NRL Report 6359

An Investigation of the Modal Interference of Very-Low-Frequency Radio Waves

F. J. Rhoads and W. E. Garner

Communication Branch
Radio Division

October 27, 1965

U.S. NAVAL RESEARCH LABORATORY
Washington, D.C.

CONTENTS

ABSTRACT

A very-low-frequency (vlf) radio-wave propagation experiment has been designed to study modal interference effects and the extent of agreement with theoretical results obtained previously. The experimental data are the field strengths of the vlf transmissions from the U.S. Navy transmitting stations NPM and Haiku in Hawaii and NPG near Seattle, Washington. These data were recorded aboard an aircraft while in flight between California, Guam, and Japan, and also at a field site near Washington, D.C. During the experiment, NPM transmitted for various periods on 16.6, 19.8, 22.3, 24.0, and 26.1 kc/s. The Haiku transmissions were on 16.6 and 19.8 kc/s, while NPG was on 18.6 kc/s continuously.

The experimental field-strength-versus-distance graphs show considerable modal interference and very good agreement with the theoretical results for the isotropic case. For frequencies above 20 kc/s the experimental data indicate the existence of at least the first three modes for propagation to the west and to the east, out to distances greater than 3 megameters. The data at 19.8 kc/s, however, indicate first-three-mode effects for propagation to the east but only two modes to the west. The fading of the field strengths at Washington, D.C., during sunrise was frequently greater than 20 db. The depth of the fades, in general, increased with frequency, whereas their time of occurrence was relatively independent of frequency over the range of 19.8 to 26.1 kc/s.

PROBLEM STATUS

This is the final report on one phase of this problem; work is continuing on other phases.

AUTHORIZATION

NRL Problem R01-39
BuShips Prob. SR 008-01-01, Task 7044

Manuscript submitted October 1, 1965.

AN INVESTIGATION OF THE MODAL INTERFERENCE OF VERY-LOW-FREQUENCY RADIO WAVES

INTRODUCTION

The U.S. Naval Research Laboratory is carrying out a comprehensive very-low-frequency (vlf) radio-wave-propagation research program. Pursuant to the objectives of this program, several series of propagation-research experiments were conducted in May, June, and July 1965, primarily to determine modal interference effects for transmissions at frequencies in the upper portion of the vlf range.

During portions of this three-month period, the U.S. Navy vlf transmitting stations at Lualualei (NPM) and Haiku, Hawaii provided special transmissions at several frequencies. The Lualualei transmitting station, to be referred to as NPM, operated for various periods at frequencies of 16.6, 19.8, 22.3, 24.0, and 26.1 kc/s. The special transmissions from the Haiku station were at 16.6 and 19.8 kc/s. The field strengths of these transmissions, along with those from the U.S. Navy transmitting station NPG near Seattle, Washington, were recorded aboard an aircraft flying between California, Guam, and Japan. In addition, the field strengths of these transmissions were recorded near Washington, D.C., to determine the diurnal pattern for the various transmission frequencies and the sunrise and sunset effects, which can be interpreted to be modal interference phenomena (2,3).

EXPERIMENTAL APPROACH

The special transmissions, at several frequencies, from the U.S. Navy transmitting stations at Lualualei (NPM) and at Haiku, both on the Island of Oahu, Hawaii, in May, June, and July 1965 offered a unique opportunity to investigate frequency-dependent propagation effects simultaneously over the same propagation paths. The experiment was designed to investigate the modal interference effects indicated by the results of the theoretical study by Wait and Spies (1). That is, it was designed to determine the extent of these modal interference effects under realistic conditions for both daylight and nighttime propagation paths over sea water by the analysis of propagation data collected in an aircraft flying between California, Guam, and Japan. Data were recorded also at an NRL field site at Hybla Valley, Virginia, near Washington, D.C., to provide additional information for a study of the modal interference phenomena producing sunrise and sunset fading at vlf (2,3).

The period of special transmissions from NPM pertinent to the experiment extended from May 9 through July 16, 1965. The Haiku special transmission period was from May 9 through June 13, 1965. During these periods, NPM and Haiku provided continuous, three-minute, key-down transmissions followed by three-minute, key-up periods once or twice an hour for the various transmitting frequencies, the schedule of which is given in Table 1. The NPG transmitting station was also providing three-minute, key-down transmissions during the period of this experiment at a constant frequency of 18.6 kc/s. The antenna currents at all three transmitting stations were recorded during these special key-down transmissions. The radiated power, P_r, for each key-down transmission could then be determined from the relation

$$P_r = I_a^2 R_r$$

Table 1
NPM and Haiku Special Transmission Schedule

Dates 1965 (UT)	Frequency (kc/s)	
	NPM	Haiku
May 9-12	19.8	16.6
13-16	22.3	19.8
17-20	24.0	19.8
21-24	26.1	19.8
25-28	24.0	19.8
29-June 1	22.3	19.8
June 2-5	24.0	19.8
6-9	26.1	19.8
10-13	19.8	16.6
14-17	22.3	
18-21	24.0	
22-25	26.1	
26-29	19.8	
30-July 4	22.3	
July 5-7	16.6	
8-15	19.8	

Table 2
NPM, Haiku, and NPG Radiation Resistances

Transmitter	Frequency (kc/s)	Radiation Resistance (ohms)
NPM	16.6	0.044
	19.8	0.062
	22.3	0.079
	24.0	0.092
	26.1	0.108
Haiku	16.6	0.119
	19.8	0.161
NPG	18.6	0.085

where I_a is the transmitting-antenna current and R_r is the radiation resistance. This calculation provided for the normalization of all field-strength data to a constant radiated power of one kilowatt. The appropriate values of radiation resistance are given in Table 2.

It was during the special three-minute, key-down transmissions that the primary field-strength data were obtained. The three-minute, key-up periods provided atmospheric noise-level measurements which were used to extract the transmission field strengths

Table 3
Aircraft Flight Schedule

Flight	Date/Time (UT)		Path Solar Condition*
	Depart	Arrive	
From San Francisco	May	May	
To Honolulu	18/1850	19/0605	Day
To Wake	21/1650	22/0245	Day
To Guam	22/1945	23/0140	Day
To Marcus Is.-Guam†	24/0930	24/1710	Night-Transition
To Koror Is.-Guam†	26/0930	26/1620	Night
To Tokyo	27/0900	27/1525	Night
To Midway	31/0835	31/1830	Night-Transition
To Honolulu	31/2000	June 01/0110	Day
To San Francisco	June 02/0155	02/1254	Transition-Night

*Listed are the solar conditions for the propagation paths from Hawaii to the aircraft during each flight and for times during which data are reported.

†Local flight out of Guam and returning to Guam.

from the signal-plus-noise recordings. Field-strength data reported during times other than the three-minute, key-down periods have been corrected for transmission duty cycle to be equivalent to the peak field strengths that would have been obtained during a continuous key-down period.

The airborne vlf propagation experiment was conducted aboard a U.S. Navy EC121K (formerly WV-2) aircraft. The vlf field strengths were recorded continuously during the flights listed in Table 3. The flight times were scheduled to provide data over a propagation path with homogeneous solar conditions, in so far as was practical. It must be realized, however, that the aircraft used had an average speed of about 200 knots, requiring between 2.5 and 3 hours to traverse one megameter. Therefore, even though propagation paths may have been all in daylight or darkness, the ionospheric condition of the path may have been changing considerably during the period of each flight.

The aircraft flights were planned to provide the greatest amount of field-strength-versus-distance data during the limited time that the aircraft was available for this experiment. The local flights out of Guam were planned to study the stability of the modal interference patterns during the night at relatively large distances. The flight from Guam to near Koror Island to Guam was approximately on a radial from Hawaii going southwest from Guam. The flight from Guam to near Marcus Island to Guam flight was in a generally northeasterly direction out of Guam.

All the airborne data were recorded using AN/URM-139 field-strength meters fed through an antenna multicoupler from a vertical whip antenna approximately six feet in length and located in the upper radome of the aircraft at the center of the intersection of the fuselage and wing. The sensitivity pattern of this antenna was verified to be circular in azimuth. The data recorded at the Hybla Valley, Virginia field site, and reported here as being at Washington, D.C., were recorded using an AN/URM-139 or an AN/URM-6 field-strength meter, both of which operated from loop antennas.

Table 4
Guide to Figure Numbers for Airborne Data

Figure Number	Transmitter and Frequency (kc/s)	Flight
1	NPM 24.0	San Francisco - Honolulu
2	Haiku 19.8	San Francisco - Honolulu
3	NPM 26.1	Honolulu - Wake Is.
4	Haiku 19.8	Honolulu - Wake Is.
5	NPM 26.1	Wake Is. - Guam
6	Haiku 19.8	Wake Is. - Guam
7	NPM 26.1	Guam - Marcus Is. - Guam
8	Haiku 19.8	Guam - Marcus Is. - Guam
9	NPM 24.0	Guam - Koror Is. - Guam
10	NPM 24.0	Guam - Koror Is. - Guam
11	NPM 24.0	Guam - Tokyo
12	Haiku 19.8	Guam - Tokyo
13	NPM 22.3	Tokyo - Midway Is. - Honolulu
14	Haiku 19.8	Tokyo - Midway Is. - Honolulu
15	NPM 24.0	Honolulu - San Francisco
16	Haiku 19.8	Honolulu - San Francisco
17	NPG 18.6	San Francisco-Honolulu-Wake Is.-Guam
18	NPG 18.6	Guam - Marcus Is. - Guam
19	NPG 18.6	Guam - Koror Is. - Guam
20	NPG 18.6	Guam - Tokyo
21	NPG 18.6	Tokyo-Midway-Honolulu-San Francisco

EXPERIMENTAL OBSERVATIONS

As stated previously, the primary field-strength data recorded aboard the aircraft and at the field site near Washington, D.C., were measured during the special three-minute, key-down transmissions from NPM, Haiku, and NPG. These special transmissions were provided twice an hour by NPM and Haiku during a portion of this experimental period and once an hour during the remainder of the time. They were provided by NPG only once an hour during the entire period. Data recorded and reported during periods of CW or frequency-shift keying (FSK) have been corrected for duty-cycle effects to be equivalent to a continuous key-down transmission. All the field-strength data presented here have been normalized to a radiated power of one kilowatt. The actual radiated power of the three transmitting stations involved differed considerably and, of course, the NPM radiated power varied with the operating frequency. The radiated powers of the three stations for this period averaged roughly 23 db above one kilowatt (200 kilowatts) for both NPM and NPG and about 10 db above one kilowatt (10 kilowatts) for Haiku.

The data recorded aboard the aircraft are presented in Figs. 1 through 21* and are individually identified in Table 4. In general these data are plotted as field-strength-

*All figures are bound consecutively at the end of this report.

Table 5
Guide to Figure Numbers for Theoretical Data
by Wait and Spies (1)

Figure Number	Frequency (kc/s)	Modes
22	16.6	1,2
23	16.6	1,2,3
24	18.6	1,2
25	18.6	1,2,3
26	19.8	1,2
27	19.8	1,2,3
28	22.3	1,2,3
29	24.0	1,2,3
30	26.1	1,2,3

versus-distance graphs, with the times of some of the special three-minute, key-down transmissions provided to show the elapsed time. Some graphs, however, are plots of field strength versus time for the flights, where the propagation-path distance did not change appreciably. In these graphs appropriate distance notations have been added. In all cases, the data for the special key-down transmissions are indicated. The initial and final data samples presented for each flight are not necessarily observations at the flight terminal points. When applicable, the times of ground sunrise (SR) and sunset (SS) are given on the graphs. Figures 1 through 21 also include curves showing the theoretically predicted field strengths given by Wait and Spies (1). These curves will be discussed in detail later in this report. In most instances, the NPG, 18.6 kc/s, data presented in Figs. 17 through 21 are for the special keydown transmissions only, and the curves are drawn point to point. In Fig. 21 some additional data were added to show large modal interference nulls.

A continuous plot of the theoretical field strengths versus distance resulting from the parameters given by Wait and Spies (1) are shown in Figs. 22 through 30. Each graph is identified in Table 5. Most of these graphs are for the summation of the first, second, and third order waveguide modes (n = 1,2,3) but some are for only the first and second modes (n = 1,2), since the computational process used by Wait and Spies (1) diverged for the third-order mode for frequencies below 20 kc/s for an ionospheric height (h) of 70 km. The curve for n = 1,2,3 for 19.8 kc/s with an ionospheric height of 70 km is a slight extrapolation of that data from 20 kc/s. It should be noted that all the theoretical curves presented here, based on the data by Wait and Spies (1), are for the isotropic case, or for propagation along a magnetic meridian. This method was necessary since theoretical values of all the parameters for three modes are not available for the anisotropic case with an ionospheric conductivity gradient, β, of 0.5 km^{-1}.

The data recorded at the field site near Washington, D.C. are presented in Figs. 31 through 62. The data covered in each graph are identified in Table 6. These data are presented in two general forms. The first form (Figs. 31 through 56) shows each data sample for periods of four days or less. These graphs not only contain the field strengths for the special key-down transmissions but also include the maxima and minima during the sunrise and sunset transition periods. In some instances, the minima as plotted are "less than" values, with the actual value below the atmospheric noise level. Generally speaking, therefore, the minima during the transition periods should not be considered as exact values. The other form used for presenting the Washington, D.C., data (Figs. 58

Table 6
Guide to Figure Numbers for Data Recorded Near Washington, D.C.

Figure Number	Transmitter and Frequency (kc/s)	Period Covered or Type of Presentation
31	NPM 22.3	May 13-16
32	Haiku 19.8	May 13-16
33	NPM 24.0	May 17-20
34	Haiku 19.8	May 17-20
35	NPM 26.1	May 21-24
36	Haiku 19.8	May 21-24
37	NPM 24.0	May 25-28
38	Haiku 19.8	May 25-28
39	NPM 22.3	May 29 - June 1
40	Haiku 19.8	May 29 - June 1
41	NPM 24.0	June 2-5
42	Haiku 19.8	June 2-5
43	NPM 26.1	June 6-9
44	Haiku 19.8	June 6-9
45	NPM 19.8	June 10-13
46	Haiku 16.6	June 10-11
47	NPM 22.3	June 14-17
48	NPM 24.0	June 18-21
49	NPM 26.1	June 22-25
50	NPM 22.3	June 30 - July 3
51	NPM 16.6	July 5-7
52	NPM 19.8	July 8-11
53	NPM 19.8	July 12-13
54	NPG 18.6	May 13-16
55	NPG 18.6	May 17-20
56	NPG 18.6	May 21-24
57	Haiku 19.8	Mean and standard deviation
58	NPM 19.8	Median and all samples
59	NPM 22.3	Median and all samples
60	NPM 24.0	Median and all samples
61	NPM 26.1	Median and all samples
62	NPG 18.6	Median and all samples

through 62) gives the median of the field strengths during the special key-down periods only. Included with each median curve are all the data samples, some of which coincide. Figure 57 is a plot of the mean and standard deviation, since there were sufficient data samples for the Haiku 19.8 kc/s transmissions to make a standard deviation calculation meaningful.

All the graphs in Figs. 31 through 62 were automatically plotted by use of an electronic computer, which generated the slight waviness in the curves. In some instances several hours of data may be missing, and, since the computer plots are point to point, a relatively long straight line (Fig. 32) results. Also, due to equipment failures and other operational difficulties, data are not available for all the special transmission periods as given in Table 1.

DISCUSSION OF OBSERVATIONS

Background

The propagation paths investigated through the experiment were generally in east-west directions, and consequently the results are influenced by any nonreciprocal effects of the anisotropic medium. It was found, however, that the experimental data did not show good agreement with the results from Wait and Spies (1) for the anisotropic case for an ionospheric conductivity gradient, β, of 0.3 km^{-1}. Consequently, since the data show better agreement with the theoretical model using $\beta = 0.5$ km^{-1}, all the theoretical curves presented herein are for the isotropic case, with $\beta = 0.5$ km^{-1}, and for an infinite ground conductivity, σ_g, which is applicable for a seawater path.

There is excellent agreement, in general, between the theoretical results and the observed daytime field strengths, as indicated in Figs. 1 through 6 and Fig. 17. The nighttime experimental data show considerable scattering, which has been found by many investigators. There were, however, some instances of fairly good agreement, where the observed nighttime field strengths showed patterns and magnitudes approximating those predicted by the theoretical model (Figs. 7, 8, 11, 15, and 16).

Daytime Propagation, Airborne Data

The observed daytime data presented in Figs. 1, 2, and 3 show excellent agreement with the theoretical, three-mode summation curve out to 3.5 Mm. The lateral displacement between the measured and predicted minima may have resulted from the exclusion of modes higher than three in the theoretical calculations. Wait and Spies (1), however, do not give values for the propagation parameters for modes higher than three. The effects of adding the third mode to the summation of modes one and two are such noticeable indications in the theoretical curves as the "ripple" at about 1.7 Mm and the broadening or distortion near 3.2 Mm for the 24.0 kc/s curve in Fig. 1. Similar effects can be seen in the other curves for the summation of three modes; the differences in the two- and three-mode models for both day and night propagation paths can readily be seen by comparing Figs. 26 and 27. Because of the lack of data, theoretical curves are presented only for nighttime (h = 90 km) for 16.6 and 18.6 kc/s for three modes (Figs. 23 and 25), but for the two-mode model both day and night curves are given (Figs. 22 and 24). The shape of the measured curves for 24.0, 19.8 and 26.1 kc/s, Figs. 1, 2, and 3, respectively, appear to indicate an observable effect of the third-order mode during daylight out to about 3.5 Mm. The propagation paths involved in Figs. 1, 2, and 3 are both to the east and to the west from the transmitters at Hawaii.

The observed 19.8 kc/s data presented in Fig. 4 for a daytime path appear to agree better with the two-mode model, which is included in the graph, than with the three-mode

model as given in Figs. 2 and 27. The readily observable differences in the three-mode model over that for only two modes are the double, relatively shallow minima around 0.75 Mm and the ripple at 1.8 Mm. The 19.8 kc/s data presented in Fig. 4 do not show either of these effects. The propagation path for these data is to the west, whereas the propagation path for the 19.8 kc/s data given in Fig. 2, which show agreement with the three-mode model, is to the east. Therefore, since the path to the west does not indicate the presence of the third-order mode even as close as 0.7 Mm, the third-order mode excitation must have been greatly reduced. The absence of any third-order mode effects for a propagation path to the west for 19.8 kc/s was demonstrated again during the return trip to Hawaii from Tokyo, as shown in Fig. 14, whereas the 22.3 kc/s data for this same flight show third-order mode effects out to 2 Mm (Fig. 13).

The experimental data presented in Figs. 1, 3, and 13 indicate the presence of the third-order mode for propagation paths to the east and to the west during the day for frequencies above 22 kc/s. Regretfully the same frequencies were not available during the flights in both directions; 22.3 and 26.1 kc/s were recorded to the west and 24.0 kc/s to the east. These data, for both directions of propagation, indicate the relative magnitude of the third-order mode to be about that predicted for the isotropic case. The 19.8 kc/s data, as discussed above, show the third-order-mode effects to be present for daytime propagation to the east but not to the west. Therefore, it appears that the nonreciprocity produced by the anisotropic medium results in a much lower excitation and/or higher attenuation of the third-order mode to the west than to the east for frequencies below 20 to 22 kc/s, but that nonreciprocity may have relatively little effect on this mode for frequencies above 22 kc/s. The results of Wait and Spies (1) indicate that the nonreciprocal effects on the excitation of the third-order mode are small for $\beta = 0.3$ km^{-1}. Data are not available for the directional effects for $\beta = 0.5$ km^{-1}.

There is other evidence of nonreciprocal effects, indicated by the data for daytime conditions. Propagation data for a path to the east from the transmitters in Hawaii are given in Figs. 1 and 2. These data, in general, lie above the theoretical isotropic curve, as would be expected from nonreciprocity theory. In Figs. 3, 4, 5, 6, and 17, which involve propagation paths to the west, the observed data tend to fall below the theoretical maxima and above the theoretical minima, both of which would be predicted by the nonreciprocity theory.

Nighttime Propagation, Airborne Data

As stated previously, the observed nighttime data were much more anomalous than the daytime observations. The most consistent agreement between the observed data and theory is exhibited at the lower frequencies, as is expected, since the roughness of the lower edge of the nighttime ionosphere appears relatively smoother for the longer wavelengths.

Figures 18, 19, 20, and 21 indicate good agreement of the observations on 18.6 kc/s, the lowest frequency observed, with the theoretical predictions. The majority of the observations in Figs. 18, 19, and 20 were made during sunrise transition, therefore no theoretical predictions are given for some measurements. The only major disagreement for the nighttime levels occurs around 3.0 Mm in Fig. 21. Better agreement is obtained for the minimum at 3.1 Mm by comparing the observed values with the value predicted considering three modes (Fig. 25). The severe minimum at 2.95 Mm in Fig. 21, however, is not predicted by either model and may possibly be attributed to ionospheric abnormalities. The three-mode model also better predicts the observed levels at 1.3 and 1.5 Mm (Fig. 21). The two-mode theoretical curve was included in Fig. 21 because the frequency was below 20 kc/s, and the receiving points were west of the transmitter; the daytime data under these conditions showed better agreement with the two-mode model. These nighttime results possibly show that the third-order mode has relatively better excitation

for propagation paths to the west at night for these lower frequencies. However, the magnetic bearing of the path during the flight from Honolulu to San Francisco was only slightly to the west; therefore definite conclusions cannot be drawn, particularly at the shorter distances.

At 19.8 kc/s there is fair agreement between the observed nighttime data and theory; however, the instability of the nighttime levels is more apparent than for 18.6 kc/s. The general levels in Figs. 8 and 16 agree with theory, but the additional maxima and minima in the observed data could be indicative of the presence of additional waveguide modes or are results of widespread irregularities in the nighttime ionosphere. Because of the distances involved during the flight covered by Fig. 8, the inclusion of a third-order mode would produce insignificant changes in the predicted levels and would predict no additional minima or maxima, as can be seen by noting Fig. 27. In Fig. 12 the bearing from the transmitter to the receiver at the beginning and end of the data is 77.5 degrees and 69.5 degrees west of true north respectively, and as indicated, the distance from the transmitter remains relatively constant. The entire propagation path is in darkness for all data, and yet the observed level gradually increases until it assumes a value near the predicted level.

Aside from the minor oscillations on the observed curve in Fig. 14, the maximum at 5.3 Mm and the minimum at 4.0 Mm are inexplicably reversed from the theoretical predictions for these distances. A simultaneous recording on 22.3 kc/s, presented in Fig. 13, indicates a similar maximum and minimum reversal at 5.6 and 4.6 Mm. The slight offset in distance for the two frequencies, 19.8 and 22.3 kc/s, could indicate that the phenomenon is frequency dependent. The measured minimum near 4.6 Mm in Fig. 13 is much sharper and more severe than the possibly associated minimum at 4.0 Mm in Fig. 14. Both frequencies have a deep minimum near 3.0 Mm which can be attributed to the effect of night-to-day transition on the path.

Figures 9 and 10 are different presentations of the same nighttime, 24.0 kc/s data; in Fig. 9 the data are plotted as a function of distance, and in Fig. 10 as a function of time. Excluding the maximum at 1130 UT, the data appear to remain fairly constant at 10 db below the predicted level. During the same period, Haiku on 19.8 kc/s was undetectable, indicating perhaps a rather widebanded degradation of signal levels. In Fig. 11 the signal level shows good agreement with theory, except for the gradual increase from 1000 to 1130 UT. A similar increase, but delayed in time, was noted on 19.8 kc/s on the same flight (Fig. 12). Figure 15 shows the same oscillatory fluctuations at 24.0 kc/s as were observed simultaneously on 19.8 kc/s (Fig. 16), which were discussed earlier. The minimum at 1.05 Mm (Fig. 15) is probably due to the occurrence of sunset at the transmitter.

The only nighttime data observed on 26.1 kc/s are presented in Fig. 7. The data show good predictability for the first half of the flight from Guam to Marcus Island and return, until an unexplainable drop occurred in the data at about 1245 UT. Then the observed level appeared to recover slowly until shortly before sunrise at the transmitter. The decay in signal level after 1530 UT probably can be attributed to sunrise transition.

Data Recorded Near Washington, D.C.

The observations made near Washington, D.C. are presented in Figs. 31 through 62, as listed in Table 6. In general, the diurnal pattern for each frequency observed was quite repeatable. Overall, there was more scatter in the nighttime observations from day to day than there was during the daytime, which is in agreement with the airborne observations. The repeatability of the time of occurrence of the sunrise minima was very remarkable. Table 7 lists the time of occurrence of the sunrise minima for each frequency observed, determined by the relative minima in the amplitude data and averaged from all days observed. The minima for 19.8 kc/s are numbered starting with 2, since

Table 7
Time of Sunrise Amplitude Minima as Observed Near Washington, D.C. for Both Haiku and NPM Transmissions

Sequence Number	Observed Time of Occurrence (UT)			
	19.8 kc/s	22.3 kc/s	24.0 kc/s	26.1 kc/s
1	*	0944	0955	1001
2	1128	1110	1103	1109
3	1315	1305	1302	1304
4	1455	1455	1455	1455

*See text.

its phase (not reported here) consistently indicated a rapid rate of phase change at approximately 0945 UT, although no associated discernible minimum could be detected in the amplitude data (see asterisk, Table 7). The time of occurrence of these minima was relatively independent of frequency, except for possibly the first and, to an even lesser degree, the second. The depth of these sunrise minima did, in general, increase with frequency and were frequently greater than 20 db. Correlation of the time of occurrence of the sunrise minima with the position of the sunrise line on the propagation path is continuing.

The average values of the data points presented in Figs. 46, 51, and 57 through 61 for daytime propagation (1600 to 2400 UT) and for nighttime propagation (0600 to 0800 UT) are listed in Table 8 along with the values predicted for propagation over seawater, neglecting the earth's magnetic field (1). The values for NPM and Haiku on 16.6 and 19.8 kc/s show some slight discrepancies. However, on 16.6 kc/s there were very little data from either transmitter. On 19.8 kc/s as well as 16.6 kc/s the data for each transmitter were observed on different days, and the discrepancies are well within the day-to-day variations. In comparing the predicted with the observed levels, it must be noted that for daytime propagation there is little, if any, nonreciprocity due to the earth's magnetic field, but due to the finite conductivity of North America the predicted daytime levels should be decreased by two to three decibels. Considering the latter, the observed daytime levels show good agreement with those predicted. For nighttime propagation, consideration of the earth's magnetic field would decrease the attenuation losses over the entire path involved, but again, the finite conductivity of North America would increase the absorption losses over that portion, thus tending to cancel the former, nonreciprocity effect. To obtain better agreement between theory and the observed nighttime values in Table 8, the effect of nonreciprocity would have to be much greater than the effect of finite conductivity. The analysis of these data is continuing.

CONCLUSIONS

There is excellent agreement between the experimental data for daylight, seawater propagation paths out to about 3.5 Mm, and the theoretical results by Wait and Spies (1). The observed frequencies above 22 kc/s indicated agreement with a three-mode model for propagation to the east as well as to the west. At frequencies below 20 kc/s, the three-mode model fits the data for propagation to the east, but there was no evidence of the presence of the third-order mode for propagation to the west. This latter result indicates the possibility of a greater directional effect on the third-order mode excitation than what might be predicted theoretically. A definite conclusion cannot be drawn concerning this effect, since Wait and Spies (1) have not published values for directional effects for the ionospheric gradient of 0.5 km^{-1} used herein for the comparison. Other directional

Table 8
Daytime and Nighttime Signal Levels from NPM and Haiku, Predicted* and Observed, near Washington, D.C.

Freq. (kc/s)	Transmitter	Daytime Field Strength (db above 1 μv/m)		Nighttime Field Strength (db above 1 μv/m)	
		Predicted*	Observed	Predicted*	Observed
16.6†	NPM	33.5(2)	31.0	30.7(3)	35.0
16.6†	Haiku	33.5(2)	27.0	30.7(3)	33.0
19.8	NPM	31.4(3)	28.0	23.2(3)	34.5
19.8	Haiku	31.4(3)	27.0	23.2(3)	33.0
22.3	NPM	28.3(3)	26.0	23.3(3)	31.5
24.0	NPM	27.7(3)	23.5	26.4(3)	31.5
26.1	NPM	21.1(3)	20.5	26.5(3)	33.5

*Wait and Spies (1). The predicted levels are for an isotropic case with infinite ground conductivity. The number in parentheses after each predicted level is the number of modes summed for the prediction.
†Very little data available.

effects were observed indicating, as expected, that the attenuation rates for propagation to the west are greater than those to the east.

The daytime data recorded aboard the aircraft for the seawater paths to the west showed good agreement with the isotropic, theoretical model out to about 9 Mm. The nighttime data, even at distances less than 2 Mm, showed considerably more scatter, as expected, and as demonstrated by the data continuously recorded near Washington, D.C. There was, however, some reasonably good agreement between the airborne, nighttime data and the theoretical model even at distances greater than 7 Mm. A predicted modal interference null at 7.2 Mm for 18.6 kc/s during the night was observed, but the repeatability of these more distant nulls predicted for nighttime conditions would not be expected to be very good because of the apparent irregularities of the nighttime ionosphere.

The nighttime field strengths recorded near Washington, D.C., at all observed frequencies between 16.6 and 26.1 kc/s, were considerably higher than those predicted by Wait and Spies (1) using the isotropic model and an infinite ground conductivity. Consideration of directional effect and the true conductivity of the path would not materially alter this result, since the two effects tend to cancel each other. The daytime data observed near Washington, D.C., would probably show good agreement with the theoretical model if all factors were considered. Analysis of the Washington, D.C., data will continue.

ACKNOWLEDGMENTS

The authors wish to thank the officers and crew of the aircraft, commanded by LCDR R.H. Davis, for their cooperation in this project. Also, the assistance of J. Sicard of the U.S. Navy Underwater Sound Laboratory and our colleagues J.E. Raudenbush, J.E. Rogerson, E.J. Elwood, III, and R.L. Schauer in the collection and processing of the data is gratefully acknowledged.

REFERENCES

1. Wait, J.R., and Spies, K.P., "Characteristics of the Earth-Ionosphere Waveguide for VLF Radio Waves," National Bureau of Standards Tech. Note No. 300, and Numerical Supplement

2. Crombie, D.D., "Periodic Fading of VLF Signals Received Over Long Paths During Sunrise and Sunset," NBS Radio Science, 68D(1):27-34 (Jan. 1964)

3. Crombie, D.D., "Further Observations of Sunrise and Sunset Fading of Very Low Frequency Signals," submitted to Environmental Science Services Administration, Radio Science, for publication Jan. 1966

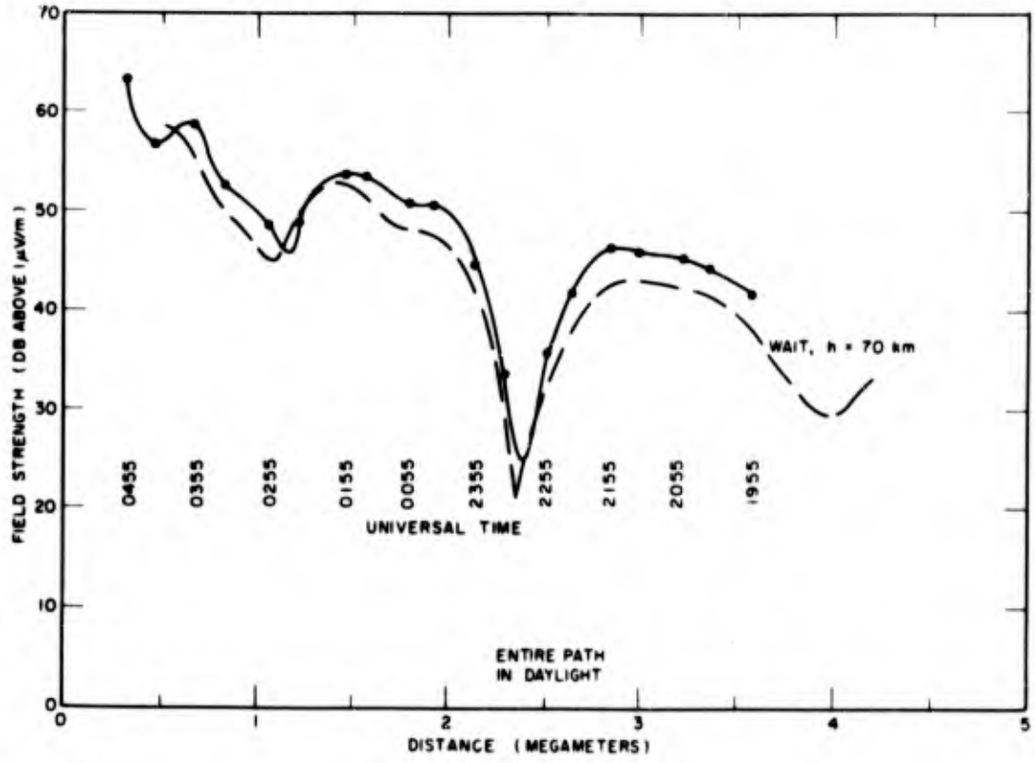

Fig. 1 - Comparison of theoretical results from Wait and Spies (1) with measured results, considering waveguide modes 1, 2, and 3 and NPM (24.0 kc/s) data recorded in flight from San Francisco to Honolulu, May 18-19, 1965; P_r = 1 kw

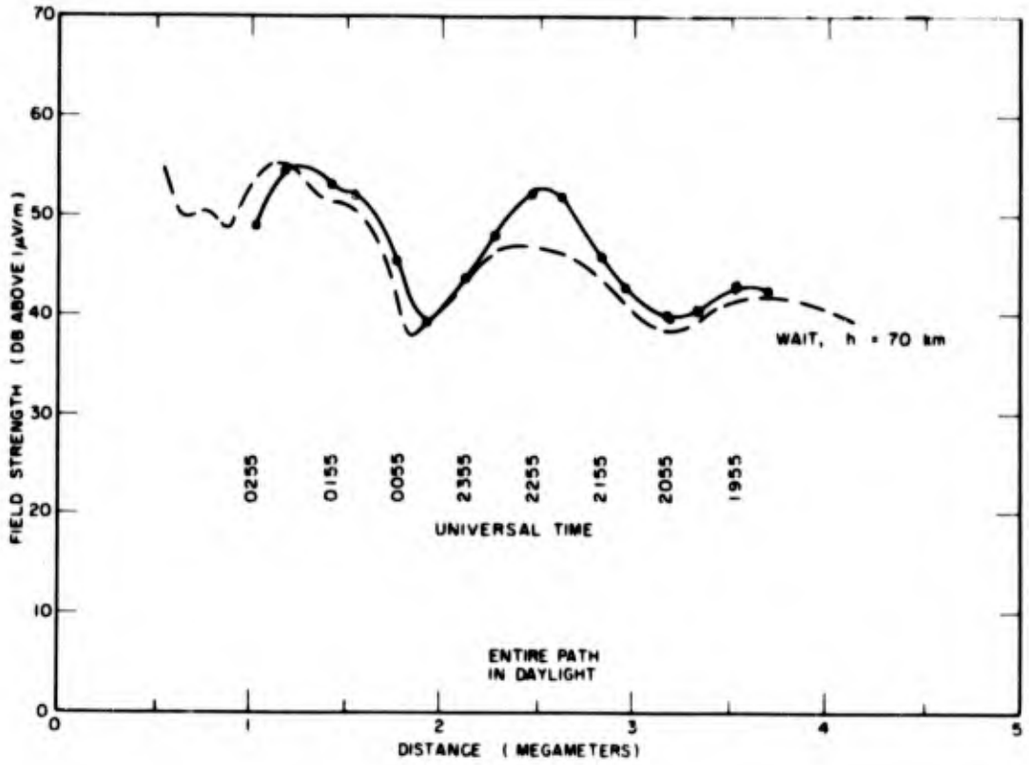

Fig. 2 - Comparison of theoretical results from Wait and Spies (1) with measured results, considering waveguide modes 1, 2, and 3 and Haiku (19.8 kc/s) data recorded in flight from San Francisco to Honolulu, May 18-19, 1965; P_r = 1 kw

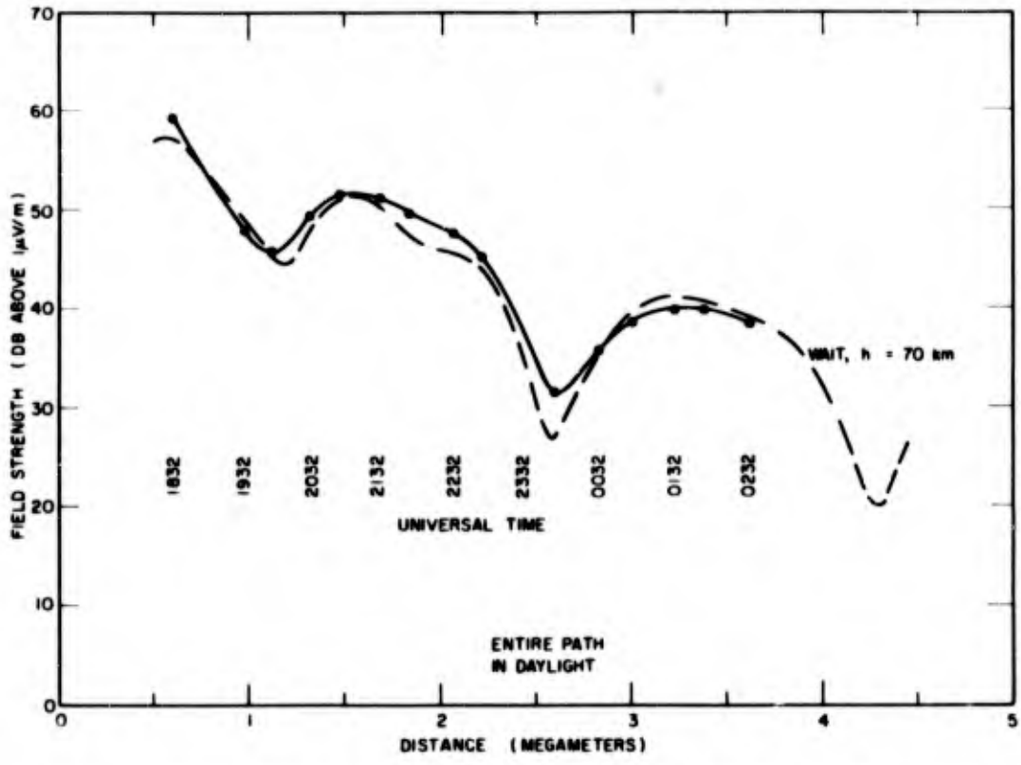

Fig. 3 - Comparison of theoretical results from Wait and Spies (1) with measured results, considering waveguide modes 1, 2, and 3 and NPM (26.1 kc/s) data recorded in flight from Honolulu to Wake Island, May 21-22, 1965; P_r = 1 kw

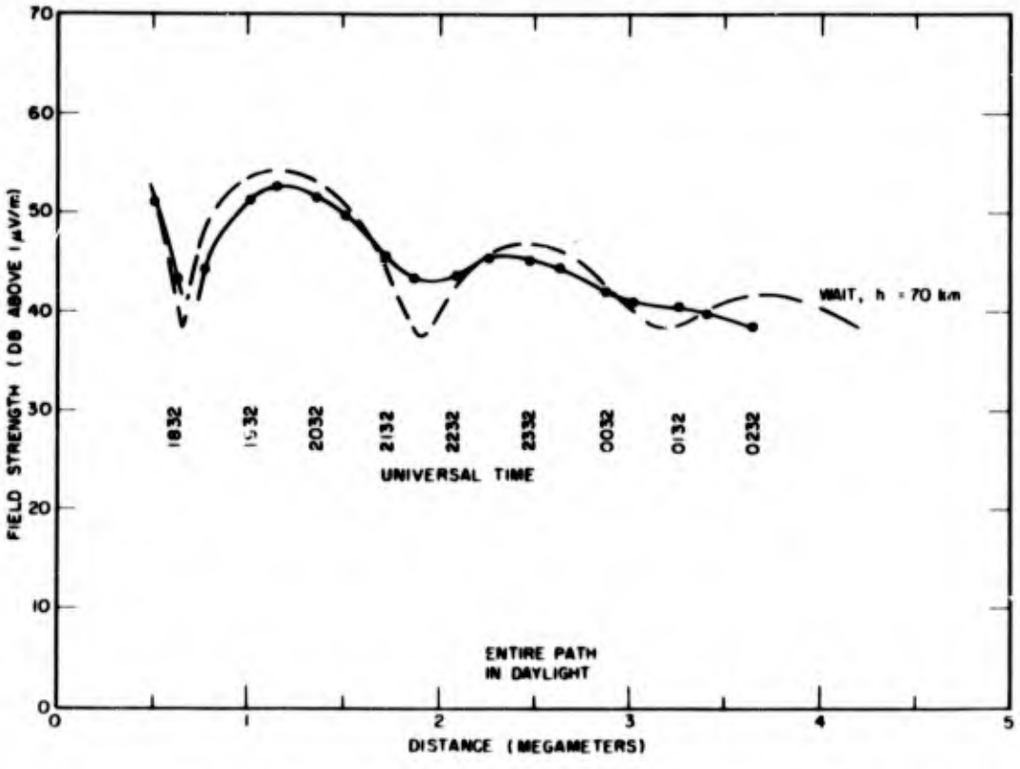

Fig. 4 - Comparison of theoretical results from Wait and Spies (1) with measured results, considering waveguide modes 1 and 2 and Haiku (19.8 kc/s) data recorded in flight from Honolulu to Wake Island, May 21-22, 1965; P_r = 1 kw

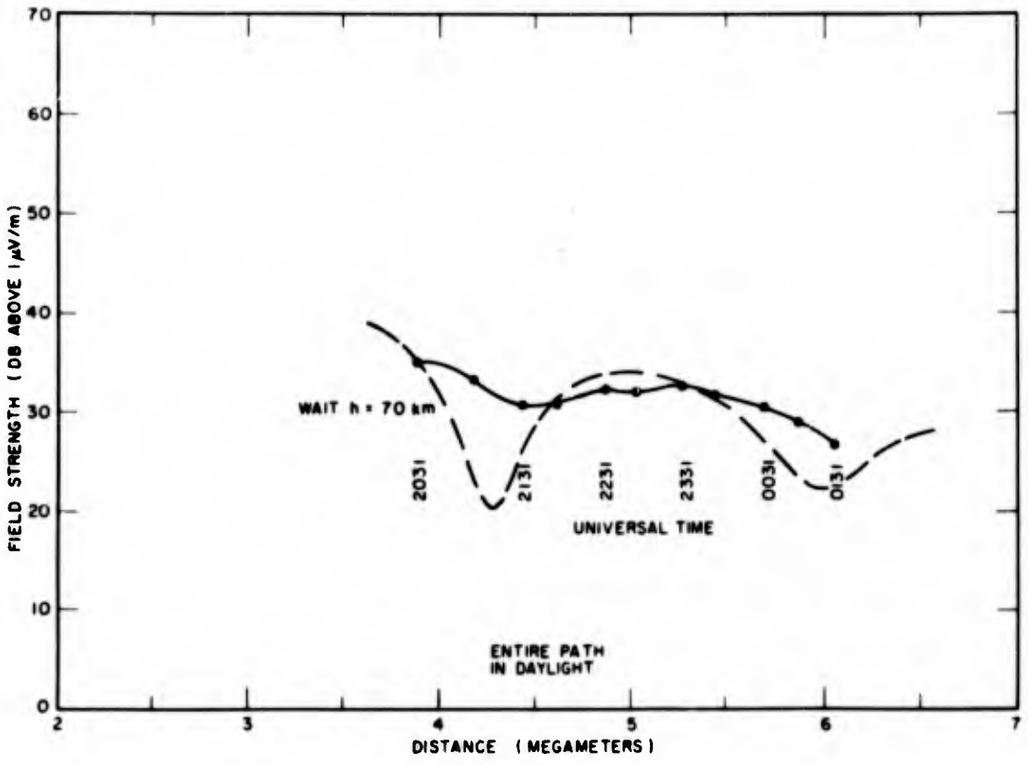

Fig. 5 - Comparison of theoretical results from Wait and Spies (1) with measured results, considering waveguide modes 1, 2, and 3 and NPM (26.1 kc/s) data recorded in flight from Wake Island to Guam, May 22-23, 1965; P_r = 1 kw

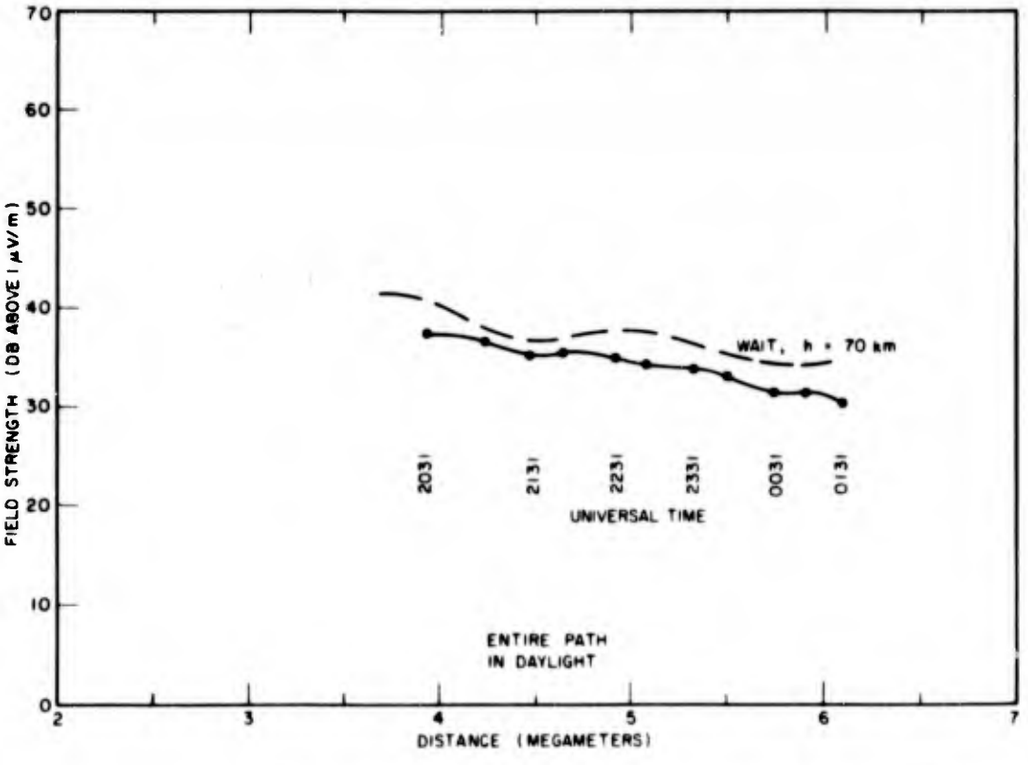

Fig. 6 - Comparison of theoretical results from Wait and Spies (1) with measured results, considering waveguide modes 1 and 2 and Haiku (19.8 kc/s) data recorded in flight from Wake Island to Guam, May 22-23, 1965; P_r = 1 kw

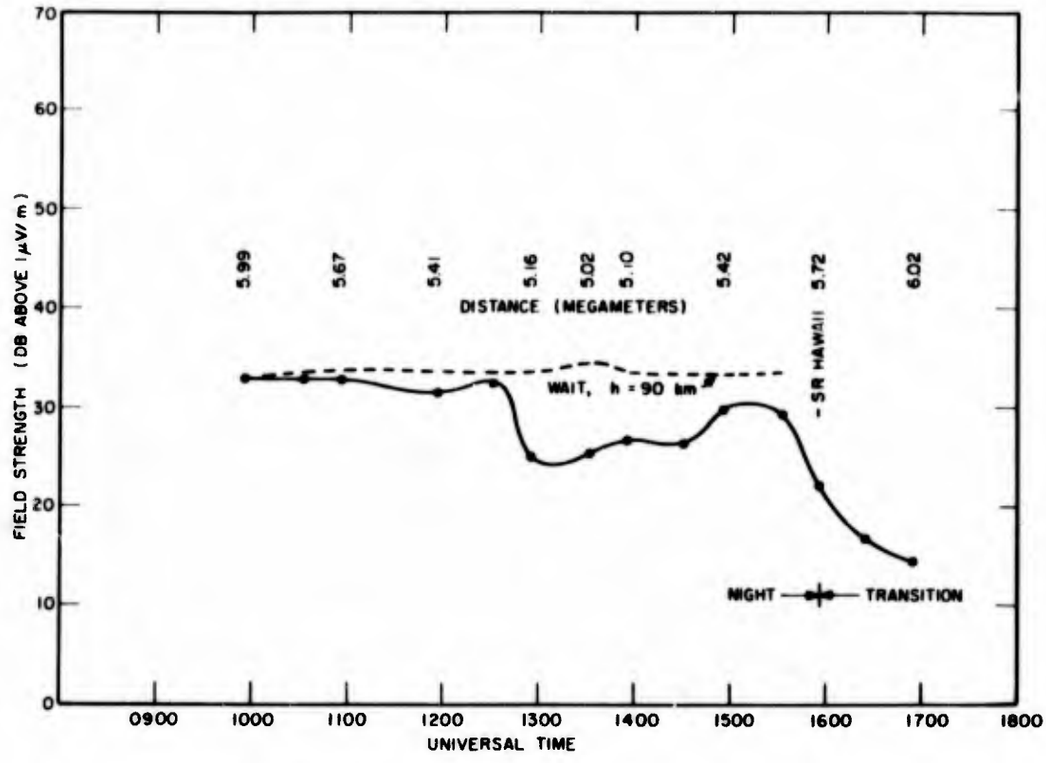

Fig. 7 - Comparison of theoretical results from Wait and Spies (1) with measured results, considering waveguide modes 1, 2, and 3 and NPM (26.1 kc/s) data recorded in flight from Guam to Marcus Island to Guam, May 24, 1965; P_r = 1 kw

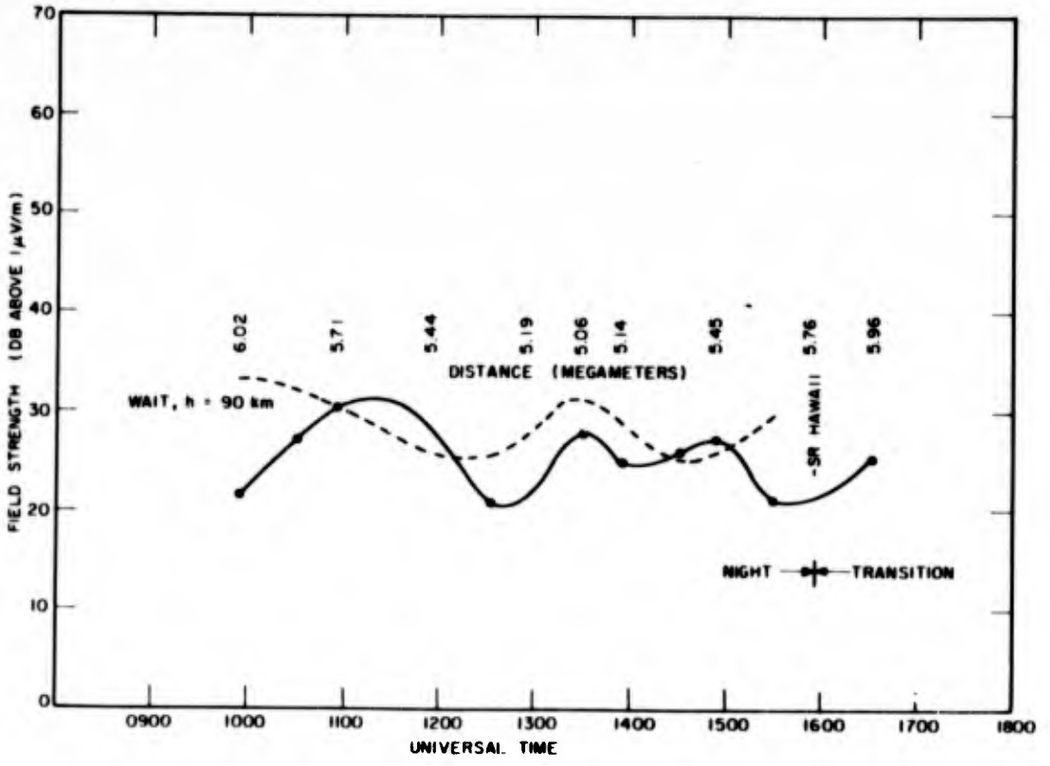

Fig. 8 - Comparison of theoretical results from Wait and Spies (1) with measured results, considering waveguide modes 1 and 2 and Haiku (19.8 kc/s) data recorded in flight from Guam to Marcus Island to Guam, May 24, 1965; P_r = 1 kw

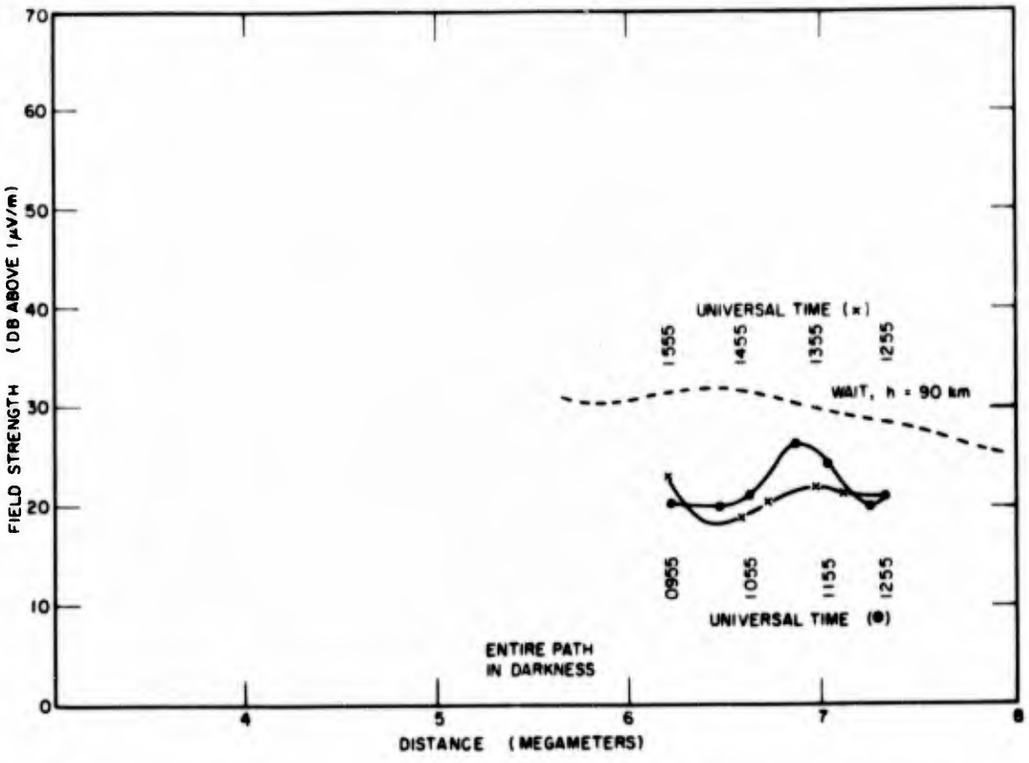

Fig. 9 - Comparison of theoretical results from Wait and Spies (1) with measured results, considering waveguide modes 1, 2, and 3 and NPM (24.0 kc/s) data recorded in flight from Guam to Koror Island to Guam, May 26, 1965; P_r = 1 kw (field strength versus distance)

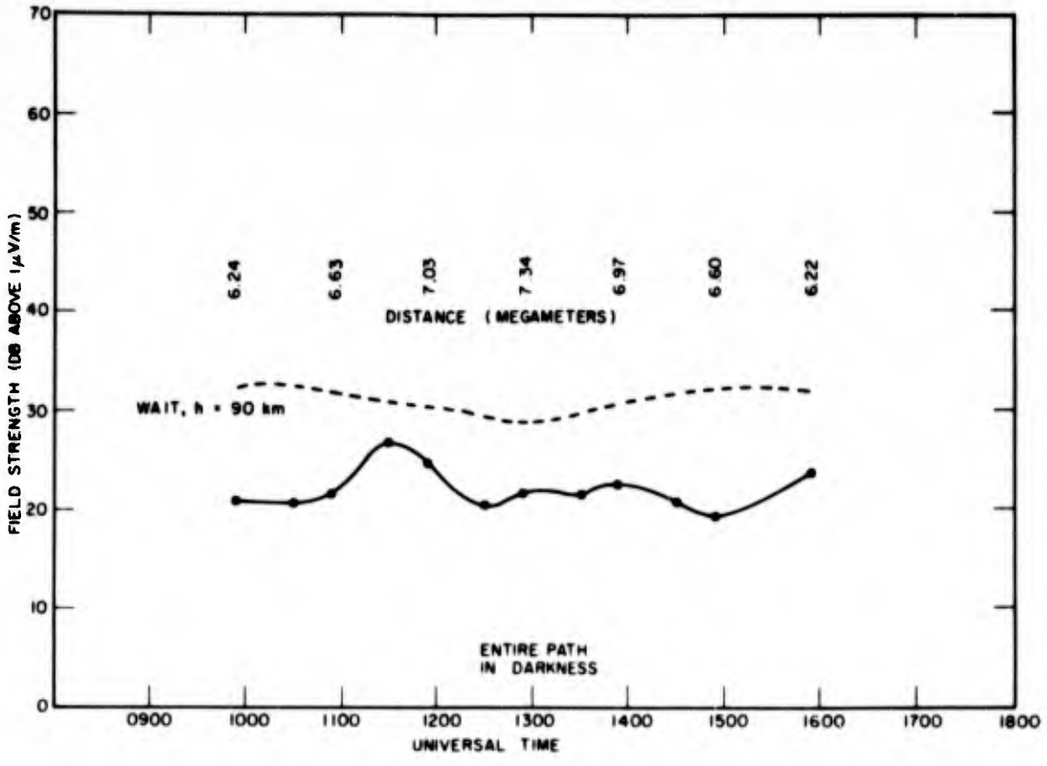

Fig. 10 - Comparison of theoretical results from Wait and Spies (1) with measured results, considering waveguide modes 1, 2, and 3 and NPM (24.0 kc/s) data recorded in flight from Guam to Koror Island to Guam, May 26, 1965; P_r = 1 kw (field strength versus time)

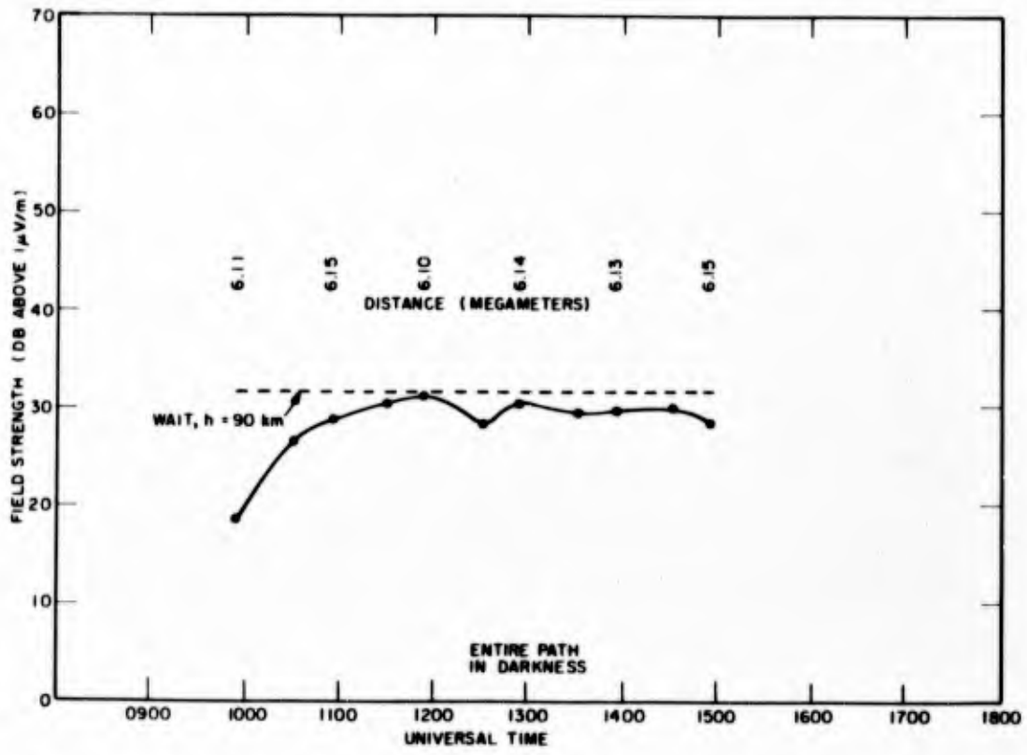

Fig. 11 - Comparison of theoretical results from Wait and Spies (1) with measured results, considering waveguide modes 1, 2, and 3 and NPM (24.0 kc/s) data recorded in flight from Guam to Tokyo, May 27, 1965; P_r = 1 kw

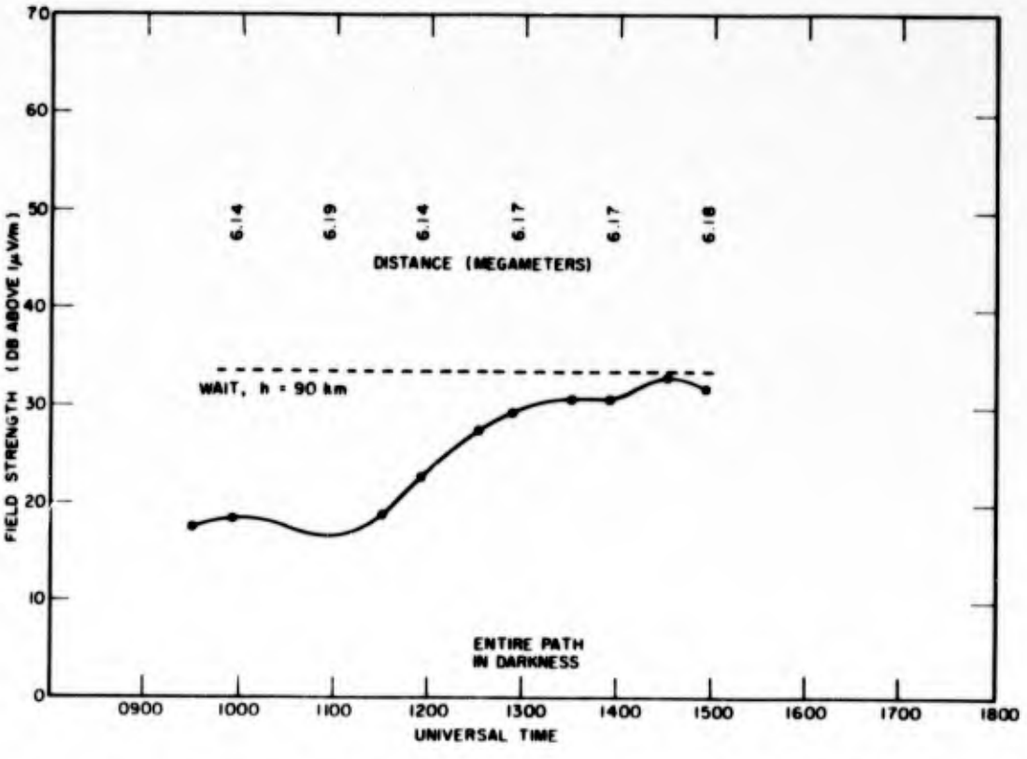

Fig. 12 - Comparison of theoretical results from Wait and Spies (1) with measured results, considering waveguide modes 1 and 2 and Haiku (19.8 kc/s) data recorded in flight from Guam to Tokyo, May 27, 1965; P_r = 1 kw

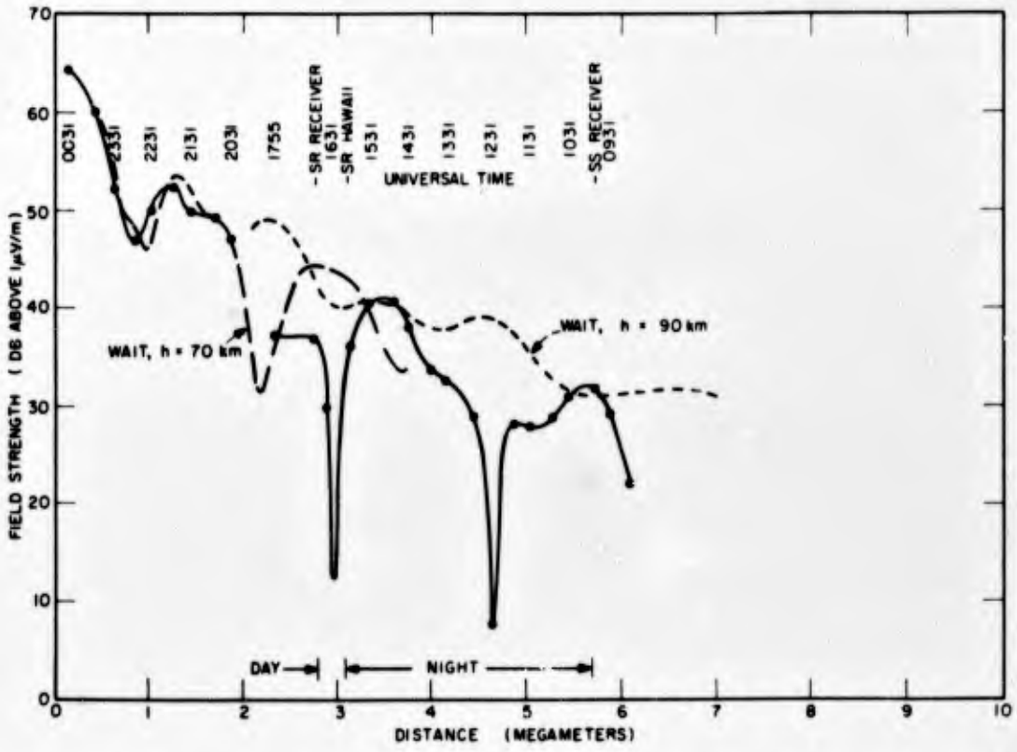

Fig. 13 - Comparison of theoretical results from Wait and Spies (1) with measured results, considering waveguide modes 1, 2, and 3 and NPM (22.3 kc/s) data recorded in flight from Tokyo to Midway Island to Honolulu, May 31 - June 1, 1965; P_r = 1 kw

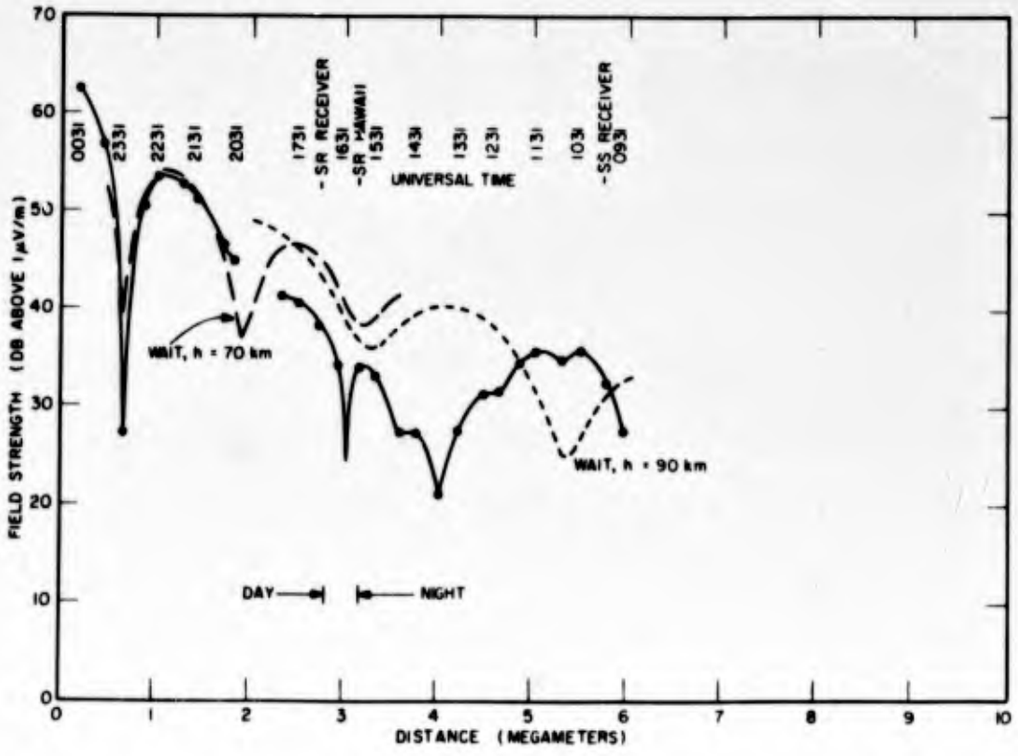

Fig. 14 - Comparison of theoretical results from Wait and Spies (1) with measured results, considering waveguide modes 1 and 2 and Haiku (19.8 kc/s) data recorded in flight from Tokyo to Midway Island to Honolulu, May 31 - June 1, 1965; P_r = 1 kw

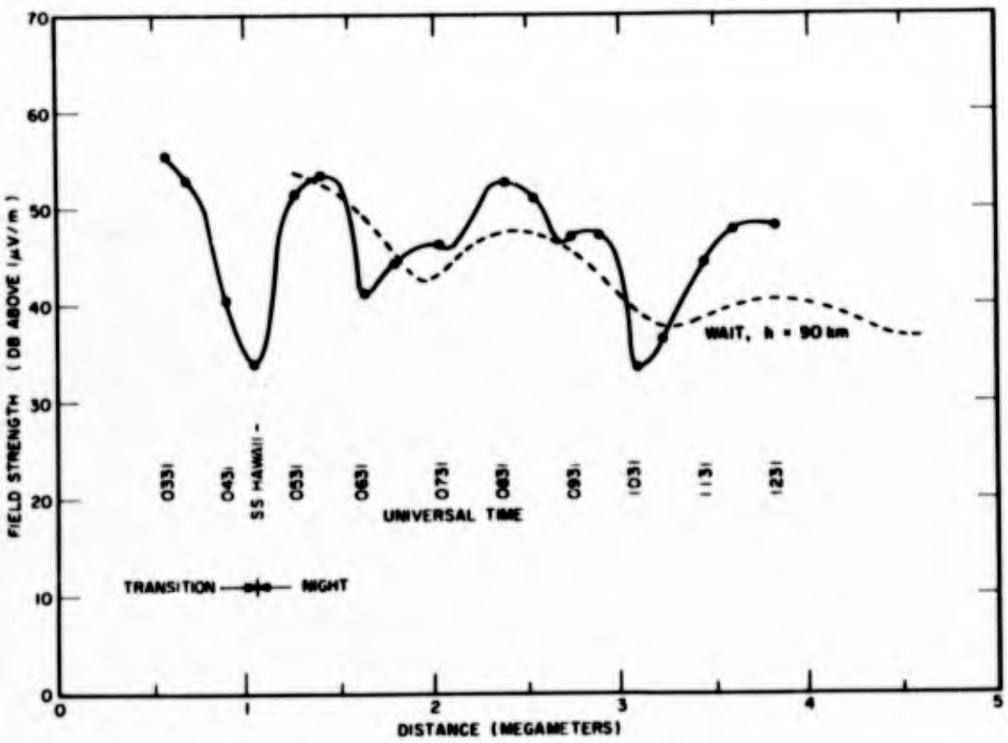

Fig. 15 - Comparison of theoretical results from Wait and Spies (1) with measured results, considering waveguide modes 1, 2, and 3 and NPM (24.0 kc/s) data recorded in flight from Honolulu to San Francisco, June 2, 1965; P_r = 1 kw

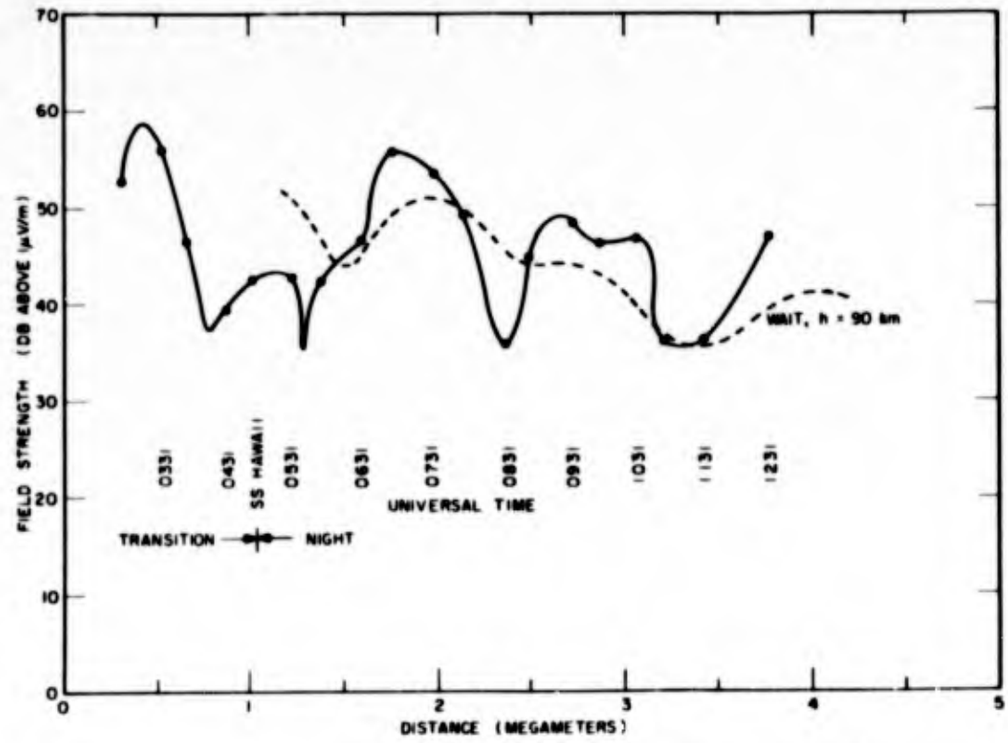

Fig. 16 - Comparison of theoretical results from Wait and Spies (1) with measured results, considering waveguide modes 1, 2, and 3 and Haiku (19.8 kc/s) data recorded in flight from Honolulu to San Francisco, June 2, 1965; P_r = 1 kw

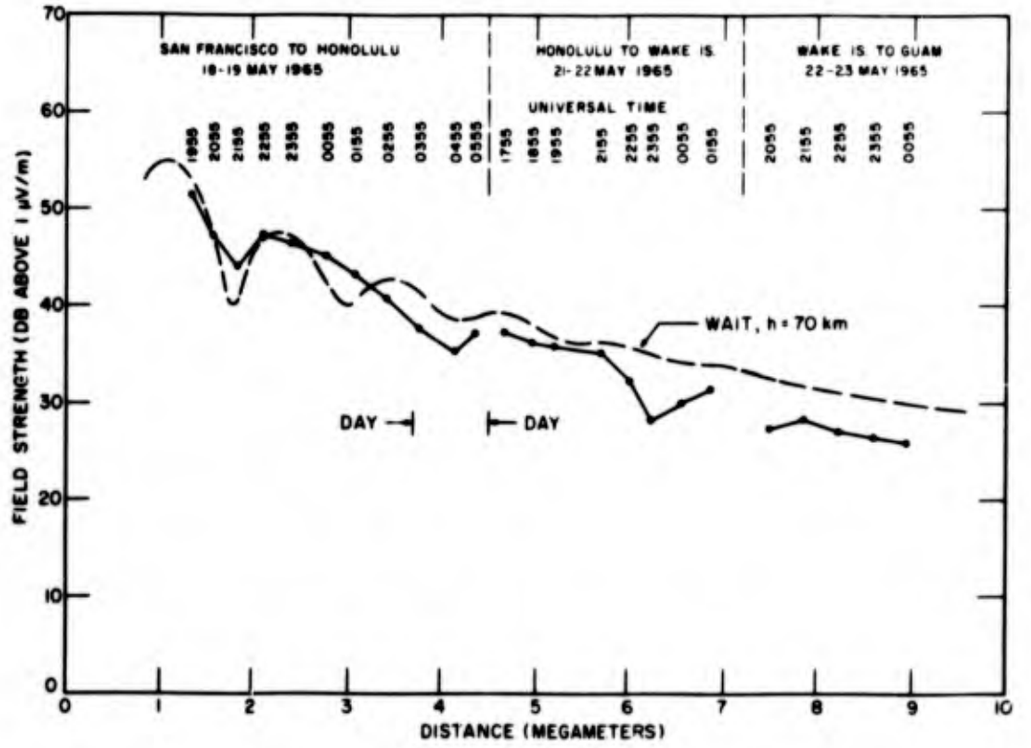

Fig. 17 - Comparison of theoretical results from Wait and Spies (1) with measured results, considering waveguide modes 1 and 2 and NPG (18.6 kc/s) data recorded in flight from San Francisco to Honolulu (May 18-19) to Wake Island (May 21-22) to Guam (May 22-23, 1965); P_r = 1 kw

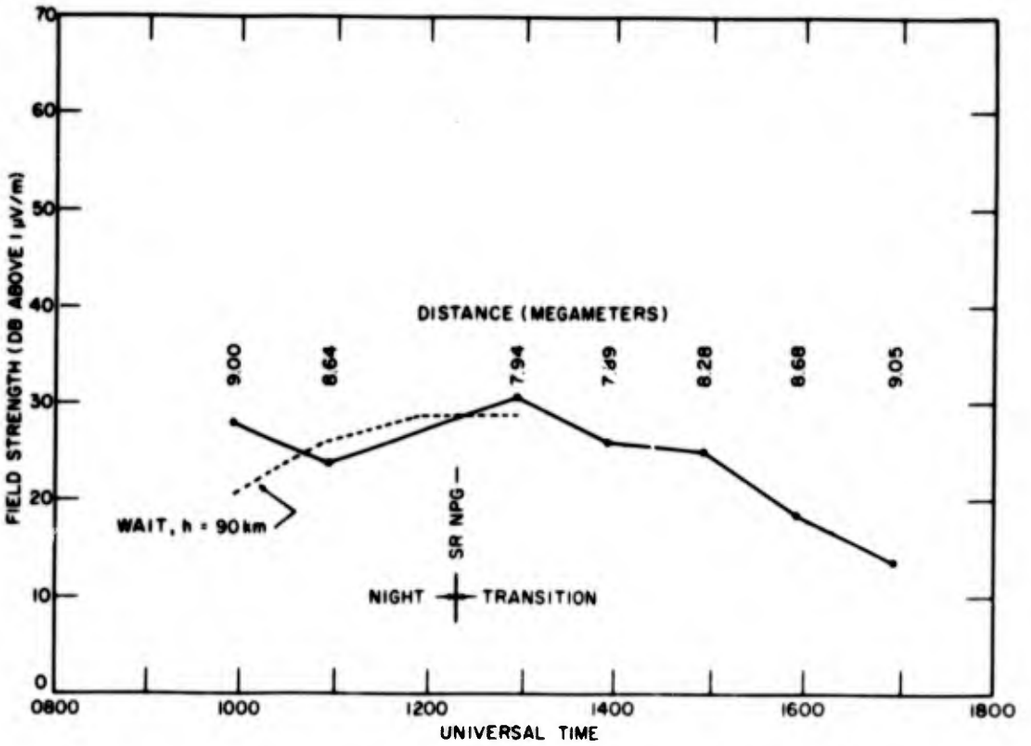

Fig. 18 - Comparison of theoretical results from Wait and Spies (1) with measured results, considering waveguide modes 1 and 2 and NPG (18.6 kc/s) data recorded in flight from Guam to Marcus Island to Guam, May 24, 1965; P_r = 1 kw

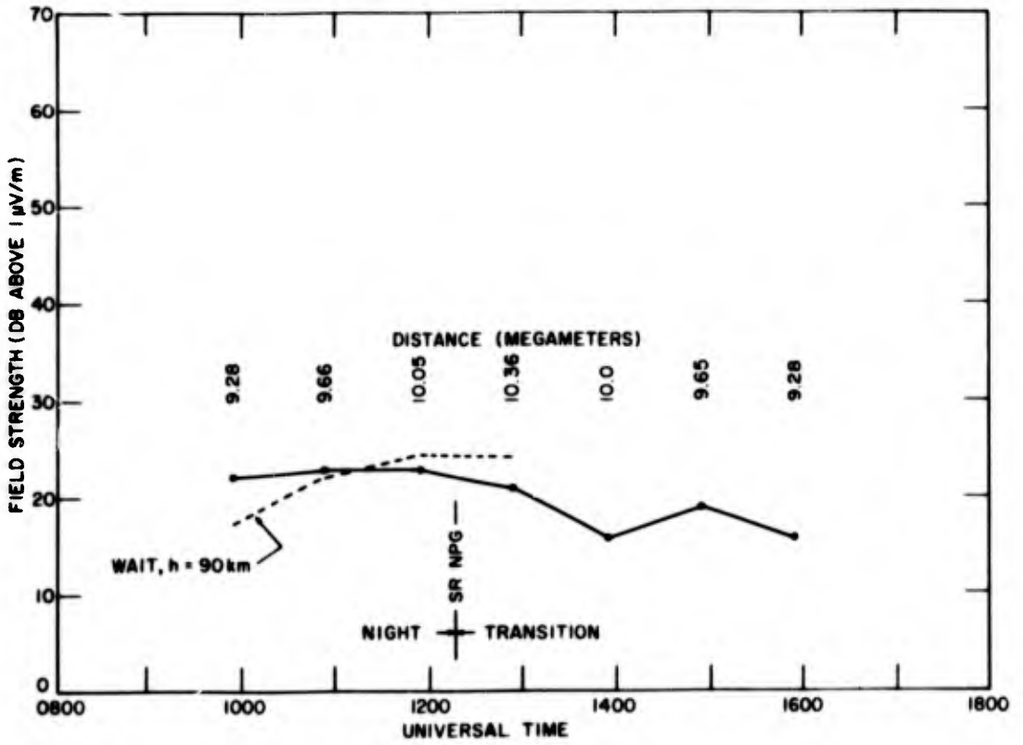

Fig. 19 - Comparison of theoretical results from Wait and Spies (1) with measured results, considering waveguide modes 1 and 2 and NPG (18.6 kc/s) data recorded in flight from Guam to Koror Island to Guam, May 26, 1965; P_r = 1 kw

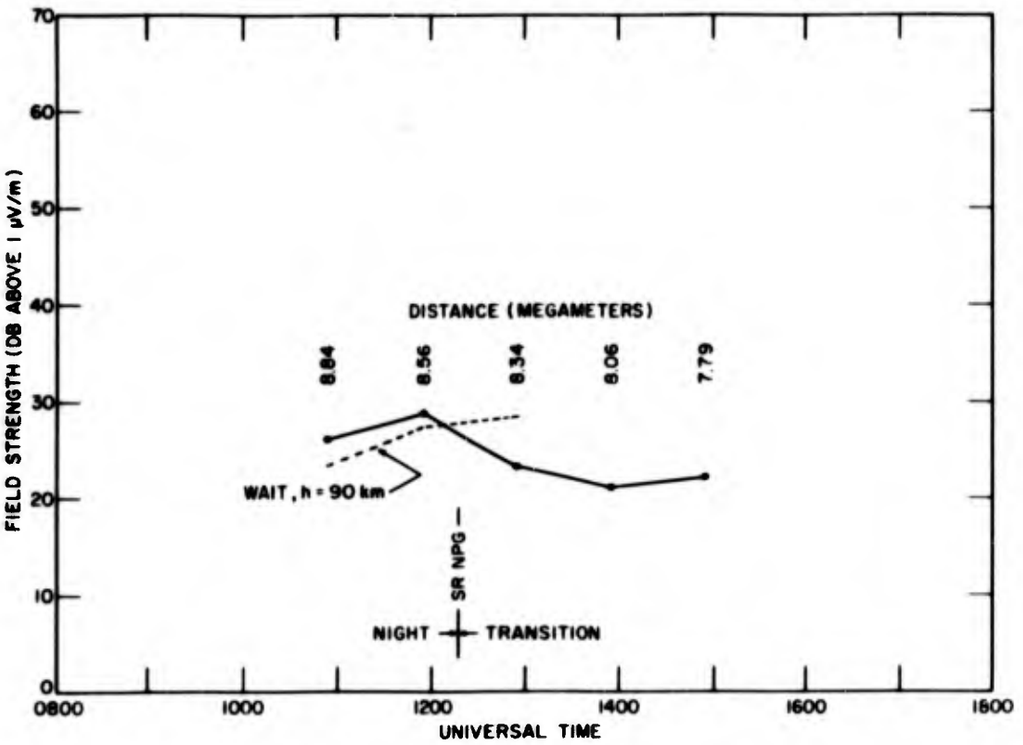

Fig. 20 - Comparison of theoretical results from Wait and Spies (1) with measured results, considering waveguide modes 1 and 2 and NPG (18.6 kc/s) data recorded in flight from Guam to Tokyo, May 27, 1965; P_r = 1 kw

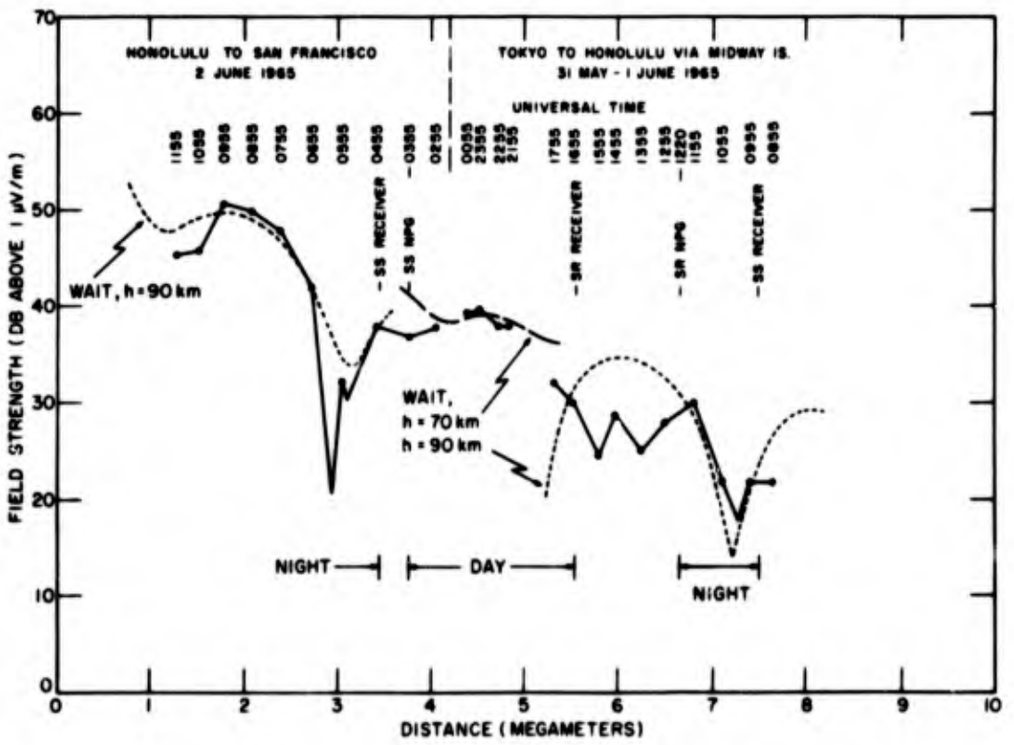

Fig. 21 - Comparison of theoretical results from Wait and Spies (1) with measured results, considering waveguide modes 1 and 2 and NPG (18.6 kc/s) data recorded in flight from Tokyo to Midway Island to Honolulu (May 31 - June 1) to San Francisco (June 2, 1965); P_r = 1 kw

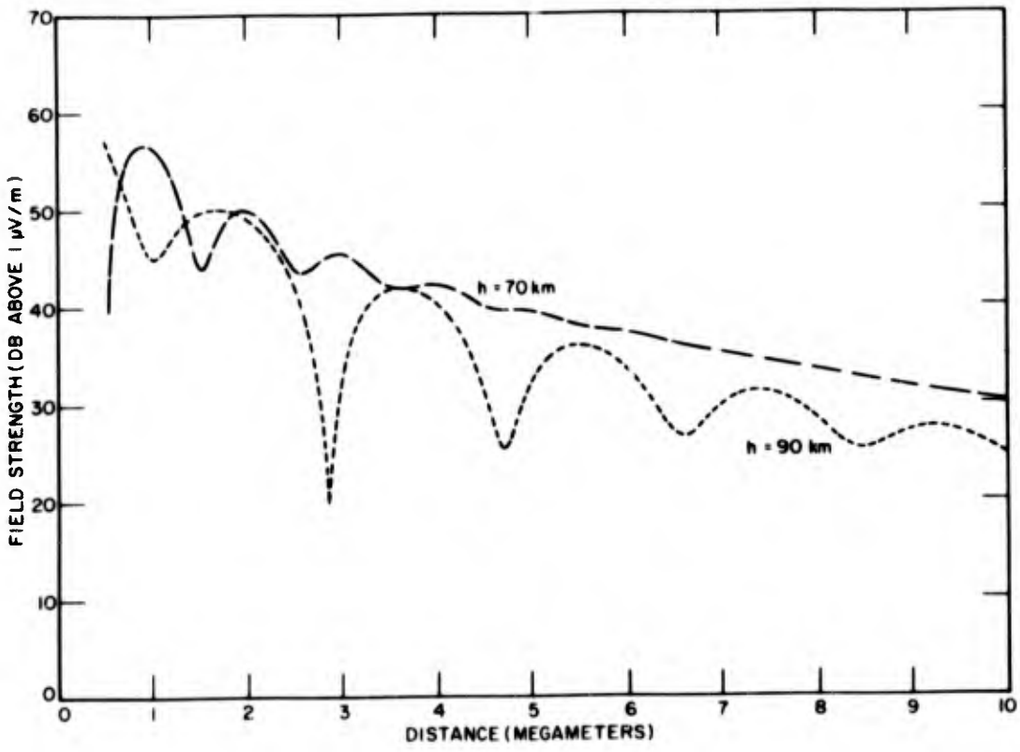

Fig. 22 - Theoretical results from Wait and Spies (1) for 16.6 kc/s considering waveguide modes 1 and 2 for the isotropic case; $\beta = 0.5$ km^{-1}, $\sigma_g = \infty$, $P_r = 1$ kw

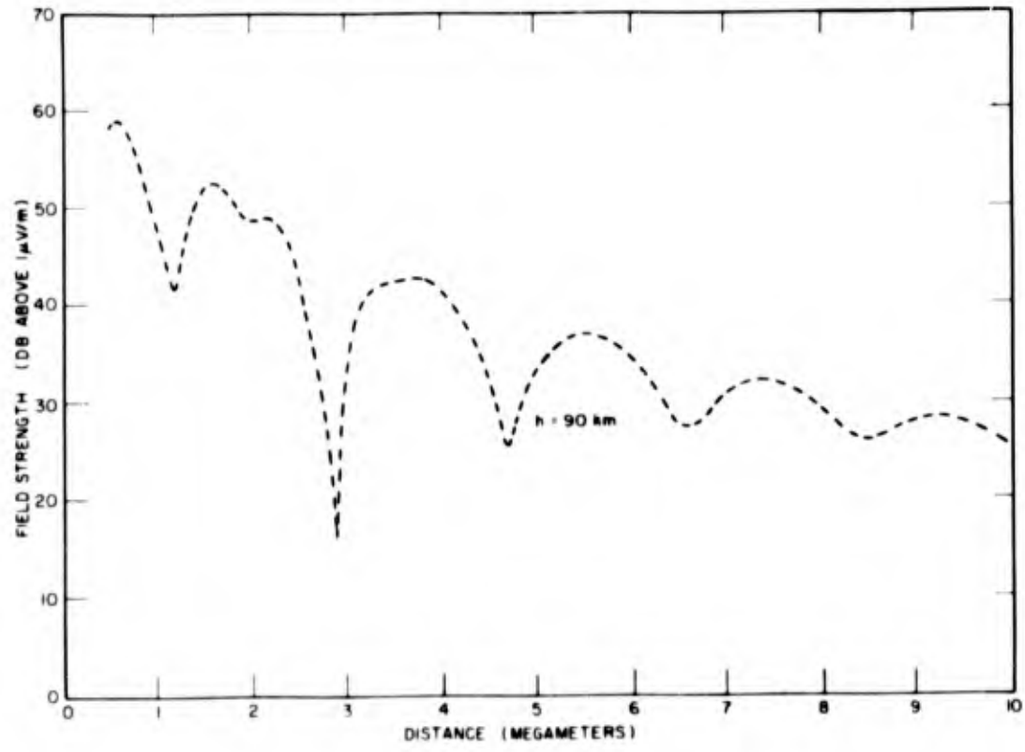

Fig. 23 - Theoretical results from Wait and Spies (1) for 16.6 kc/s considering waveguide modes 1, 2, and 3 for the isotropic case; $\beta = 0.5$ km^{-1}, $\sigma_g = \infty$, $P_r = 1$ kw

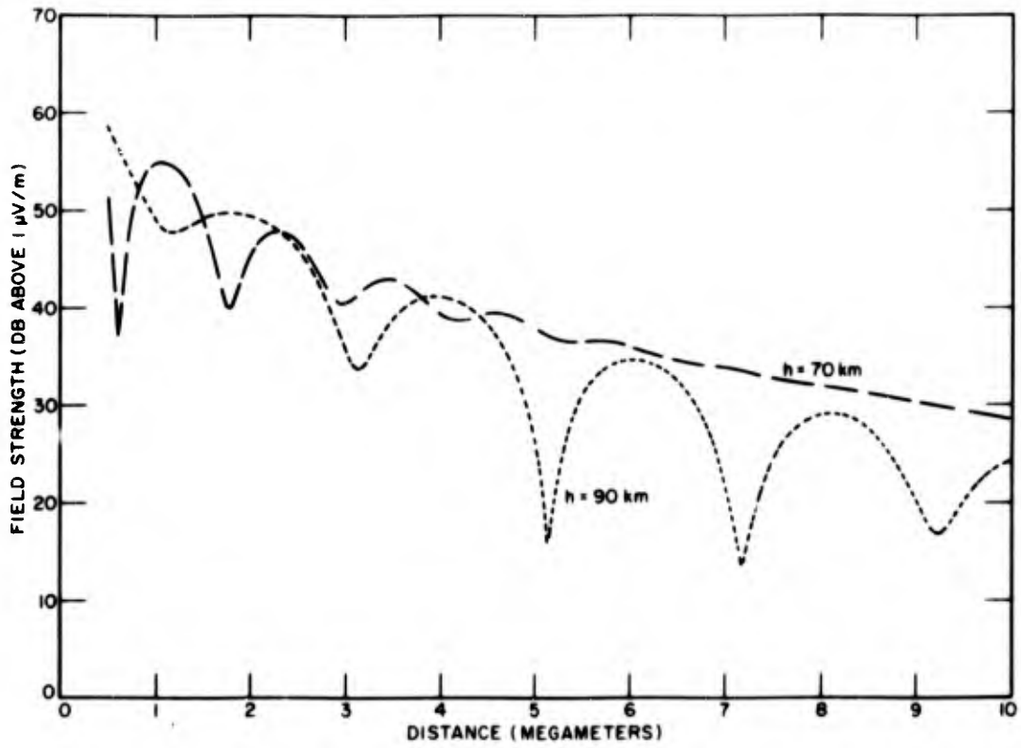

Fig. 24 - Theoretical results from Wait and Spies (1) for 18.6 kc/s considering waveguide modes 1 and 2 for the isotropic case; $\beta = 0.5$ km^{-1}, $\sigma_g = \infty$, $P_r = 1$ kw

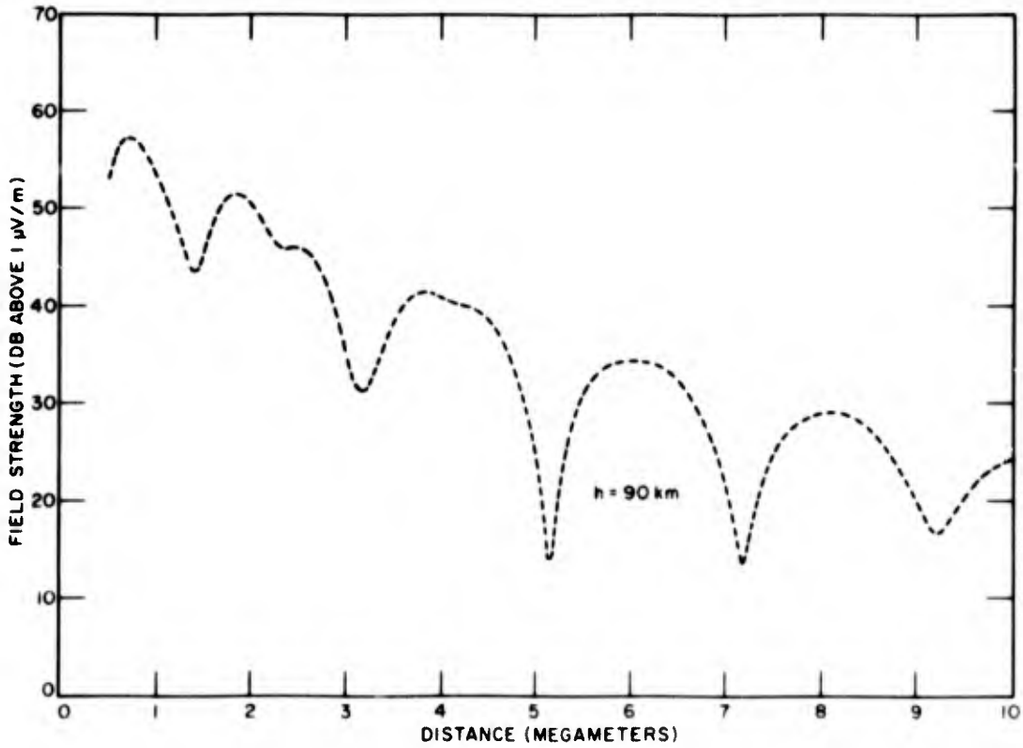

Fig. 25 - Theoretical results from Wait and Spies (1) for 18.6 kc/s considering waveguide modes 1, 2, and 3 for the isotropic case; $\beta = 0.5$ km^{-1}, $\sigma_g = \infty$, $P_r = 1$ kw

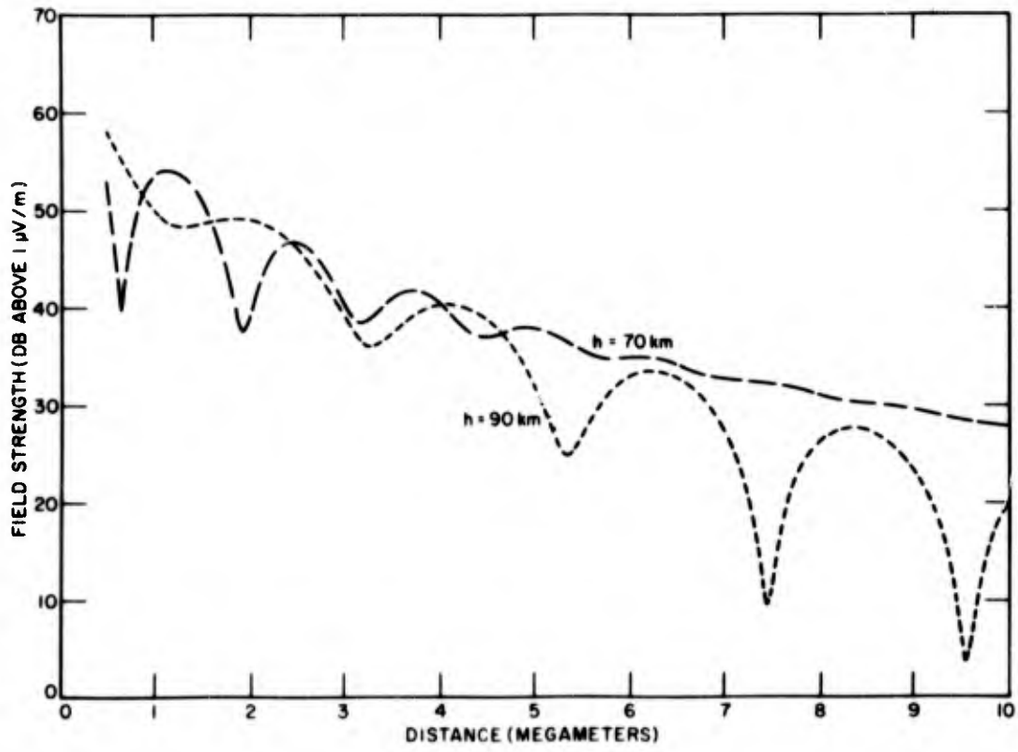

Fig. 26 - Theoretical results from Wait and Spies (1) for 19.8 kc/s considering waveguide modes 1 and 2 for the isotropic case; $\beta = 0.5$ km^{-1}, $\sigma_g = \infty$, $P_r = 1$ kw

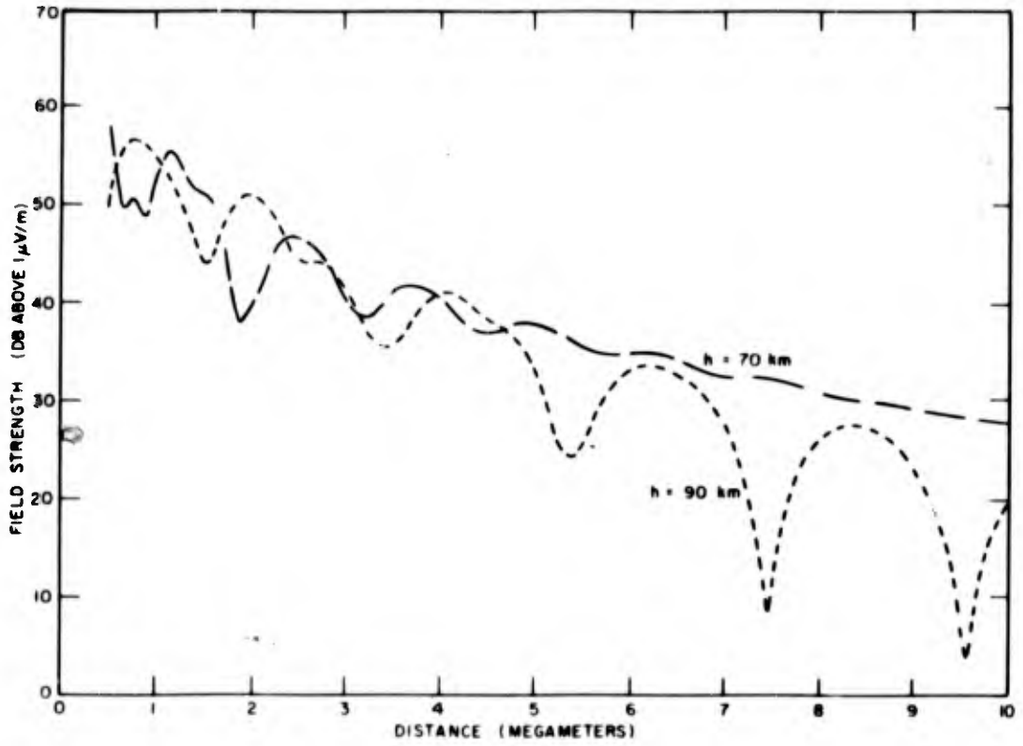

Fig. 27 - Theoretical results from Wait and Spies (1) for 19.8 kc/s considering waveguide modes 1, 2, and 3 for the isotropic case; $\beta = 0.5$ km^{-1}, $\sigma_g = \infty$, $P_r = 1$ kw

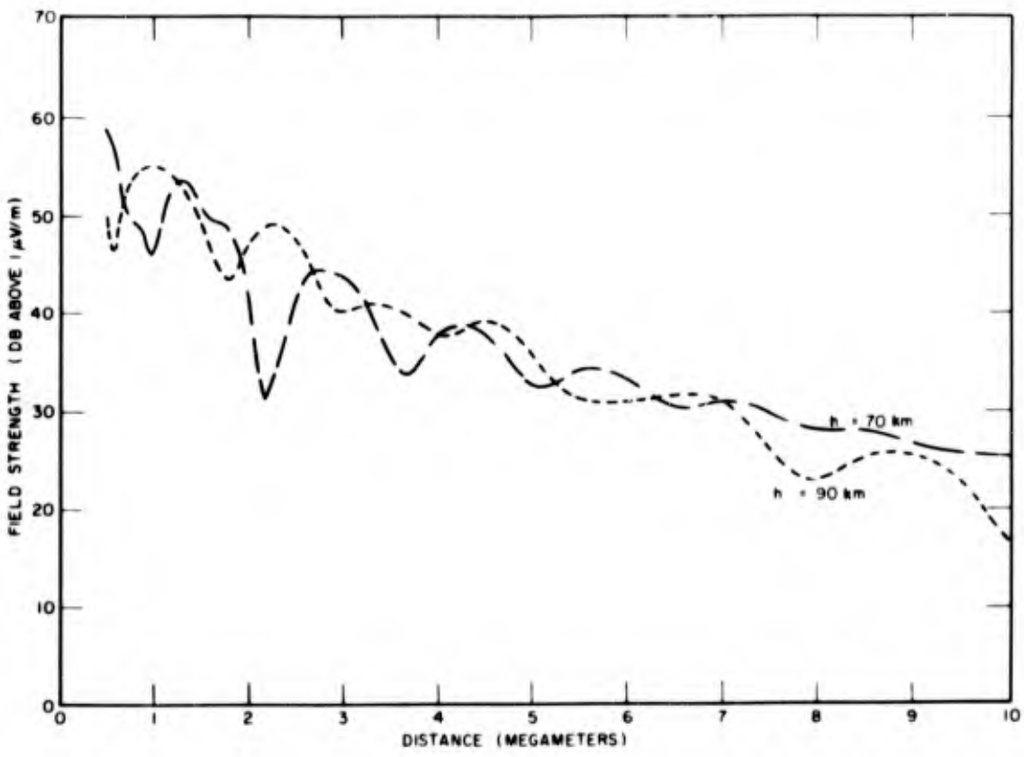

Fig. 28 - Theoretical results from Wait and Spies (1) for 22.3 kc/s considering waveguide modes 1, 2, and 3 for the isotropic case; β = 0.5 km^{-1}, $\sigma_g = \infty$, P_r = 1 kw

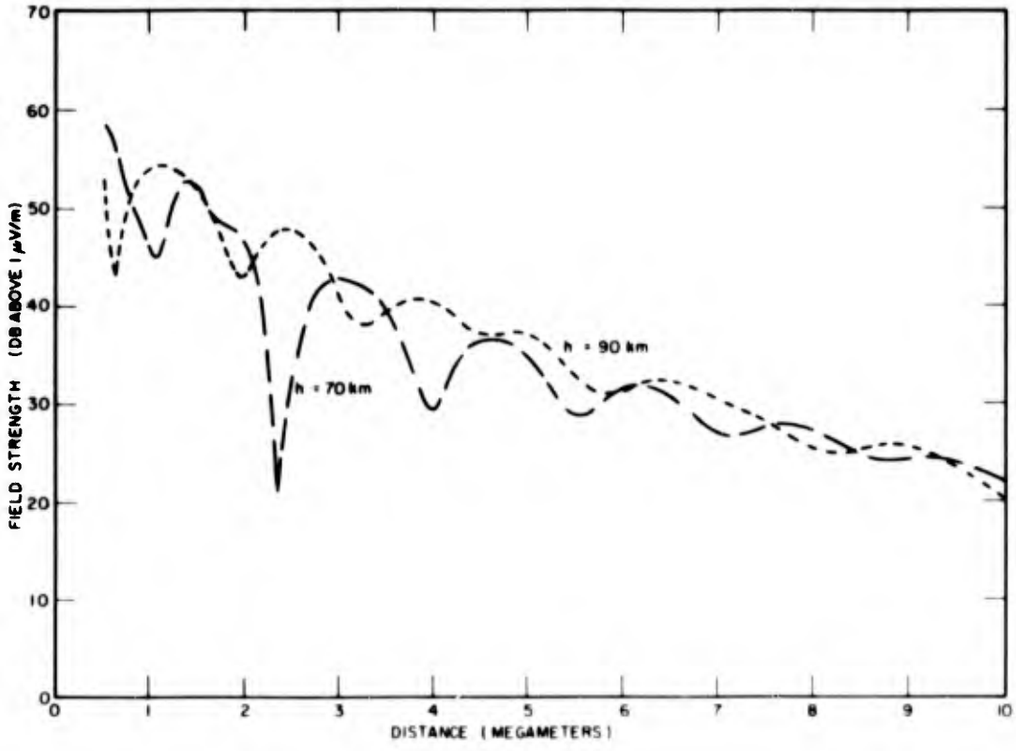

Fig. 29 - Theoretical results from Wait and Spies (1) for 24.0 kc/s considering waveguide modes 1, 2, and 3 for the isotropic case; β = 0.5 km^{-1}, $\sigma_g = \infty$, P_r = 1 kw

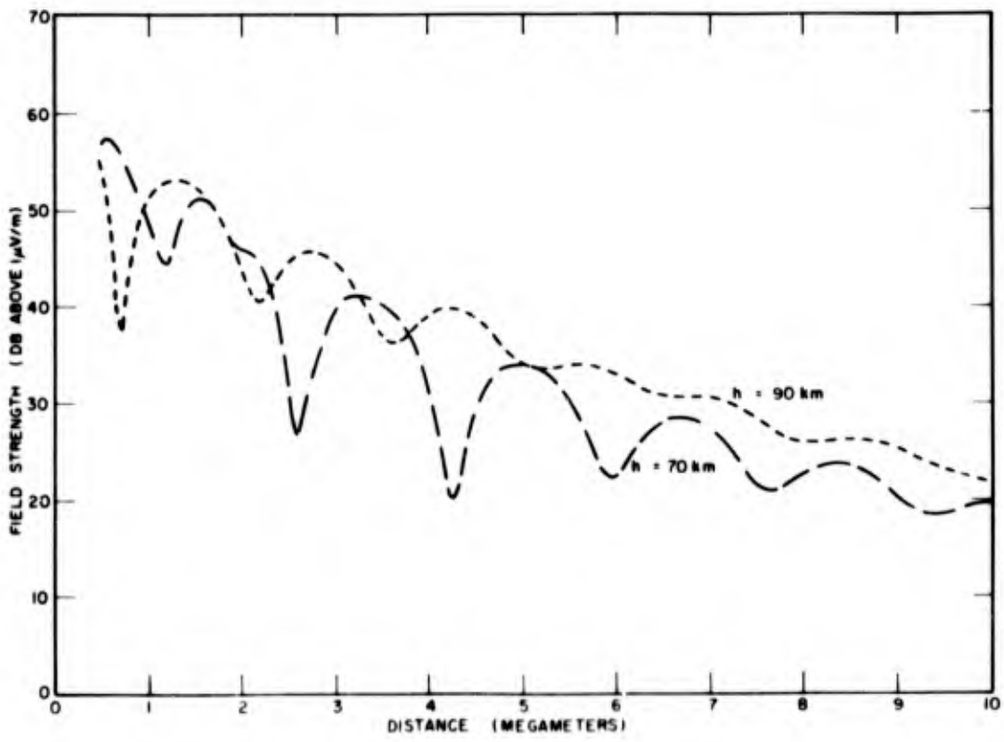

Fig. 30 - Theoretical results from Wait and Spies (1) for 26.1 kc/s considering waveguide modes 1, 2, and 3 for the isotropic case; $\beta = 0.5$ km^{-1}, $\sigma_g = \infty$, $P_r = 1$ kw

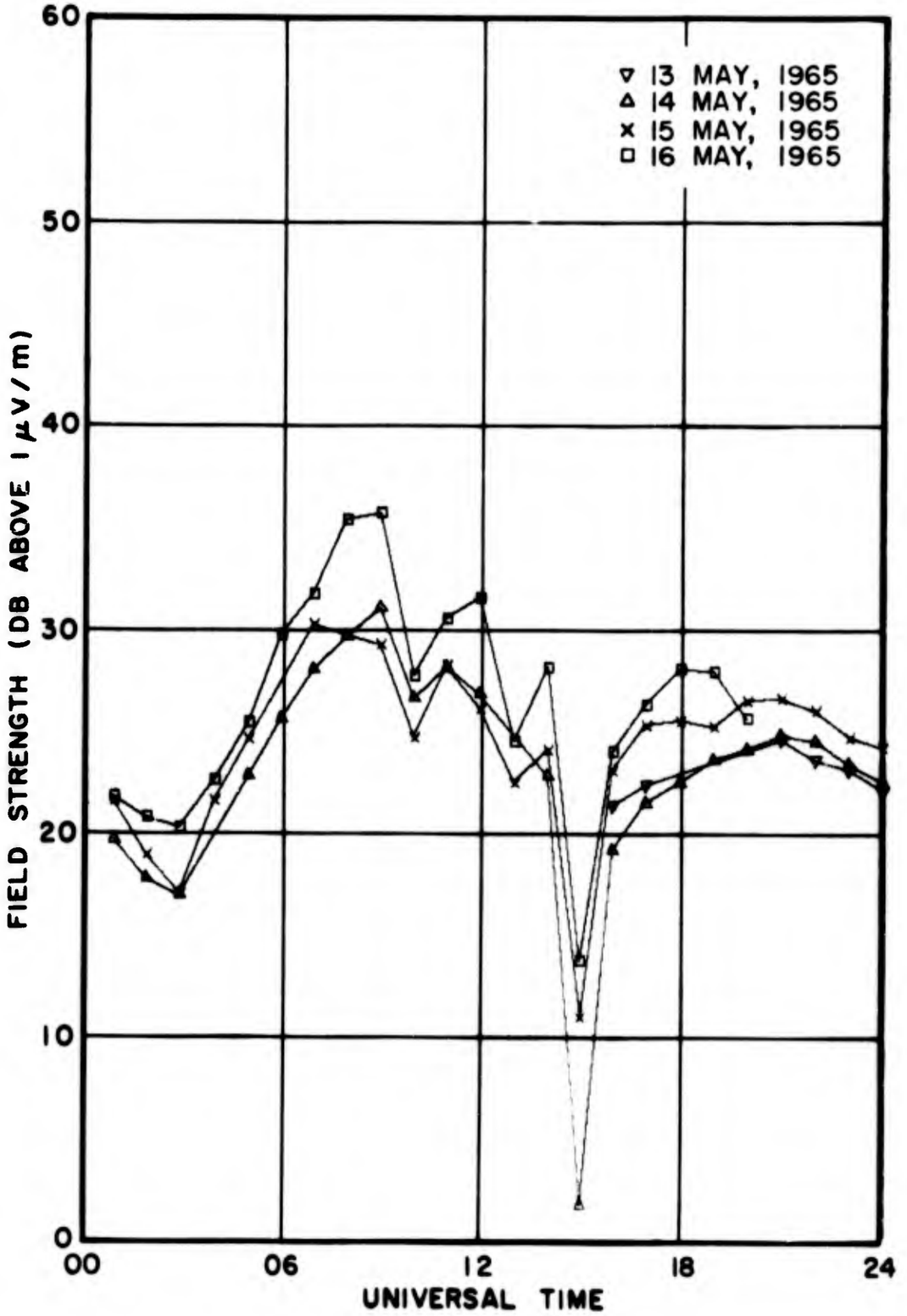

Fig. 31 - NPM (22.3 kc/s) data recorded May 13, 14, 15, 16, near Washington, D.C.

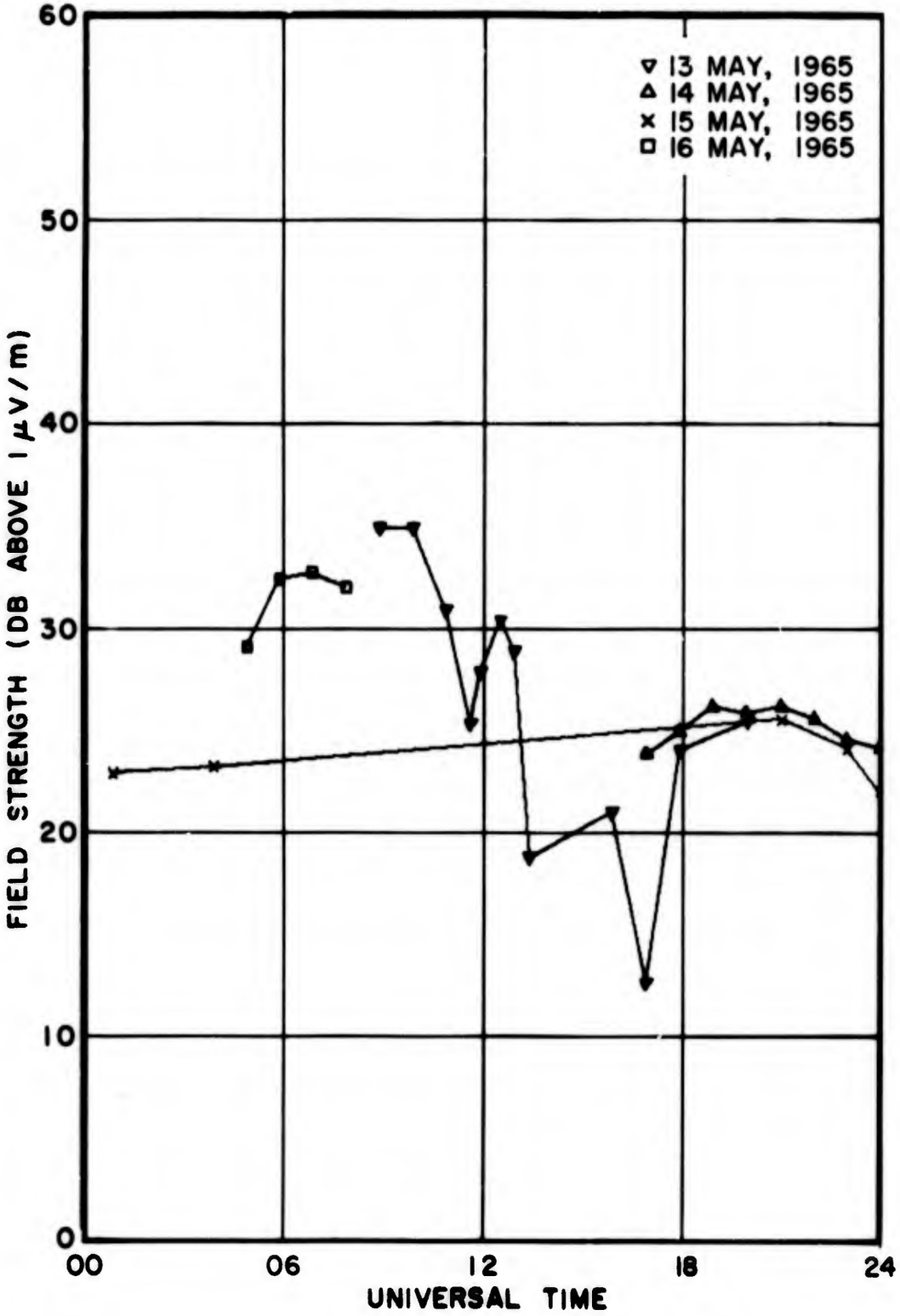

Fig. 32 - Haiku (19.8 kc/s) data recorded May 13, 14, 15, 16, near Washington, D.C.

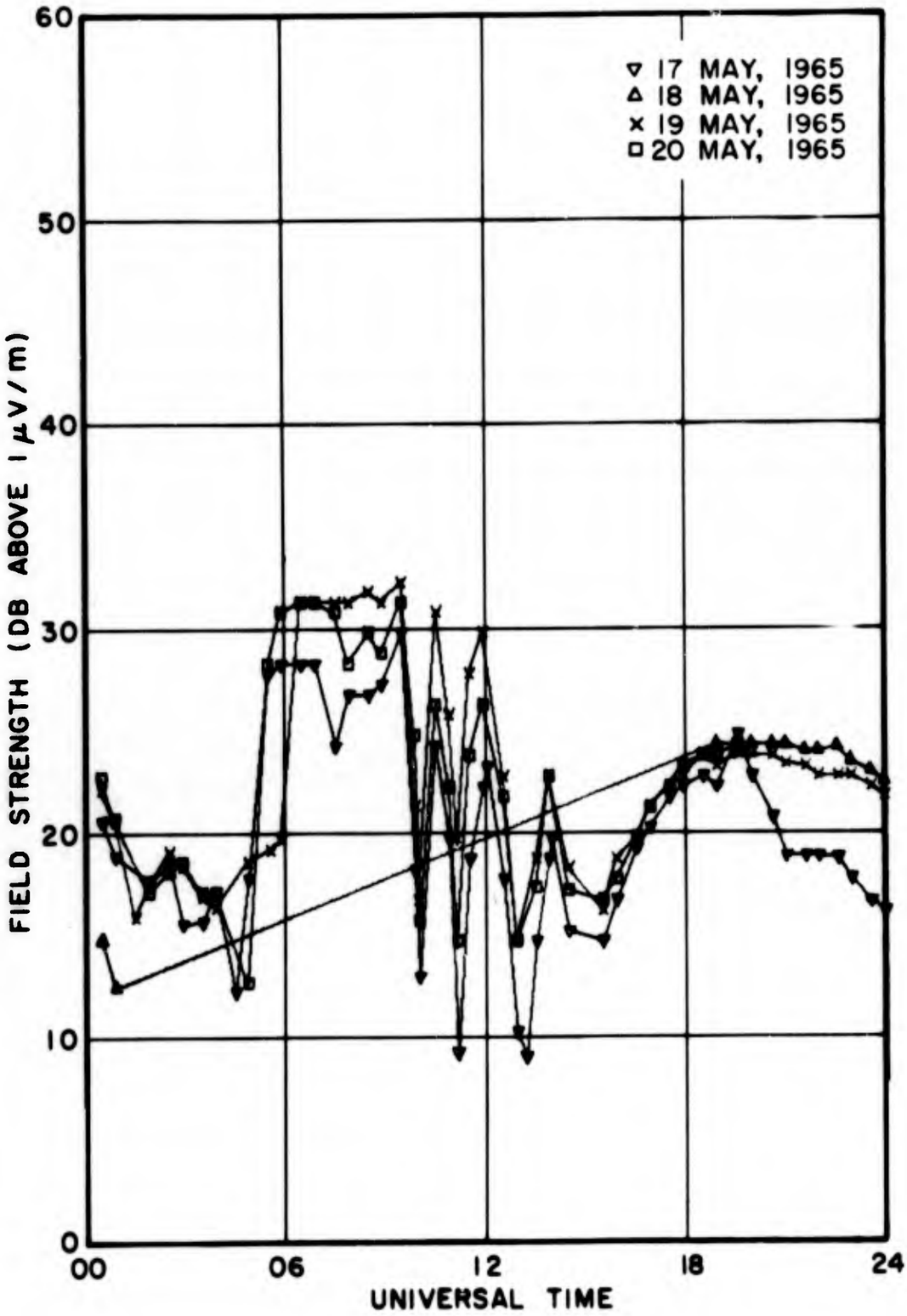

Fig. 33 - NPM (24.0 kc/s) data recorded May 17, 18, 19, 20, near Washington, D.C.

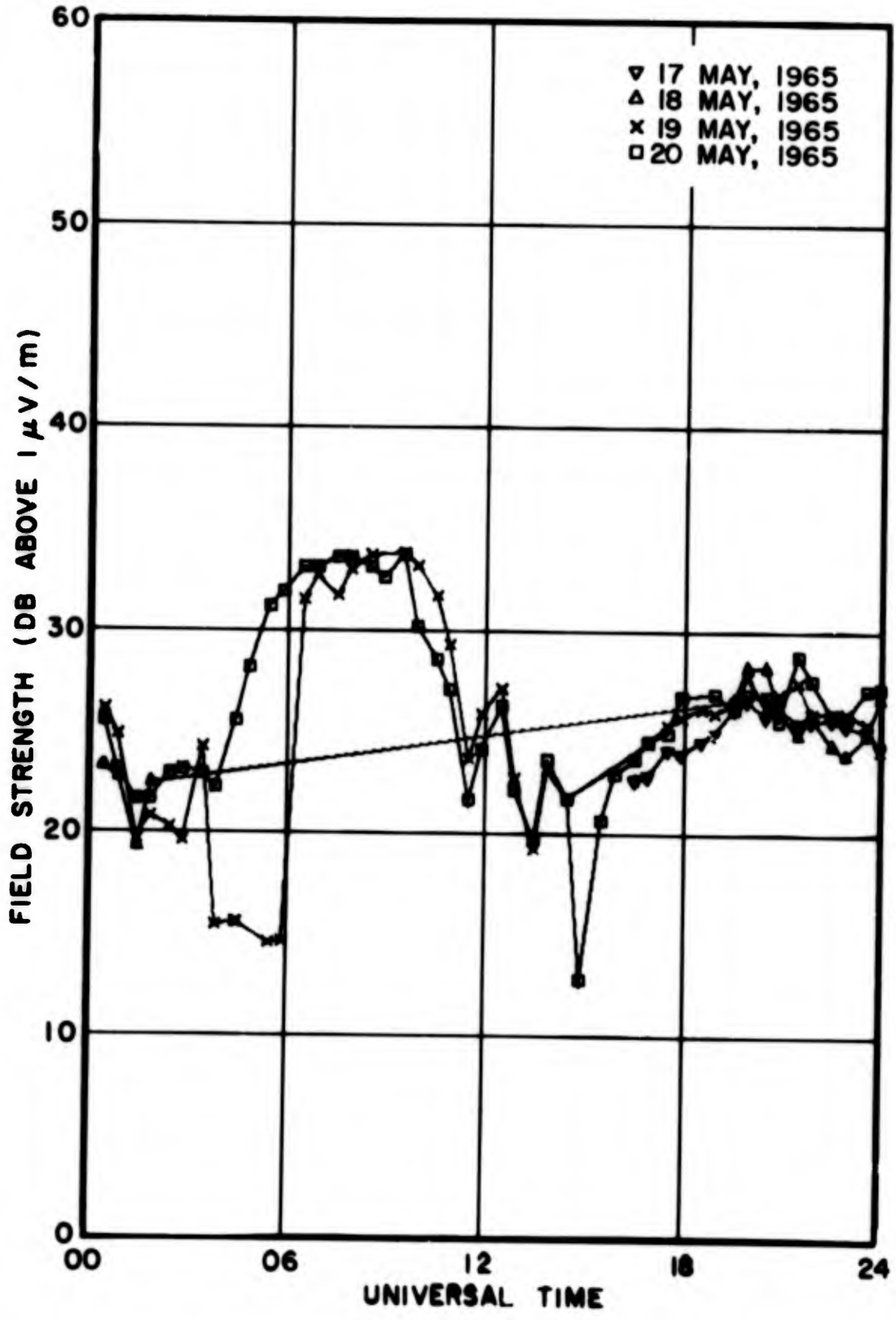

Fig. 34 - Haiku (19.8 kc/s) data recorded May 17, 18, 19, 20, near Washington, D.C.

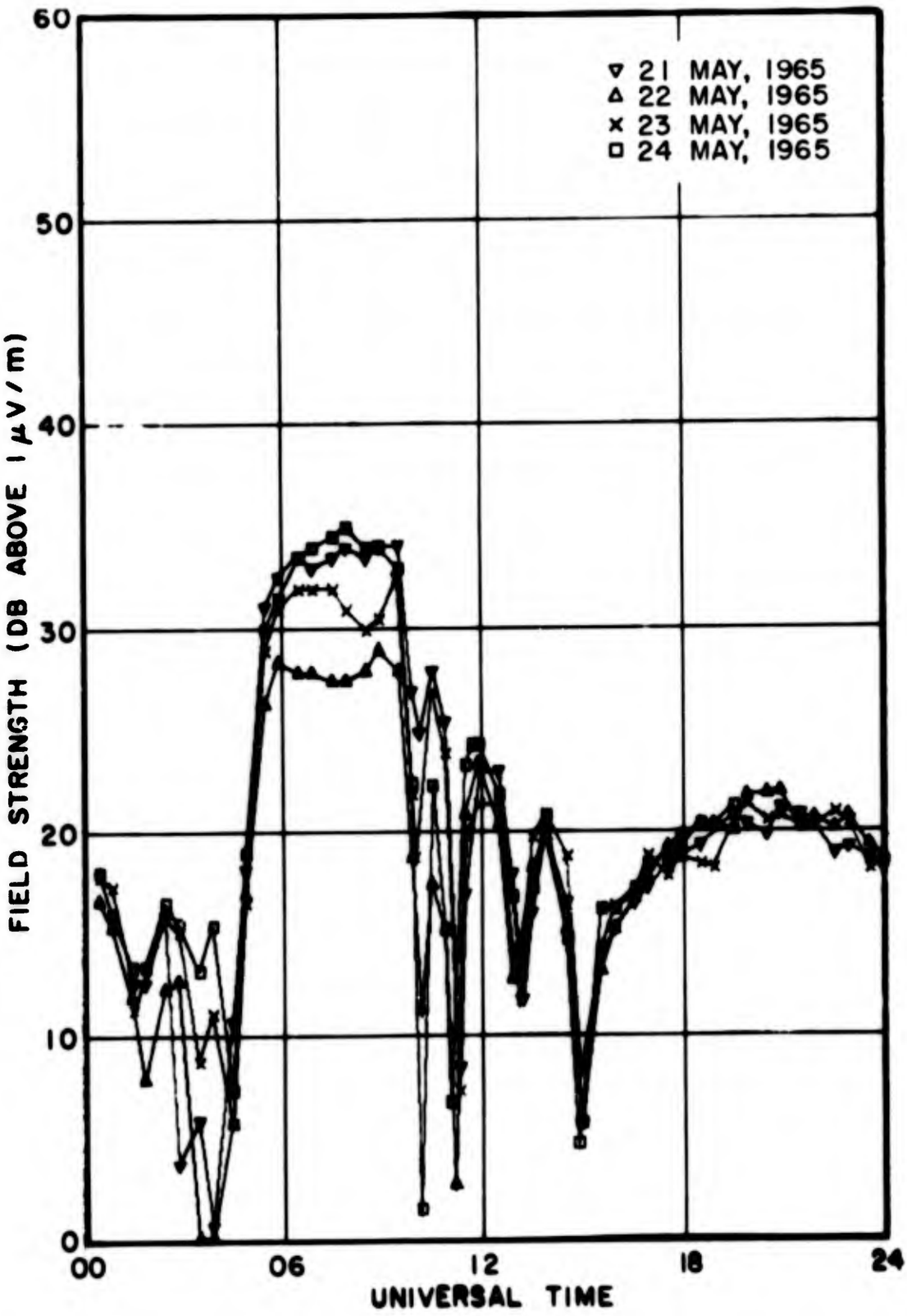

Fig. 35 - NPM (26.1 kc/s) data recorded May 21, 22, 23, 24, near Washington, D.C.

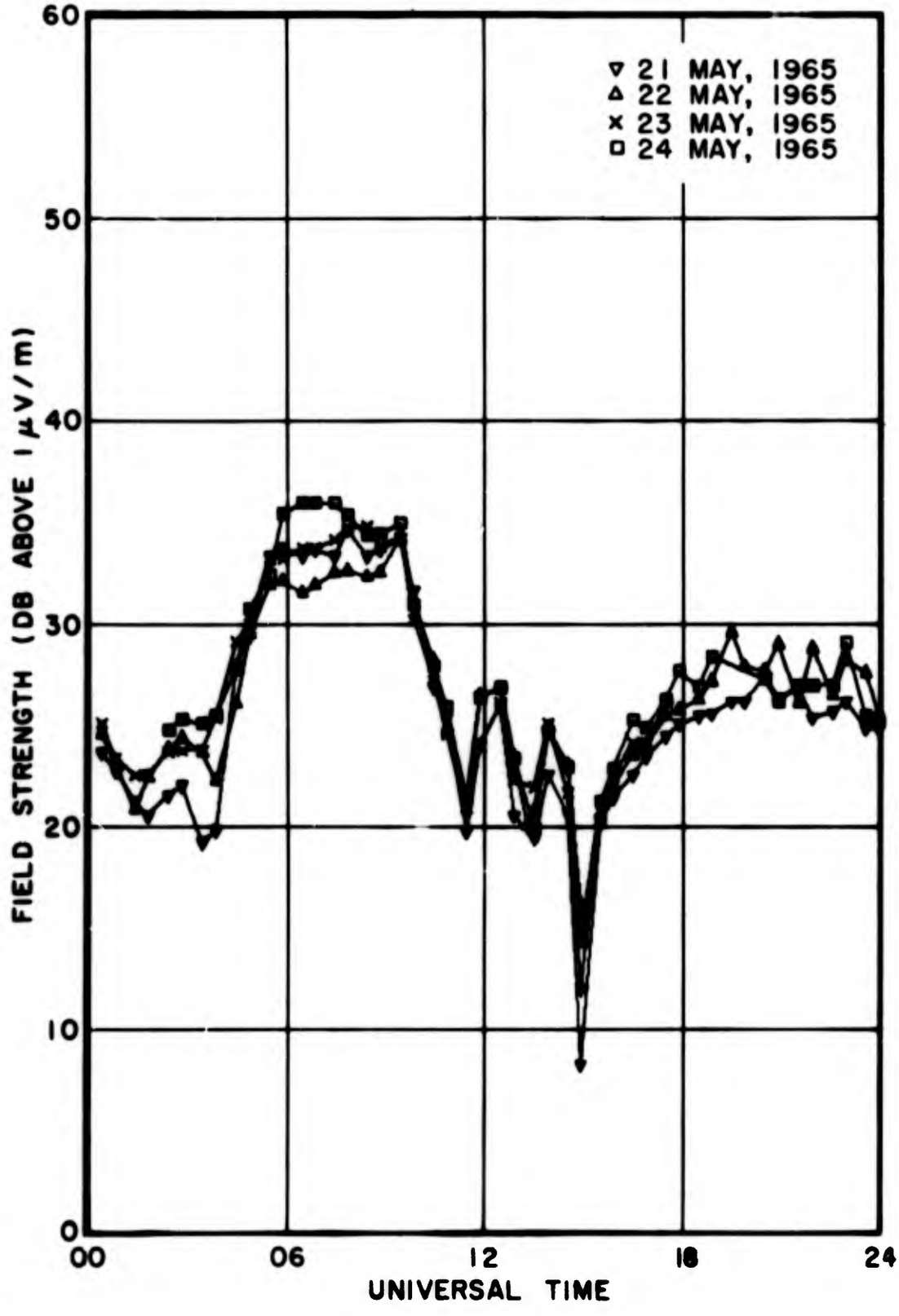

Fig. 36 - Haiku (19.8 kc/s) data recorded May 21, 22, 23, 24, near Washington, D.C.

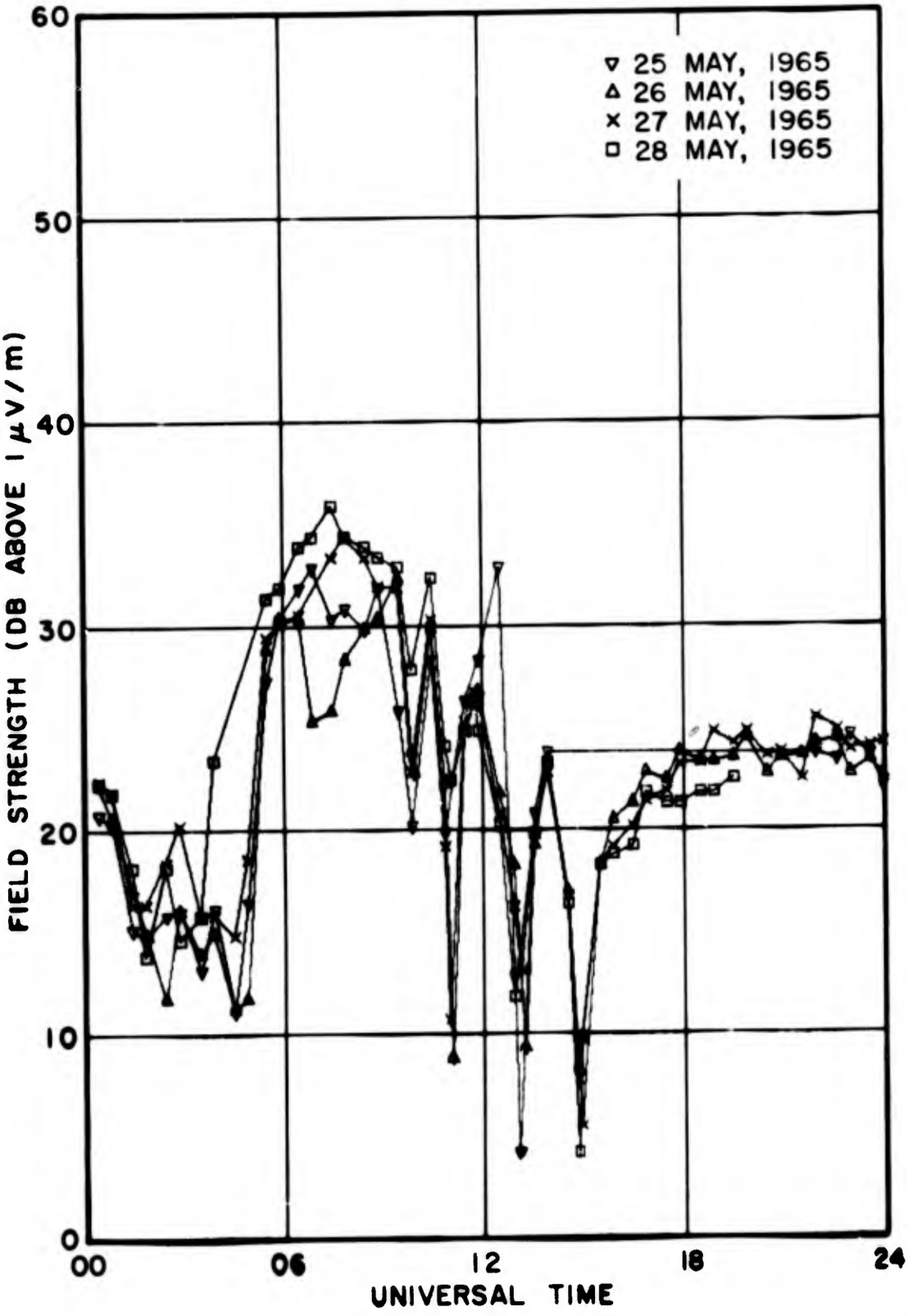

Fig. 37 - NPM (24.0 kc/s) data recorded May 25, 26, 27, 28, near Washington, D.C.

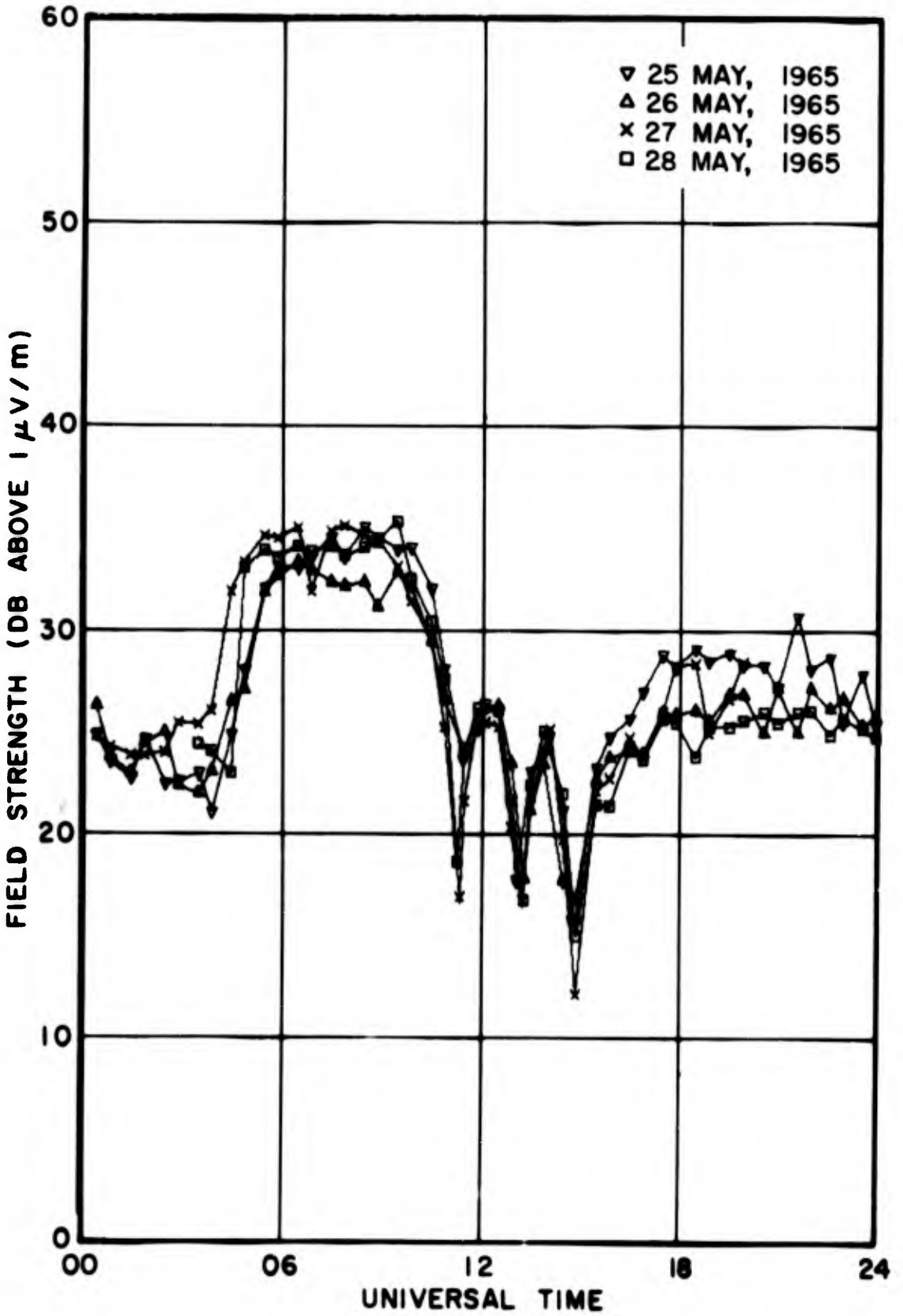

Fig. 38 - Haiku (19.8 kc/s) data recorded May 25, 26, 27, 28, near Washington, D.C.

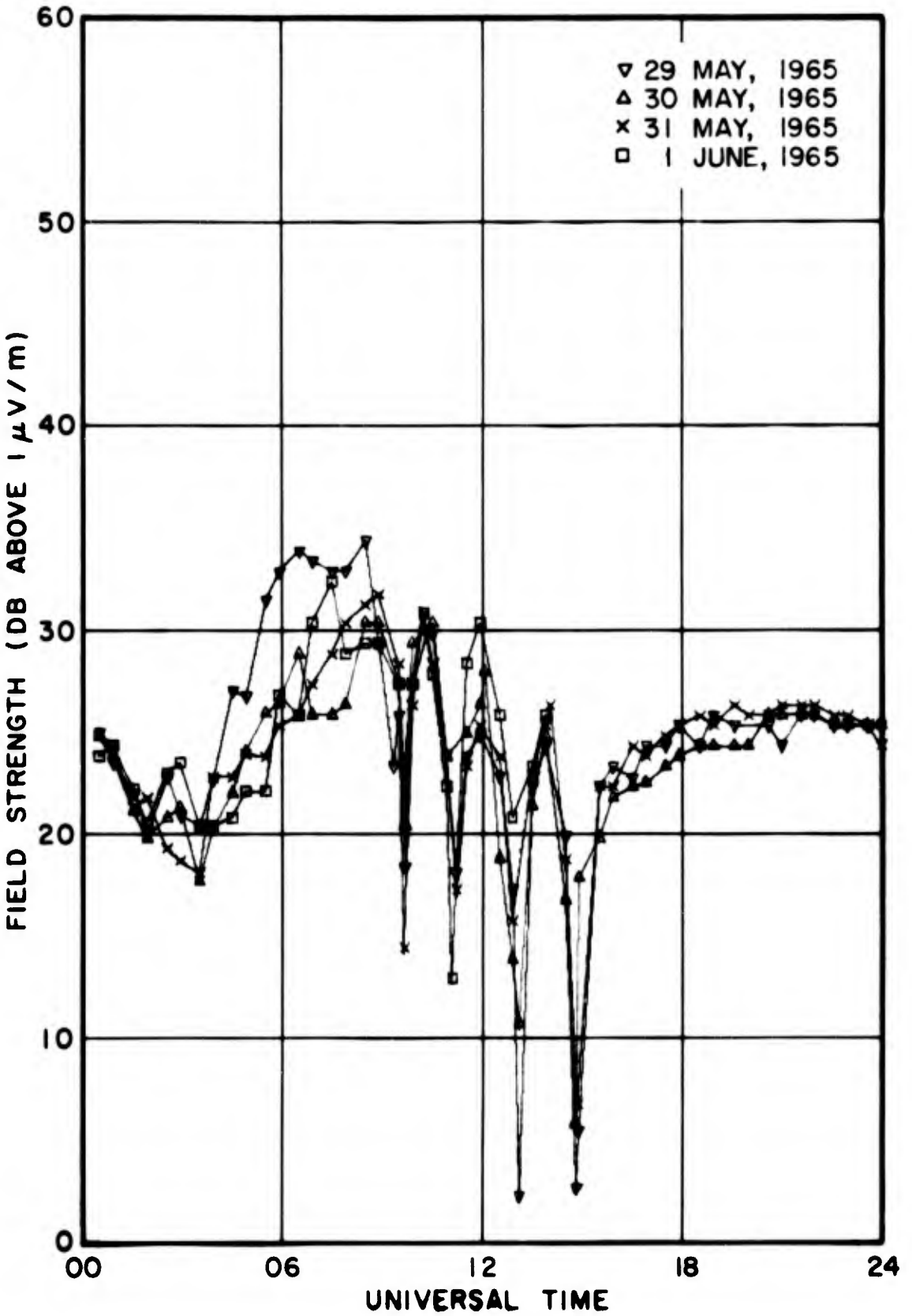

Fig. 39 - NPM (22.3 kc/s) data recorded May 29, 30, 31, June 1, near Washington, D.C.

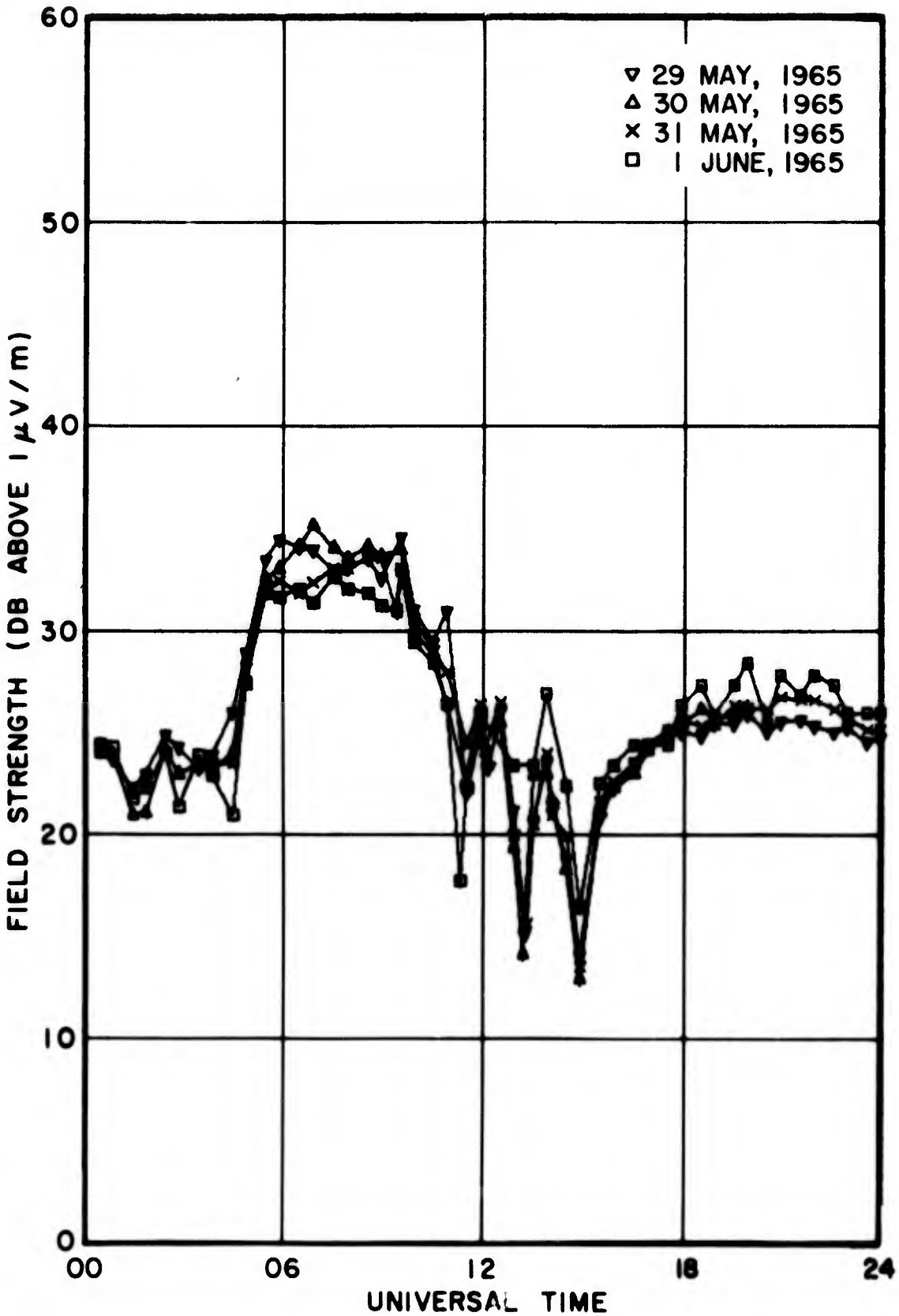

Fig. 40 - Haiku (19.8 kc/s) data recorded May 29, 30, 31, June 1, near Washington, D.C.

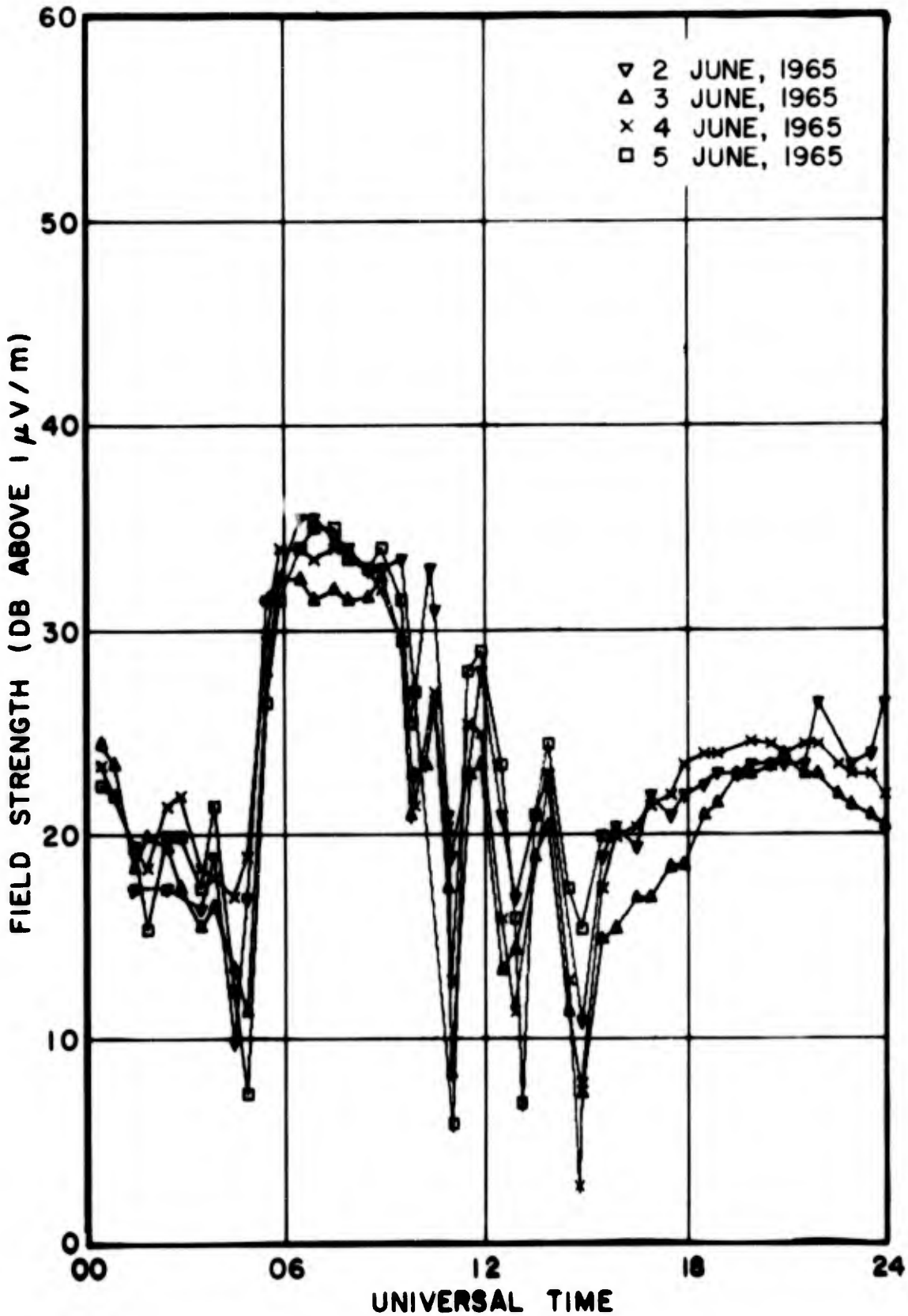

Fig. 41 - NPM (24.0 kc/s) data recorded June 2, 3, 4, 5, near Washington, D.C.

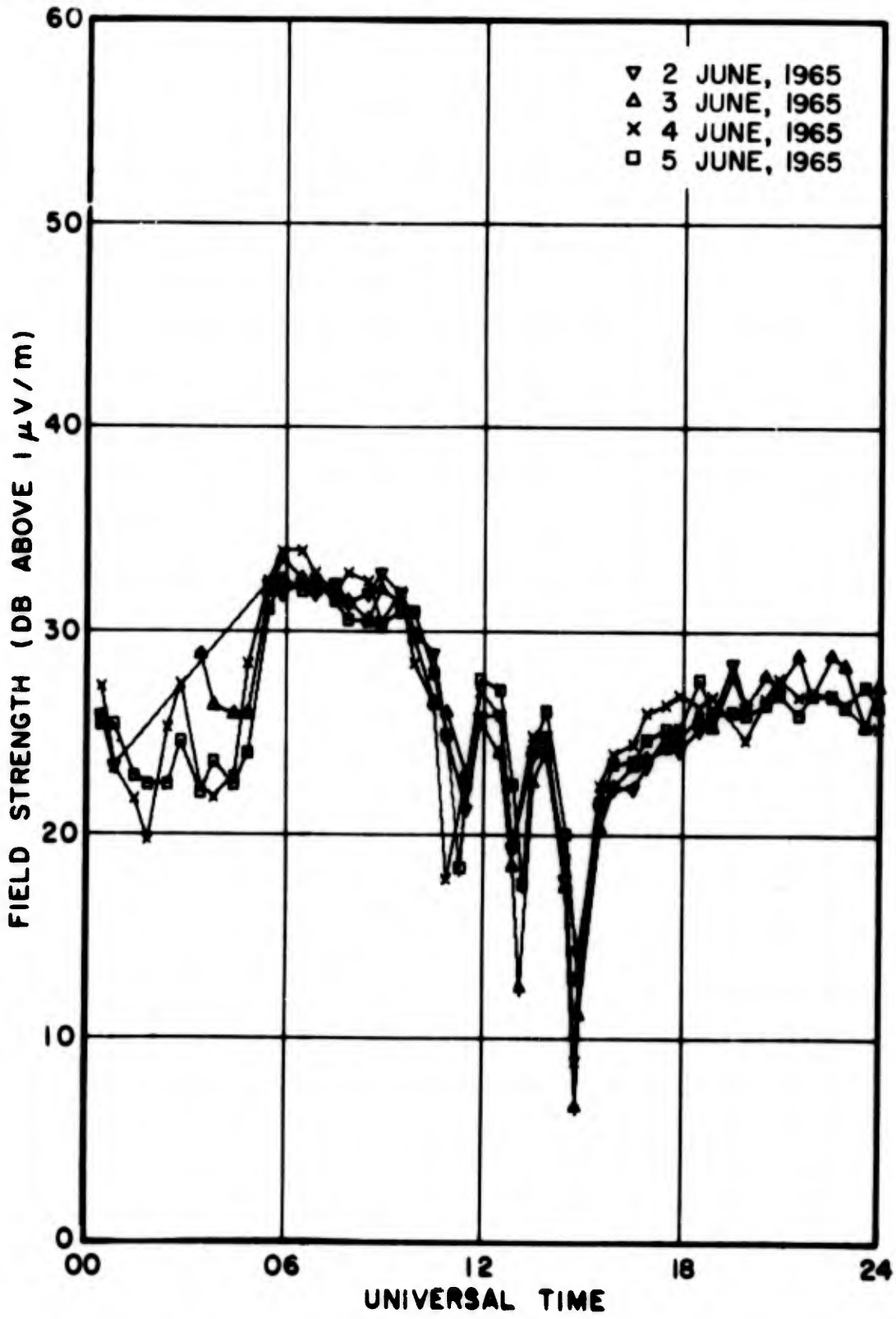

Fig. 42 - Haiku (19.8 kc/s) data recorded June 2, 3, 4, 5, near Washington, D.C.

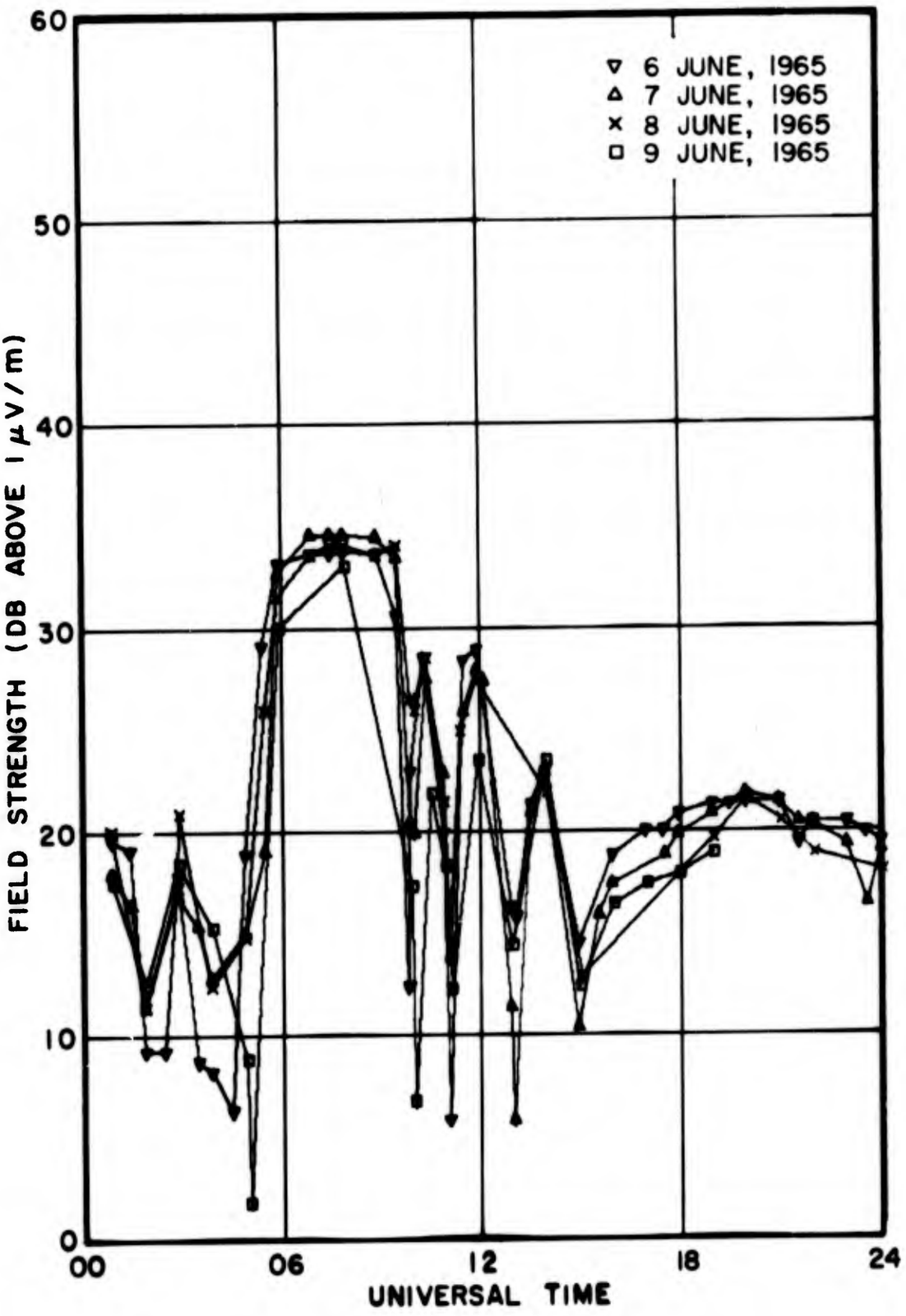

Fig. 43 - NPM (26.1 kc/s) data recorded June 6, 7, 8, 9, near Washington, D.C.

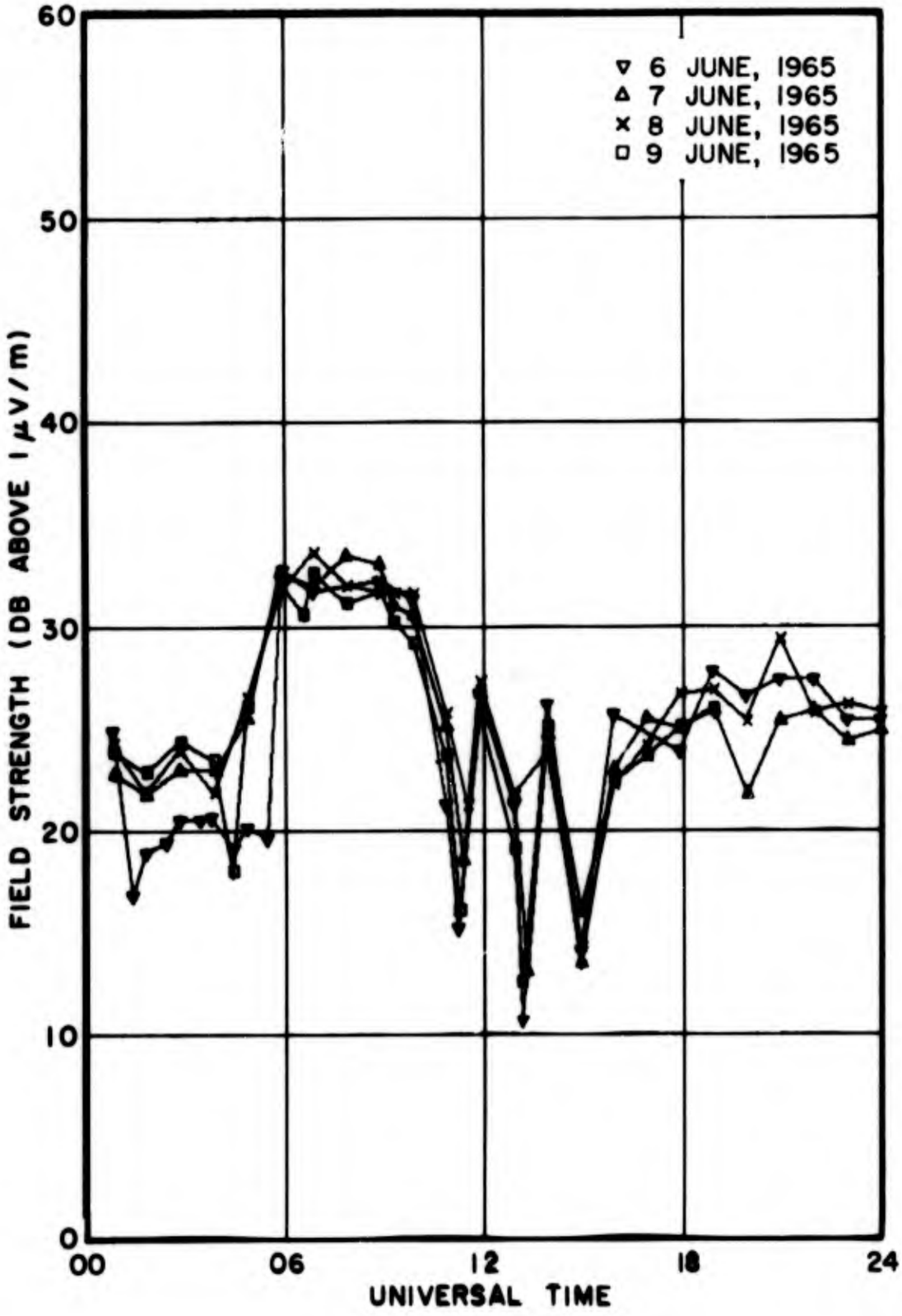

Fig. 44 - Haiku (19.8 kc/s) data recorded June 6, 7, 8, 9, near Washington, D.C.

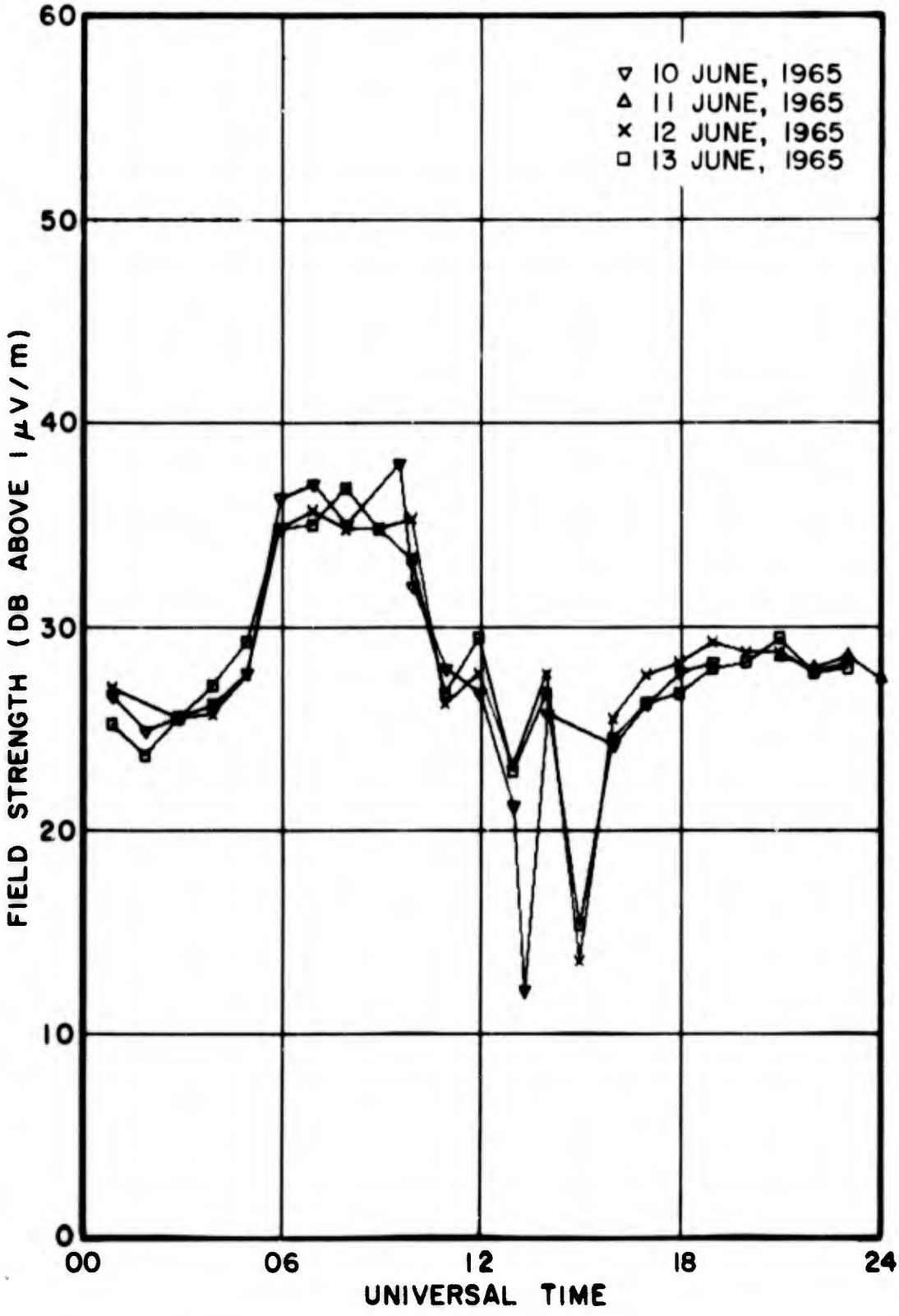

Fig. 45 - NPM (19.8 kc/s) data recorded June 10, 11, 12, 13, near Washington, D.C.

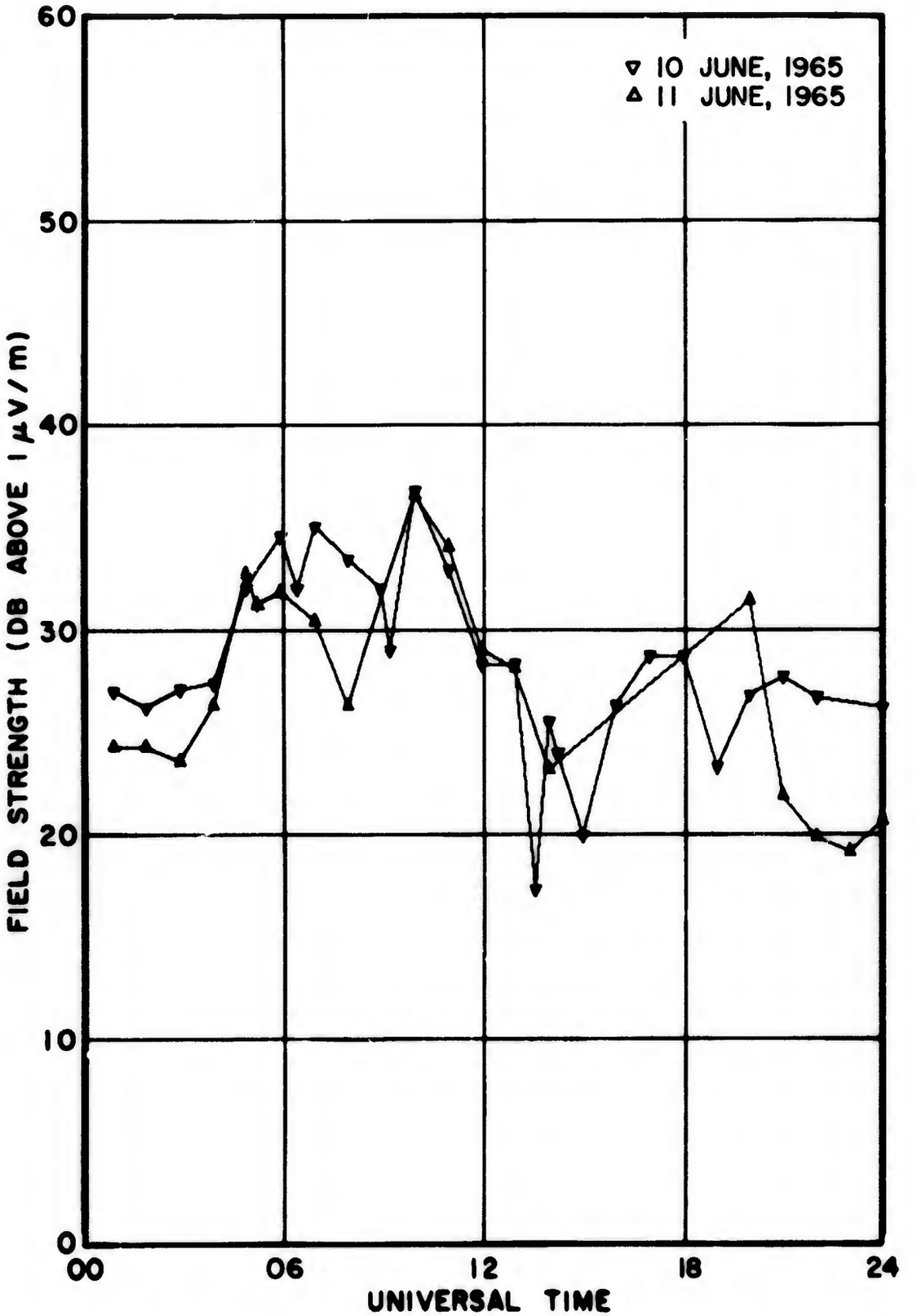

Fig. 46 - Haiku (16.6 kc/s) data recorded June 10, 11, near Washington, D.C.

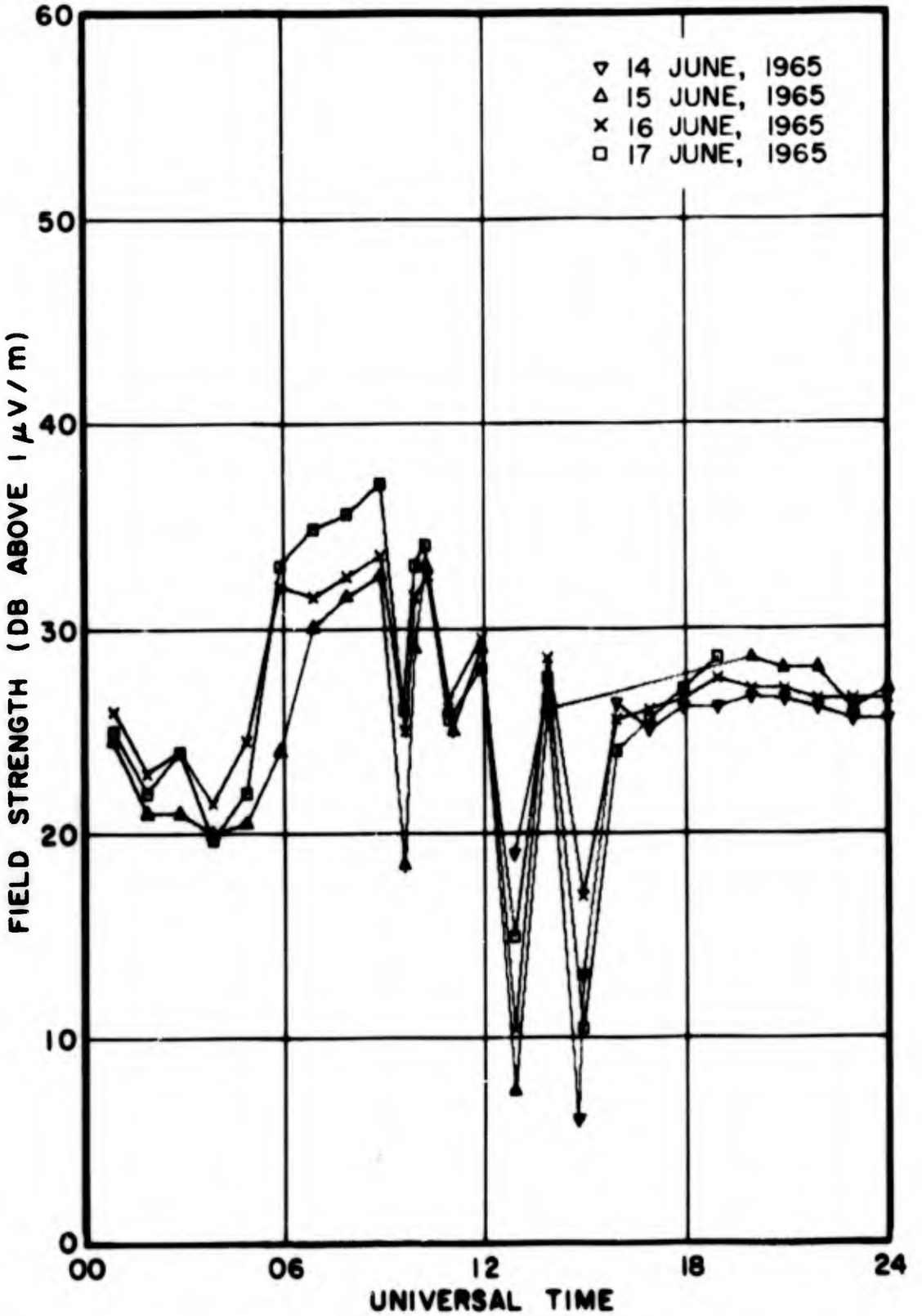

Fig. 47 - NPM (22.3 kc/s) data recorded June 14, 15, 16, 17, near Washington, D.C.

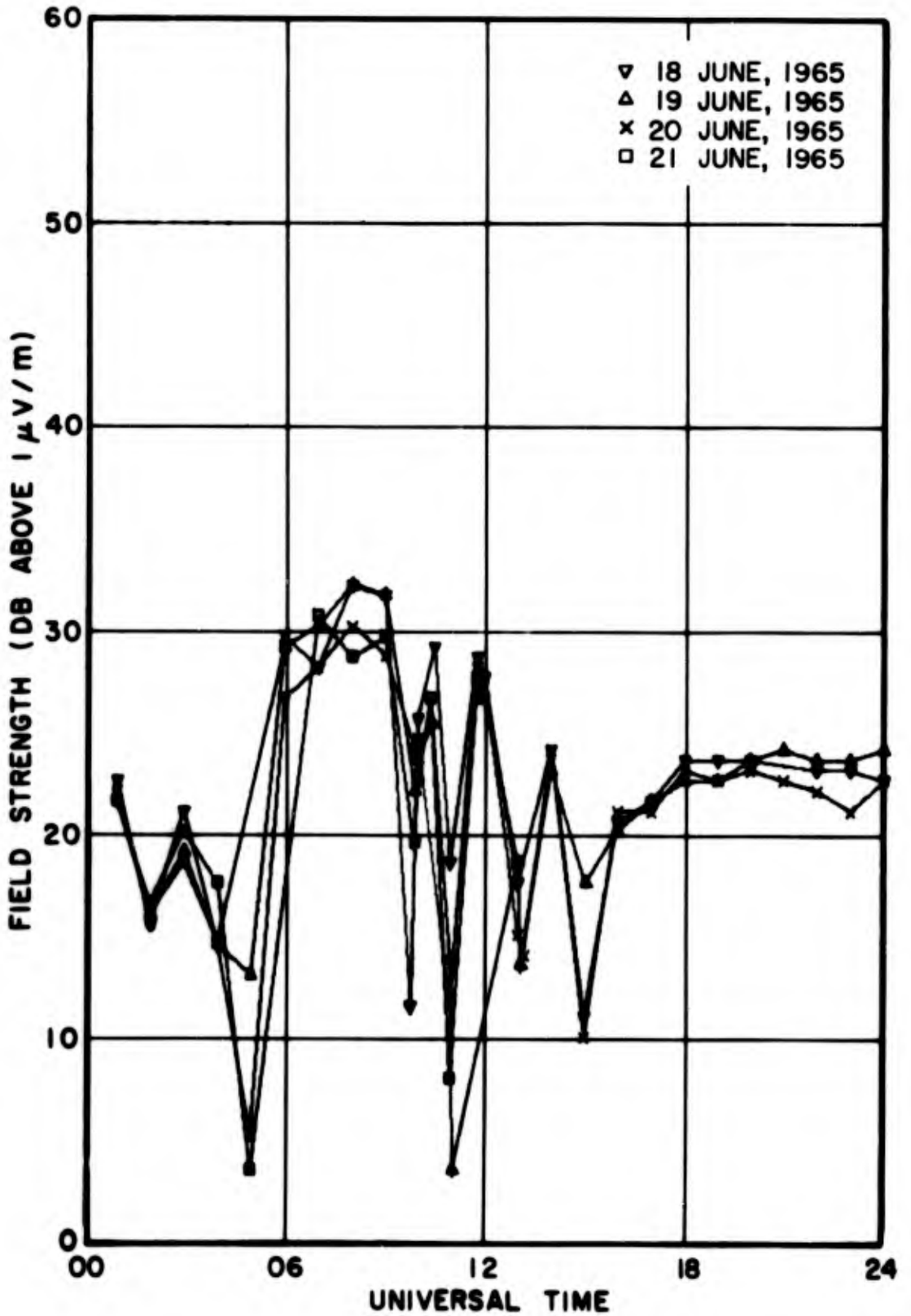

Fig. 48 - NPM (24.0 kc/s) data recorded June 18, 19, 20, 21, near Washington, D.C.

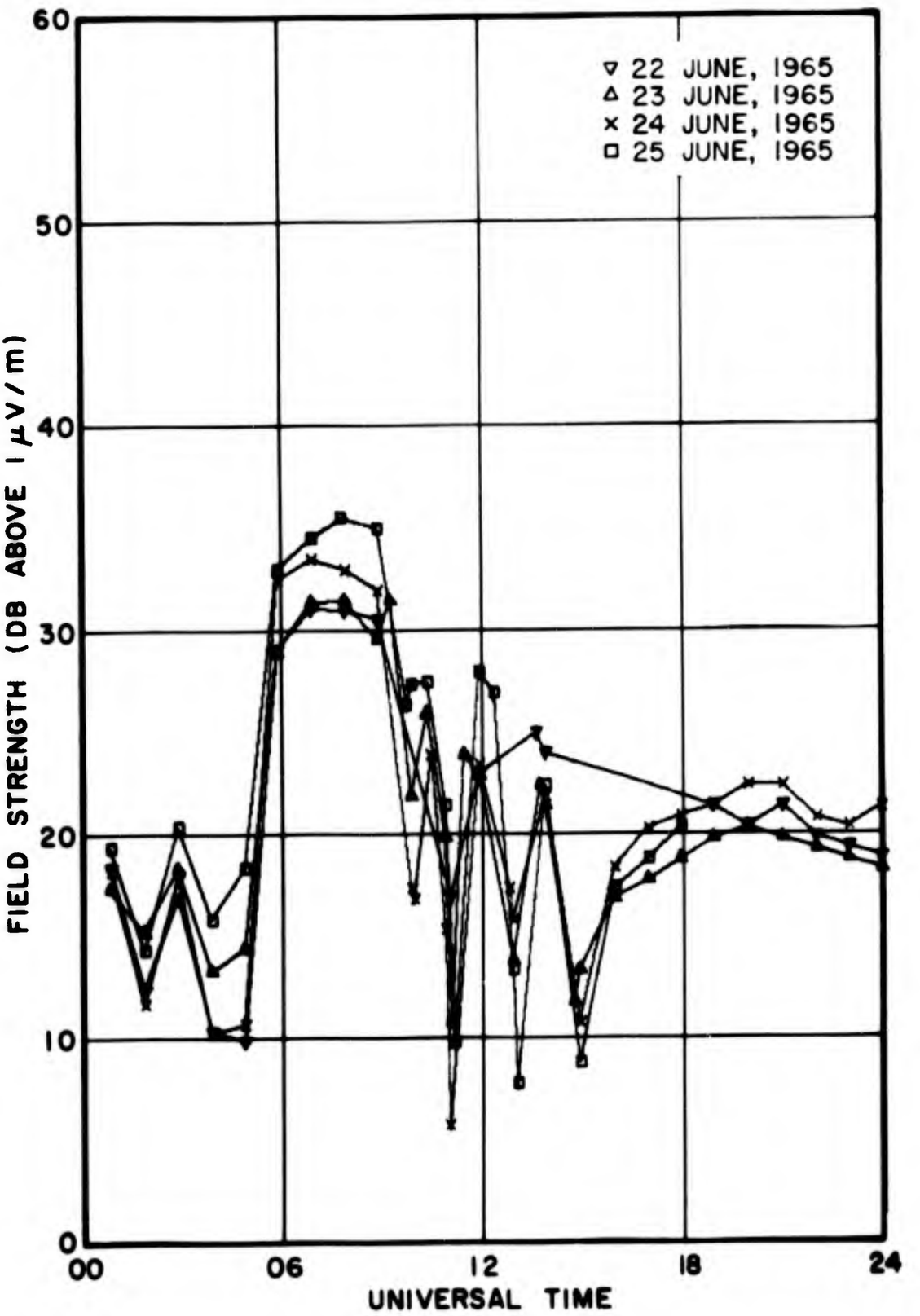

Fig. 49 - NPM (26.1 kc/s) data recorded June 22, 23, 24, 25, near Washington, D.C.

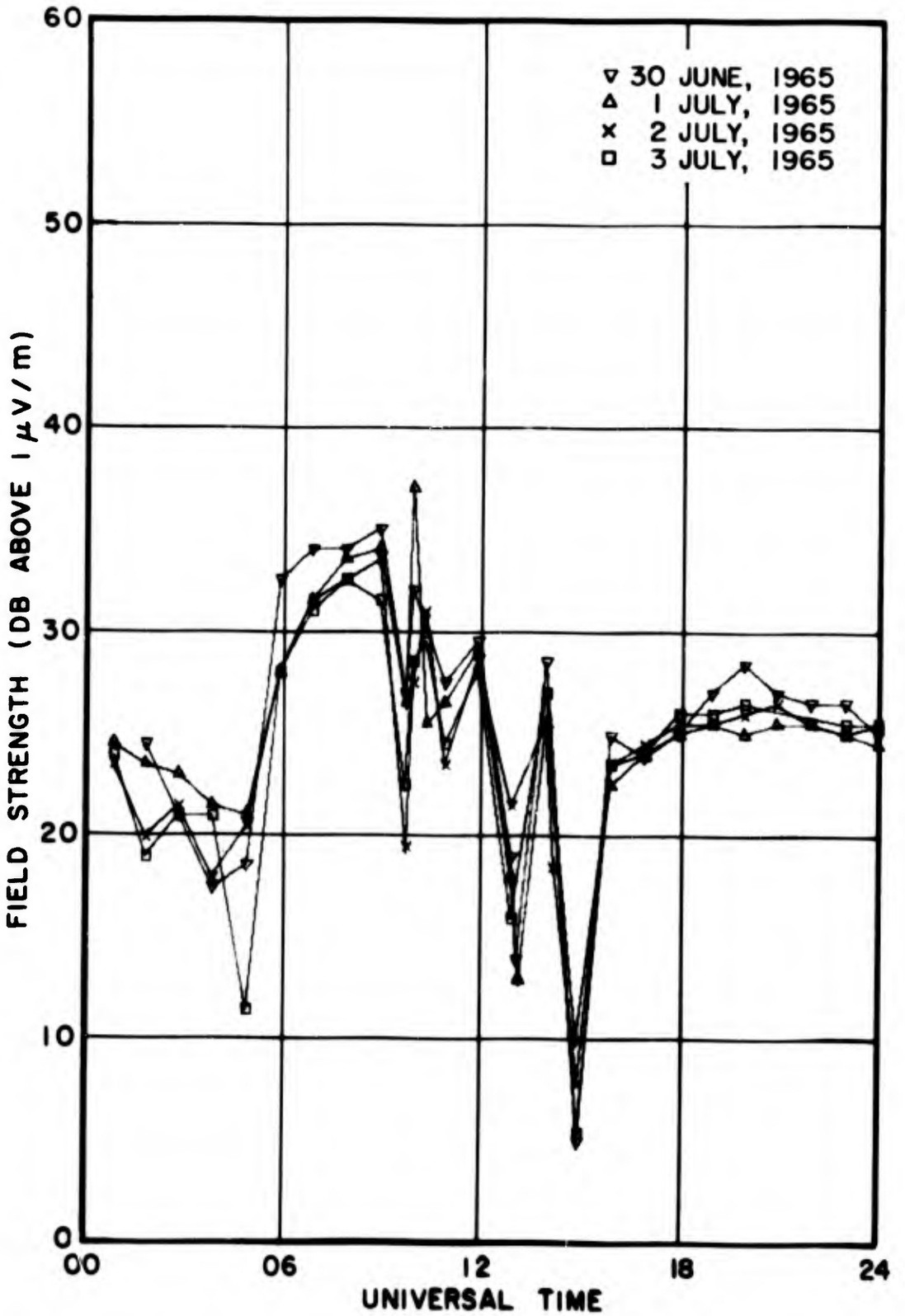

Fig. 50 - NPM (22.3 kc/s) data recorded June 30, July 1, 2, 3, near Washington, D.C.

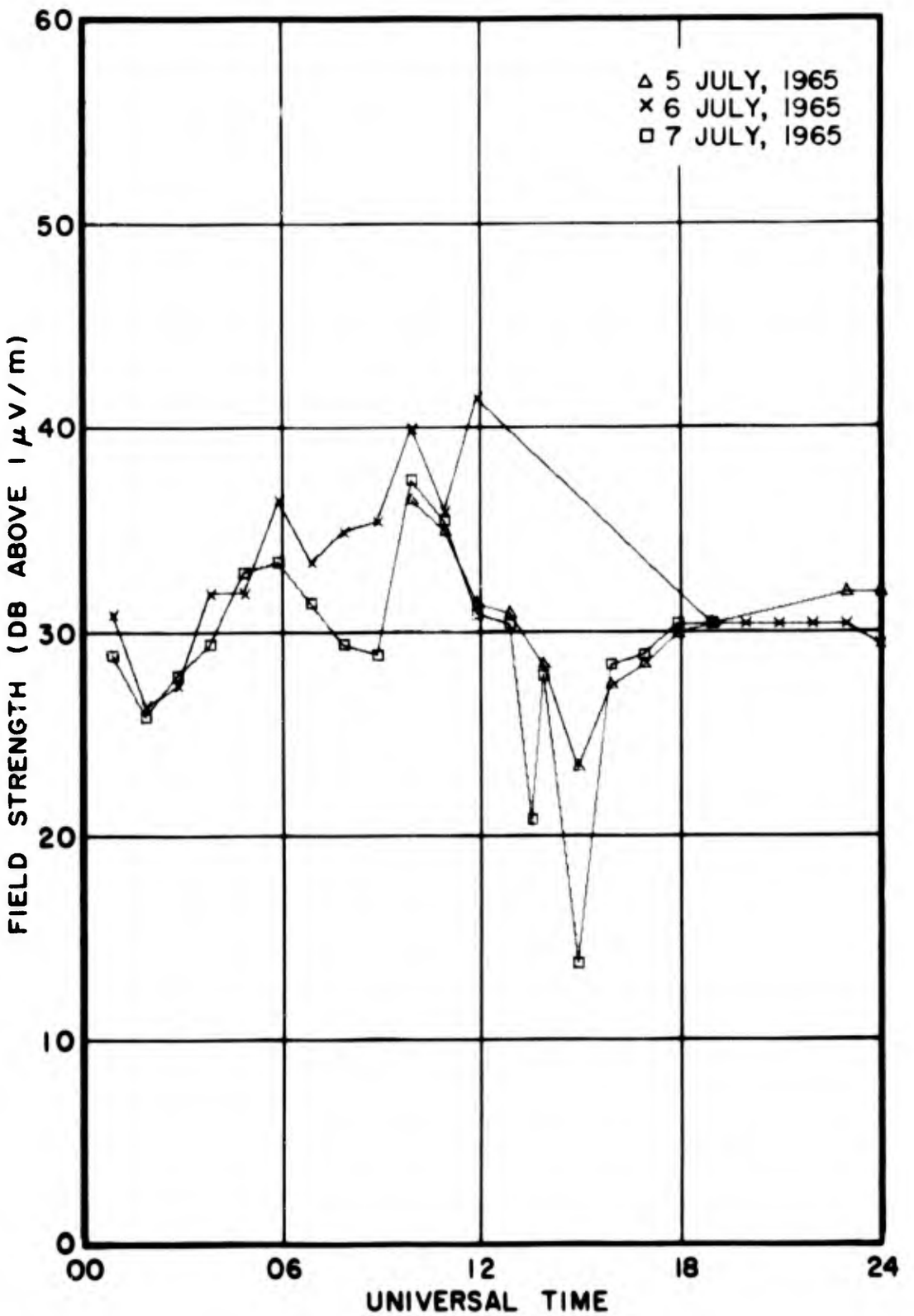

Fig. 51 - NPM (16.6 kc/s) data recorded July 5, 6, 7, near Washington, D.C.

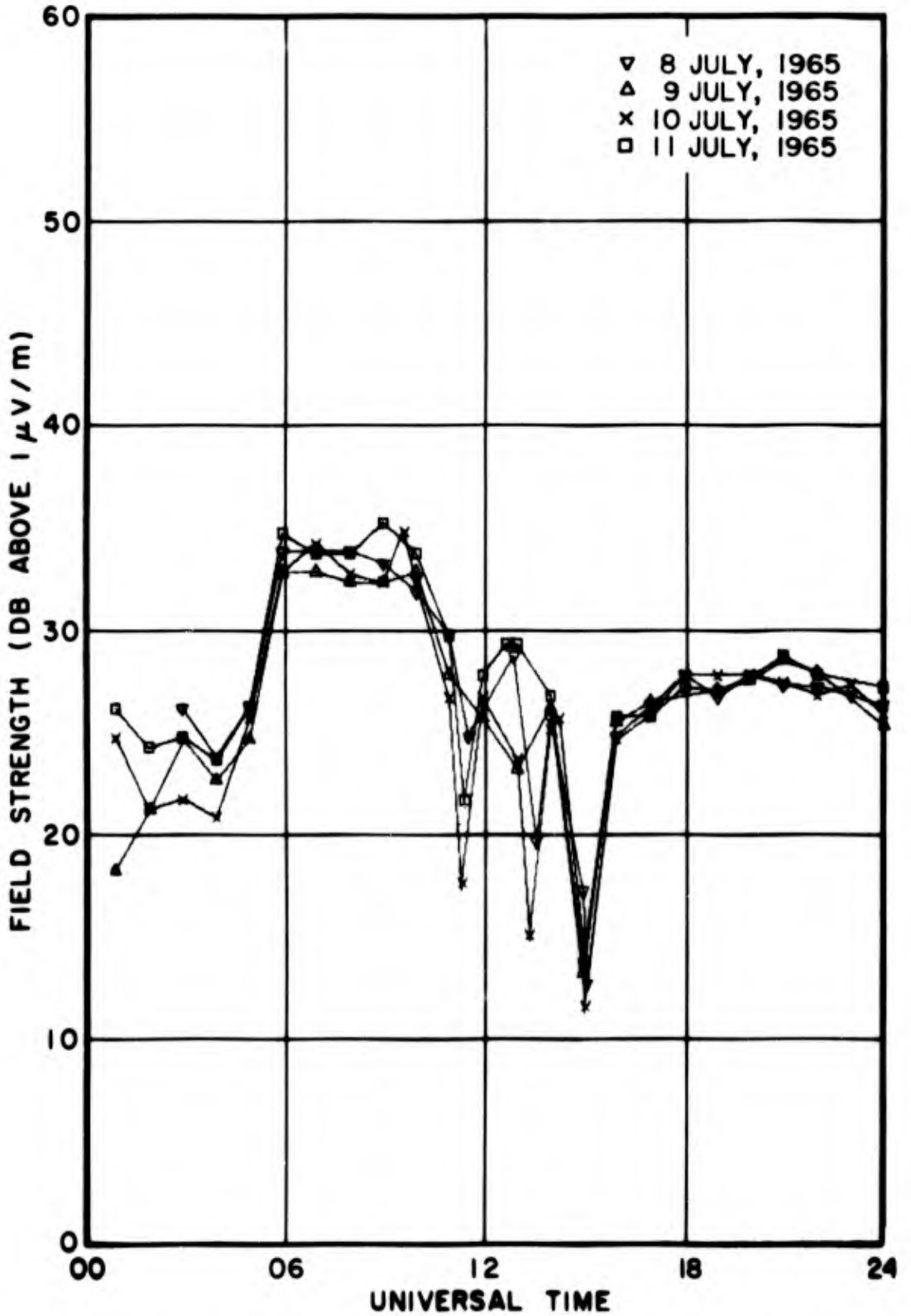

Fig. 52 - NPM (19.8 kc/s) data recorded July 8, 9, 10, 11, near Washington, D.C.

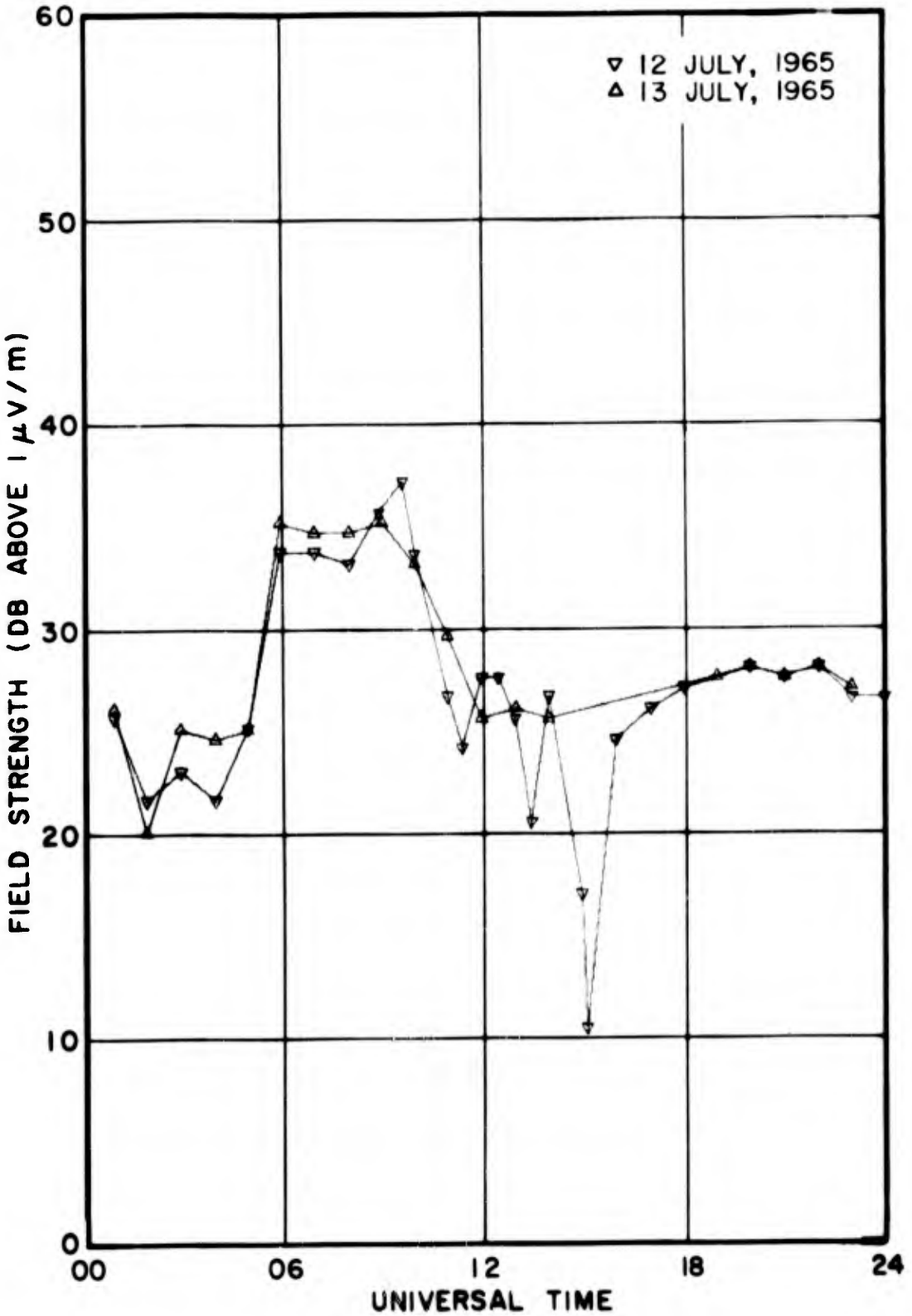

Fig. 53 - NPM (19.8 kc/s) data recorded July 12, 13, near Washington, D.C.

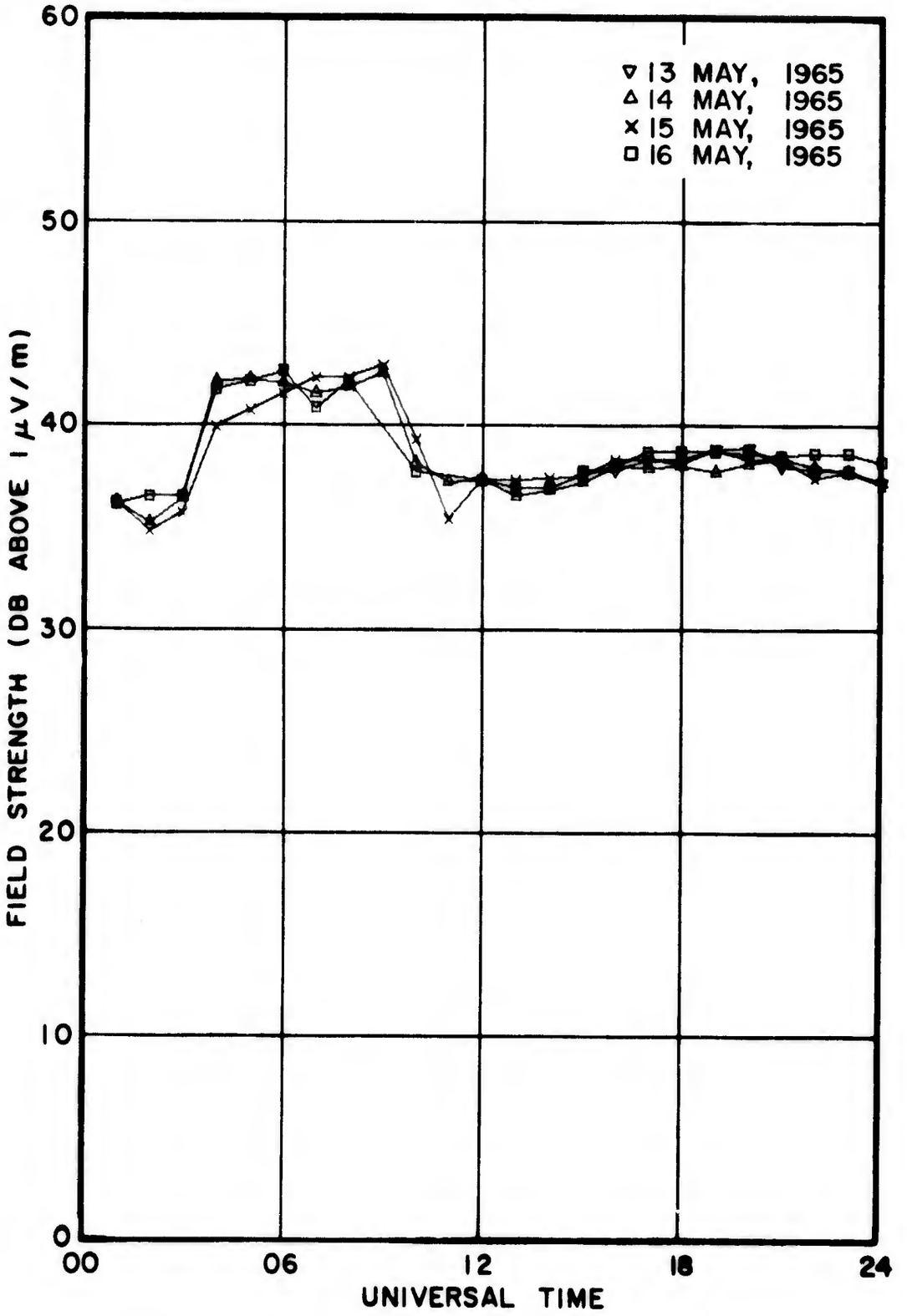

Fig. 54 - NPG (18.6 kc/s) data recorded May 13, 14, 15, 16, near Washington, D.C.

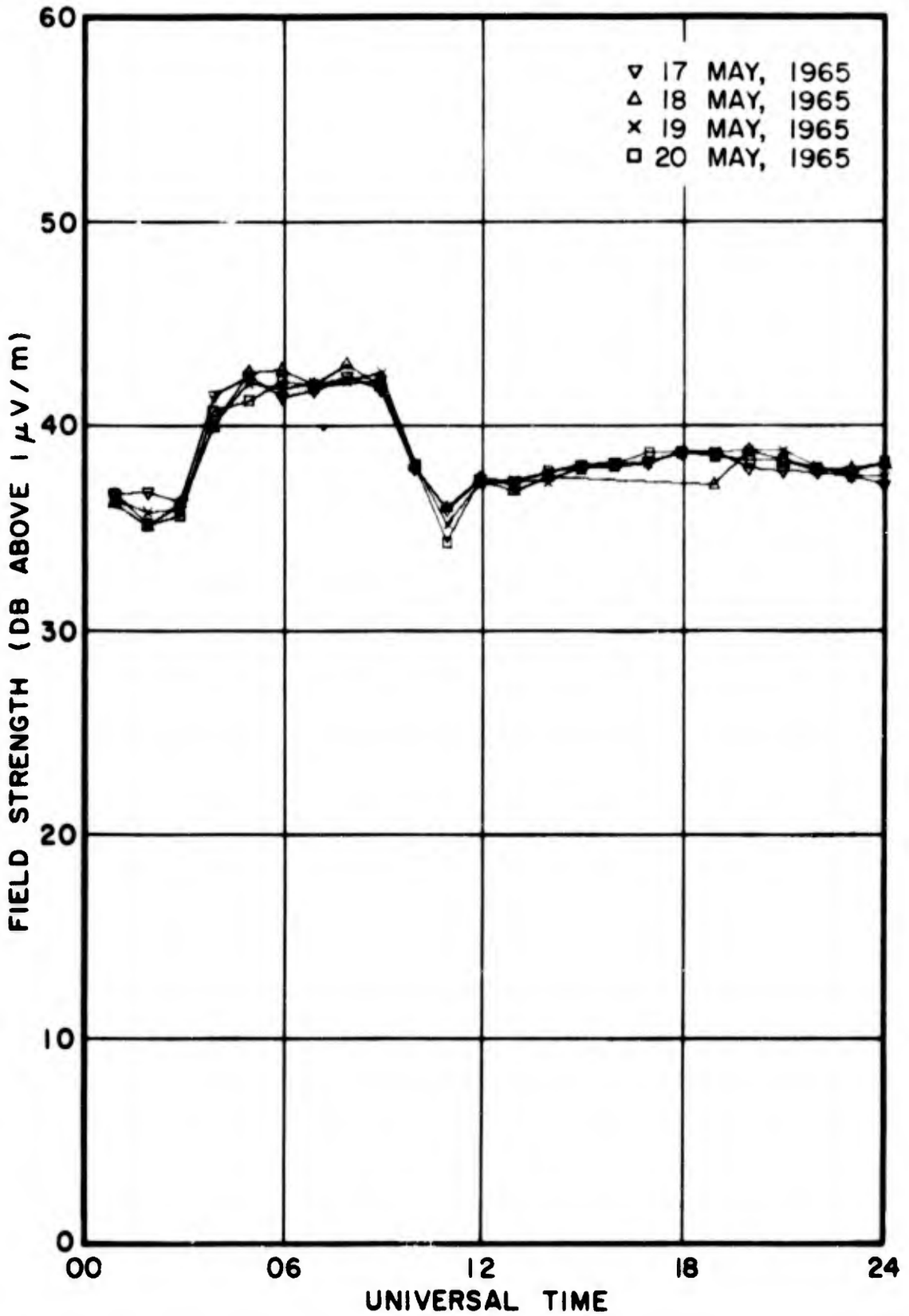

Fig. 55 - NPG (18.6 kc/s) data recorded May 17, 18, 19, 20, near Washington, D.C.

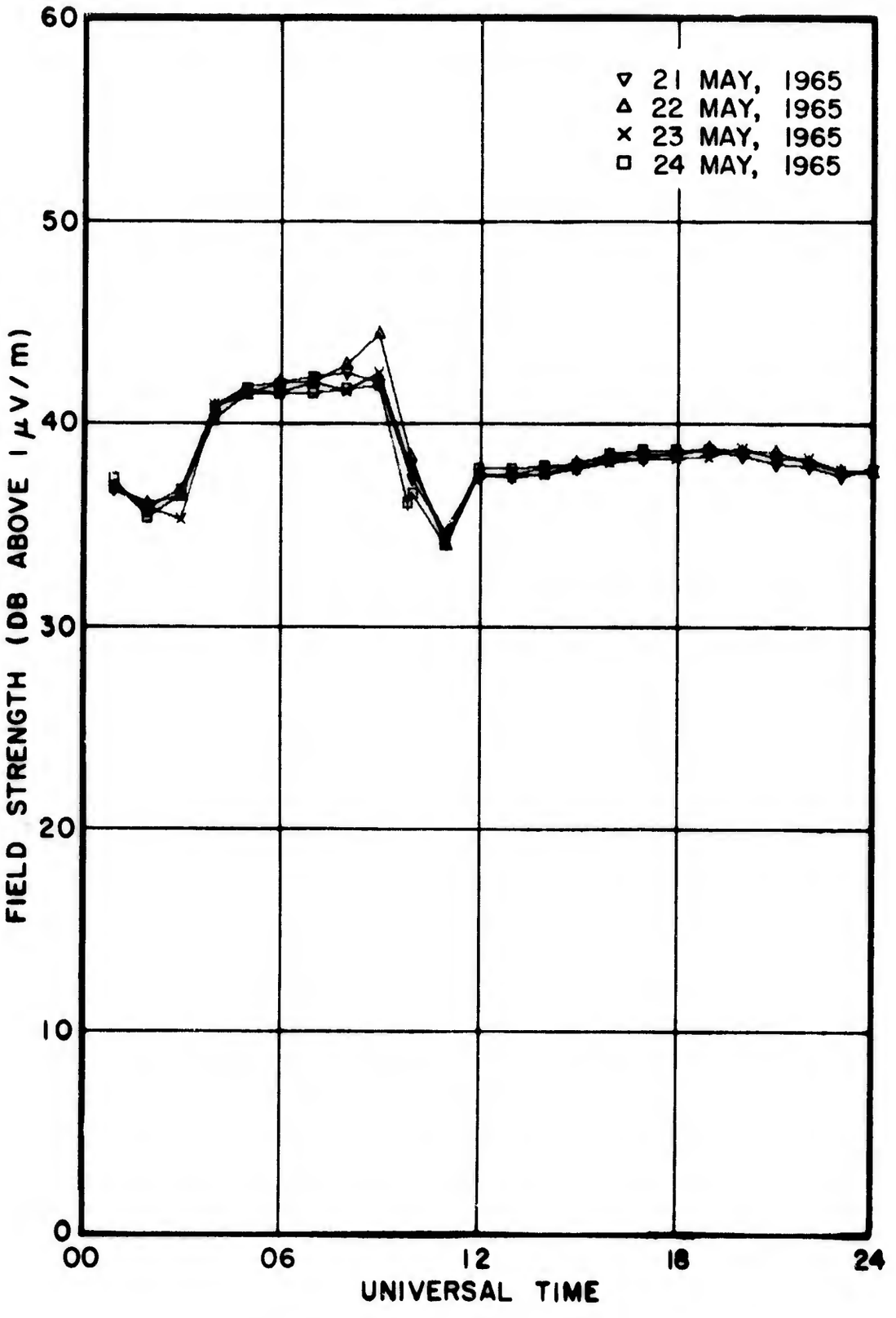

Fig. 56 - NPG (18.6 kc/s) data recorded May 21, 22, 23, 24, near Washington, D.C.

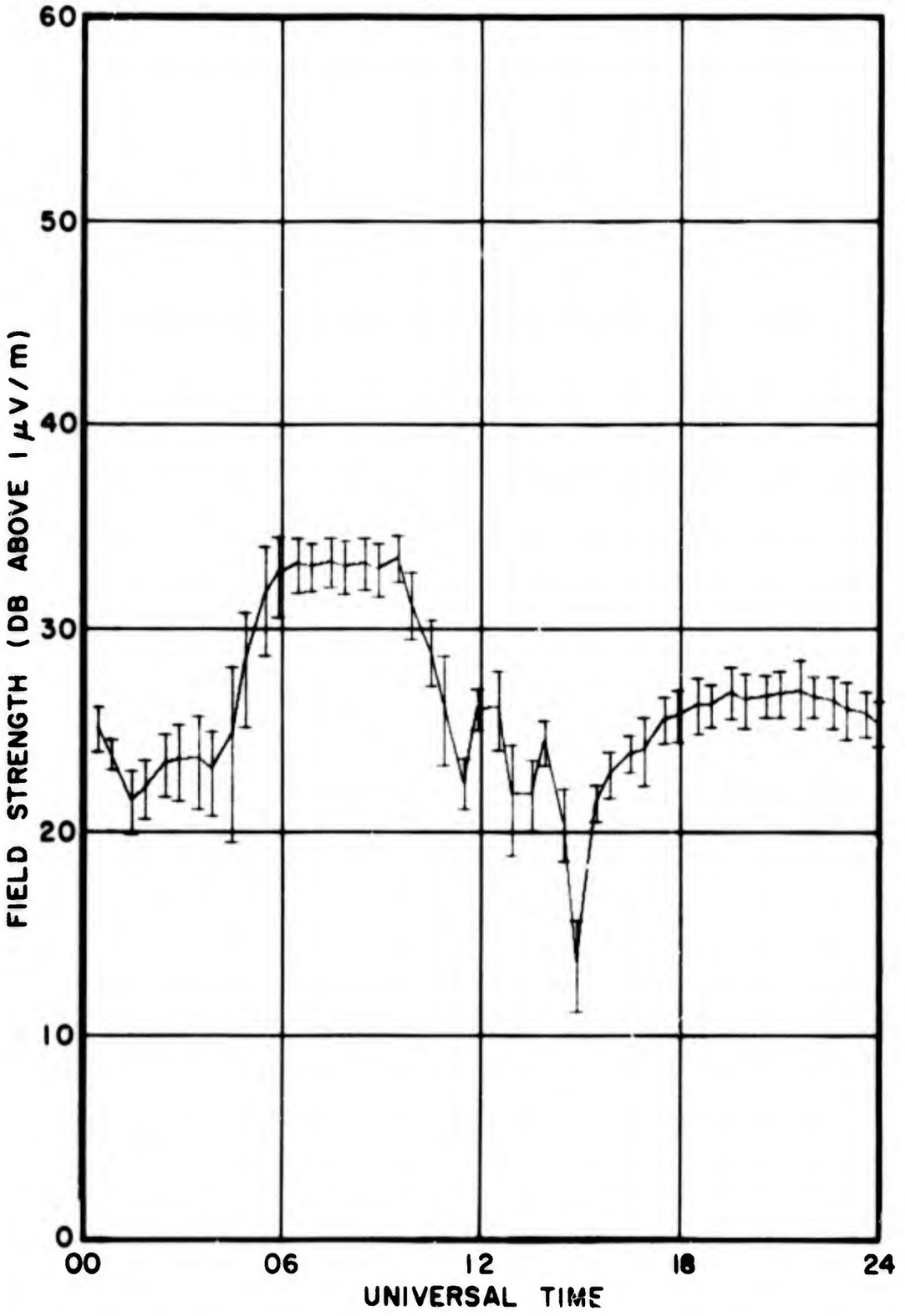

Fig. 57 - Mean and standard deviation for Haiku (19.8 kc/s) data recorded near Washington, D.C.; May 13 - June 9, 1965

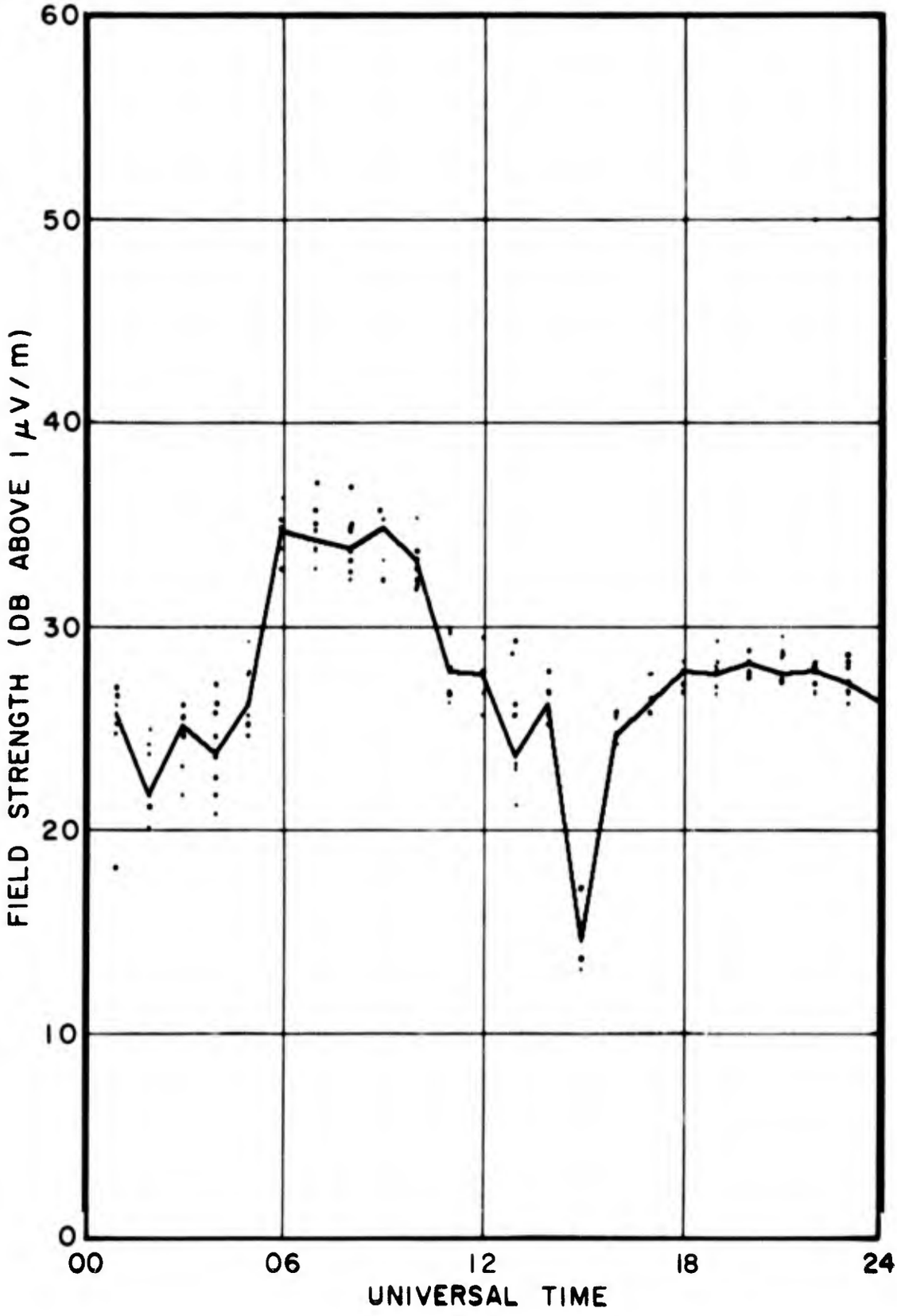

Fig. 58 - All data samples and median for NPM (19.8 kc/s) recorded near Washington, D.C.; June 10-13, and July 8-13, 1965

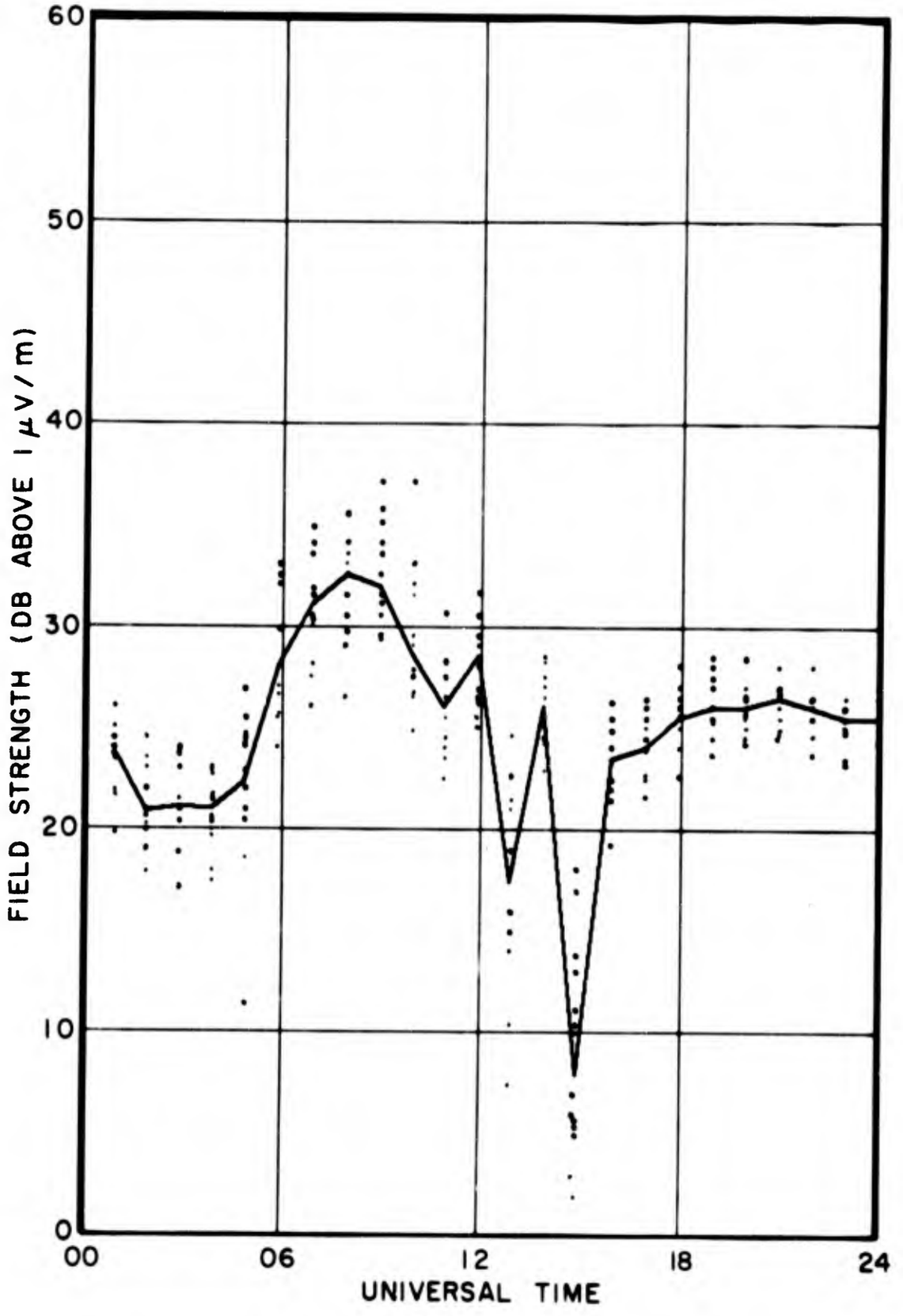

Fig. 59 - All data samples and median for NPM (22.3 kc/s) recorded near Washington, D.C.; May 13-16, May 29 - June 1, June 14-17, and June 30 - July 3, 1965

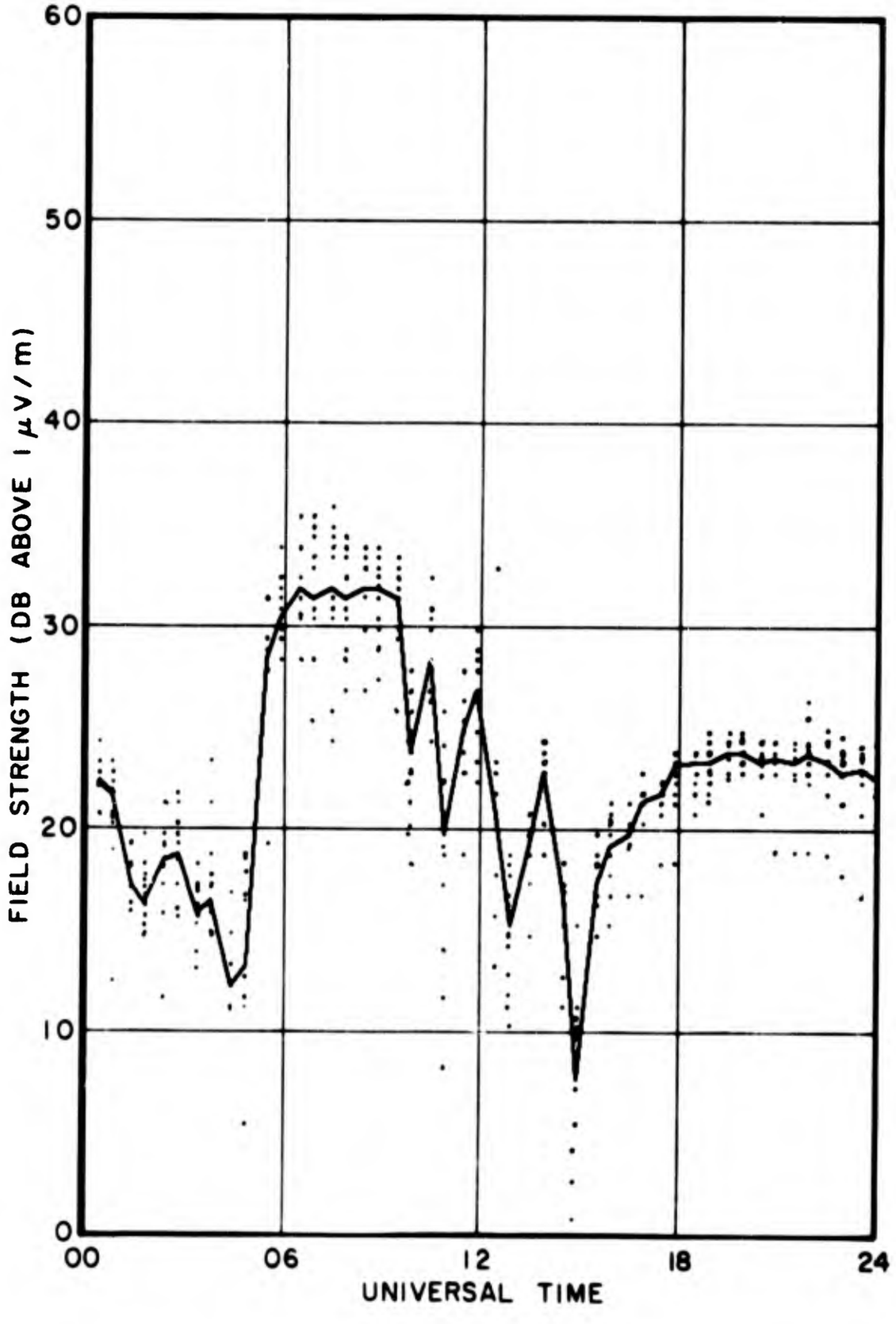

Fig. 60 - All data samples and median for NPM (24.0 kc/s) recorded near Washington, D.C.; May 17-20, May 25-28, June 2-5, and June 18-21, 1965

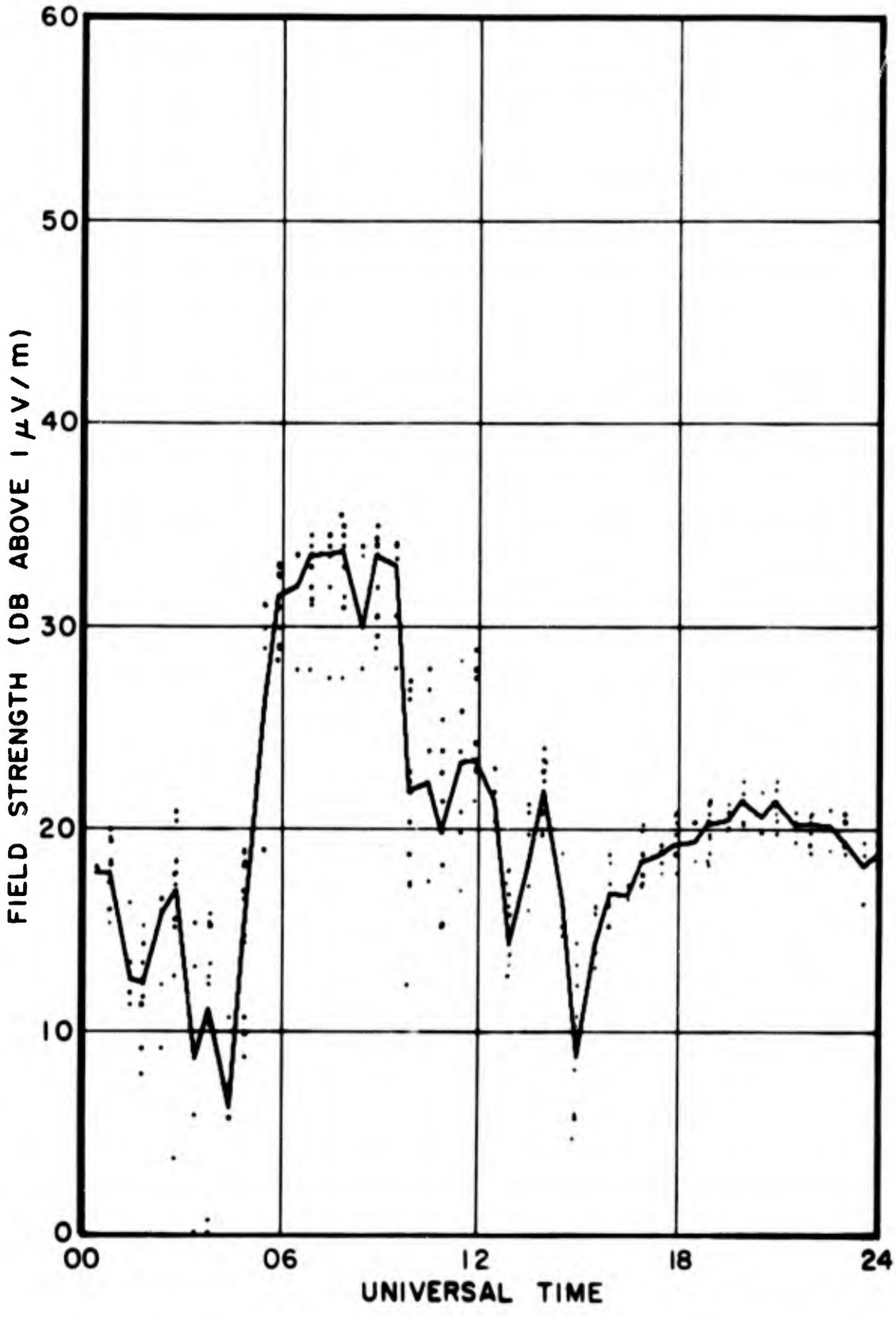

Fig. 61 - All data samples and median for NPM (26.1 kc/s) recorded near Washington, D.C.; May 21-24, June 6-9, and June 22-25, 1965

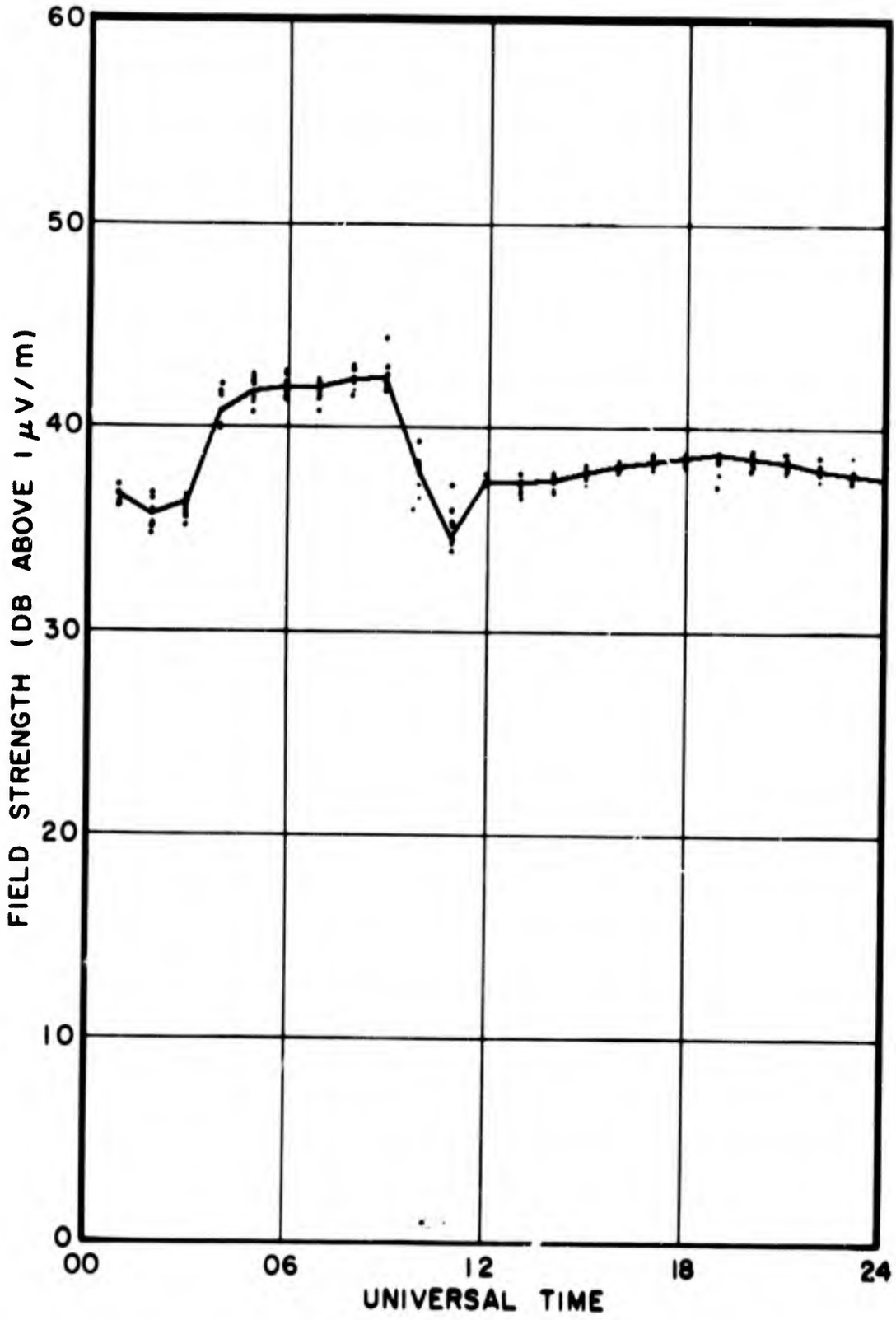

Fig. 62 - All data samples and median for NPG (18.6 kc/s) recorded near Washington, D.C.; May 13-24, 1965

Security Classification

DOCUMENT CONTROL DATA - R&D

(Security classification of title, body of abstract and indexing annotation must be entered when the overall report is classified)

1. ORIGINATING ACTIVITY *(Corporate author)*

U.S. Naval Research Laboratory
Washington, D.C., 20390

2a. REPORT SECURITY CLASSIFICATION

Unclassified

2b. GROUP

-

3. REPORT TITLE

AN INVESTIGATION OF THE MODAL INTERFERENCE OF VERY-LOW-FREQUENCY RADIO WAVES

4. DESCRIPTIVE NOTES *(Type of report and inclusive dates)*

A final report on one phase of the problem.

5. AUTHOR(S) *(Last name, first name, initial)*

Rhoads, F.J., and Garner, W.E.

6. REPORT DATE	7a. TOTAL NO. OF PAGES	7b. NO. OF REFS
October 27, 1965	64	3

8a. CONTRACT OR GRANT NO.	9a. ORIGINATOR'S REPORT NUMBER(S)
NRL Problem R01-39 b. PROJECT NO. BuShips No. SR 008-01-01 c. Task 7044 d.	NRL Report 6359
	9b. OTHER REPORT NO(S) *(Any other numbers that may be assigned this report)*

10. AVAILABILITY/LIMITATION NOTICES

Distribution of this document is unlimited.

11. SUPPLEMENTARY NOTES	12. SPONSORING MILITARY ACTIVITY
	Department of the Navy (Bureau of Ships)

13. ABSTRACT

A very-low-frequency (vlf) radio-wave propagation experiment has been designed to study modal interference effects and the extent of agreement with theoretical results obtained previously. The experimental data are the field strengths of the vlf transmissions from the U.S. Navy transmitting stations NPM and Haiku in Hawaii and NPG near Seattle, Washington. These data were recorded aboard an aircraft while in flight between California, Guam, and Japan, and also at a field site near Washington, D.C. During the experiment, NPM transmitted for various periods on 16.6, 19.8, 22.3, 24.0, and 26.1 kc/s. The Haiku transmissions were on 16.6 and 19.8 kc/s, while NPG was on 18.6 kc/s continuously.

The experimental field-strength-versus-distance graphs show considerable modal interference and very good agreement with the theoretical results for the isotropic case. For frequencies above 20 kc/s the experimental data indicate the existence of at least the first three modes for propagation to the west and to the east, out to distances greater than 3 megameters. The data at 19.8 kc/s, however, indicate first-three-mode effects for propagation to the east but only two modes to the west. The fading of the field strengths at Washington, D.C., during sunrise was frequently greater than 20 db. The depth of the fades, in general, increased with frequency, whereas their time of occurrence was relatively independent of frequency over the range of 19.8 to 26.1 kc/s.

DD FORM 1 JAN 64 1473

Security Classification

14. ♦ KEY WORDS	LINK A		LINK B		LINK C	
	ROLE	WT	ROLE	WT	ROLE	WT
Radio Waves Very low frequency Propagation Modal interference Field strength versus distance U.S. Navy transmitting stations						

INSTRUCTIONS

1. ORIGINATING ACTIVITY: Enter the name and address of the contractor, subcontractor, grantee, Department of Defense activity or other organization *(corporate author)* issuing the report.

2*a*. REPORT SECURITY CLASSIFICATION: Enter the overall security classification of the report. Indicate whether "Restricted Data" is included. Marking is to be in accordance with appropriate security regulations.

2*b*. GROUP: Automatic downgrading is specified in DoD Directive 5200.10 and Armed Forces Industrial Manual. Enter the group number. Also, when applicable, show that optional markings have been used for Group 3 and Group 4 as authorized.

3. REPORT TITLE: Enter the complete report title in all capital letters. Titles in all cases should be unclassified. If a meaningful title cannot be selected without classification, show title classification in all capitals in parenthesis immediately following the title.

4. DESCRIPTIVE NOTES: If appropriate, enter the type of report, e.g., interim, progress, summary, annual, or final. Give the inclusive dates when a specific reporting period is covered.

5. AUTHOR(S): Enter the name(s) of author(s) as shown on or in the report. Enter last name, first name, middle initial. If military, show rank and branch of service. The name of the principal author is an absolute minimum requirement.

6. REPORT DATE: Enter the date of the report as day, month, year; or month, year. If more than one date appears on the report, use date of publication.

7*a*. TOTAL NUMBER OF PAGES: The total page count should follow normal pagination procedures, i.e., enter the number of pages containing information.

7*b*. NUMBER OF REFERENCES: Enter the total number of references cited in the report.

8*a*. CONTRACT OR GRANT NUMBER: If appropriate, enter the applicable number of the contract or grant under which the report was written.

8*b*, 8*c*, & 8*d*. PROJECT NUMBER: Enter the appropriate military department identification, such as project number, subproject number, system numbers, task number, etc.

9*a*. ORIGINATOR'S REPORT NUMBER(S): Enter the official report number by which the document will be identified and controlled by the originating activity. This number must be unique to this report.

9*b*. OTHER REPORT NUMBER(S): If the report has been assigned any other report numbers *(either by the originator or by the sponsor)*, also enter this number(s).

10. AVAILABILITY/LIMITATION NOTICES: Enter any limitations on further dissemination of the report, other than those imposed by security classification, using standard statements such as:

(1) "Qualified requesters may obtain copies of this report from DDC."

(2) "Foreign announcement and dissemination of this report by DDC is not authorized."

(3) "U. S. Government agencies may obtain copies of this report directly from DDC. Other qualified DDC users shall request through

_____."

(4) "U. S. military agencies may obtain copies of this report directly from DDC. Other qualified users shall request through

_____."

(5) "All distribution of this report is controlled. Qualified DDC users shall request through

_____."

If the report has been furnished to the Office of Technical Services, Department of Commerce, for sale to the public, indicate this fact and enter the price, if known.

11. SUPPLEMENTARY NOTES: Use for additional explanatory notes.

12. SPONSORING MILITARY ACTIVITY: Enter the name of the departmental project office or laboratory sponsoring *(paying for)* the research and development. Include address.

13. ABSTRACT: Enter an abstract giving a brief and factual summary of the document indicative of the report, even though it may also appear elsewhere in the body of the technical report. If additional space is required, a continuation sheet shall be attached.

It is highly desirable that the abstract of classified reports be unclassified. Each paragraph of the abstract shall end with an indication of the military security classification of the information in the paragraph, represented as *(TS), (S), (C), or (U)*

There is no limitation on the length of the abstract. However, the suggested length is from 150 to 225 words.

14. KEY WORDS: Key words are technically meaningful terms or short phrases that characterize a report and may be used as index entries for cataloging the report. Key words must be selected so that no security classification is required. Identifiers, such as equipment model designation, trade name, military project code name, geographic location, may be used as key words but will be followed by an indication of technical context. The assignment of links, roles, and weights is optional.